



annual report
2015 / 2016

INSTITUT FÜR
TECHNISCHE OPTIK
UNIVERSITÄT STUTTGART



Universität Stuttgart

INSTITUT FÜR TECHNISCHE OPTIK
UNIVERSITÄT STUTTGART

Prof. Dr. W. Osten



Pfaffenwaldring 9
D-70569 Stuttgart
Tel.: +49(0)711 685-66075
Fax: +49(0)711 685-66586
<http://www.ito.uni-stuttgart.de>

ANNUAL REPORT 2015/2016



Dear Reader,

Another two years filled with many activities in different fields and enriched with fruitful national and global cooperation have passed since the ITO staff reported in 2015 about their current and past research activities. Thus it is again time to inform our partners, sponsors and customers about our recent advances in the field of Applied Optics.

The basic understanding that determines our work remains unchanged: striving for excellence in research and teaching, together with a good balance of continuity and systematic renewing. Keeping this in mind, it is quite certain that our work is not unaffected by the so-called megatrends. Less than a minute goes by, in which politicians, economists and strategists of all shapes don't report about the promises and challenges of Digitalization, Industry 4.0, Health, Mobility, Nano, Security, and Ecology and want to convey to us the certainty that it is high time to address these trends in a sustainable way. This position is likely to be difficult to disregard. But the strength and omnipresence with which these demands are expressed cause a new

quality. Some of these trends such as Digitalization, Health, and Nano have been continuously in our focus already. However, the constant striving for renewal, what sounds logic for scientists, means not only the devotion to hot topics but even more the guarantee of increasing infrastructural requirements. And this is an ongoing challenge for all university institutes in times of declining financial resources. But what is the way out, if one does not want to lose the connection? Greater alliances within the framework of megaprojects, more and new allies particularly outside the academically perfect world to pay tribute to the magical trend of open innovation, shared infrastructures, more risky and demanding projects? Yes and no! All of these ways have pros and cons. While greater alliances often assure a longer duration and stronger financial background, they generate on its own terms an increasing administrative overhead with the result of declining flexibility. The strong handshake between industry and academia is often the direct way out of the ivory tower and widens the view for real economic and social challenges. But it also contains the risk of mutating into a prolonged workbench and causes in general a new level of commitment. This is – without a doubt – often a challenge, yet an important aspect for engineering and applied science from our point of understanding. In general, there is no golden way and the quest for the right strategic decisions is a daily demand. We at ITO tried to shape our future on the one hand by a continued strong commitment for basic research which is enabled by a series of challenging projects mainly supported by the German Research Association DFG. Here we can report of about 90% of allowance rate for our submitted DFG projects and a share of 35% of DFG funding in our entire

budget. The latter could be continuously increased over the years to an annual amount of 3,2 million Euro. On the other hand, long-term cooperation with companies like Mahr and ASML in the field of asphere and free-form metrology, semiconductor inspection and mask alignment is a fixed part of our strategy. Such lasting academia-industry-alliances mean for ITO an unfailing source of inspiration for future research activities and an effective way for the generation of high-level scientific output in terms of disserta-

tions and publications as well. But for both a continued investment in infrastructure is mandatory. One of our latest achievements in this context is the opening of our Nano-Fabrication and –Measurement Center with the new Nano-Measurement and –Positioning Machine NPMM 200 (fig. 1), dedicated nano-fabrication tools such as the FEI Helios NanoLab 600 and the Super-Inkjet-Printer SIJ-S030. Further sophisticated equipment for nano-machining and measurement is already a fixed part of our mid-term agenda.



Fig. 1: The NPMM-200 constructed at the Technical University Ilmenau and almost ready for shipping to the ITO.

Ongoing activities are directed to the profound investigation of our strategic research topics such as multi-scale sensor fusion, computational microscopy, resolution enhancement, model-based reconstruction of measurement data, asphere and freeform metrology, optical systems design, hybrid optics, digital holography, and inverse scattering. Let me cite only some recent results which caused international attention:

- a new miniaturized image sensor with increased resolution in the center of the field of view fabricated with 2-photon polymerization (fig. 2a)¹,
- the commercial launch of the new tilted wave interferometer TWI 60 by the company Mahr as result of the long-term cooperation between ITO and Mahr (fig. 2b)²,

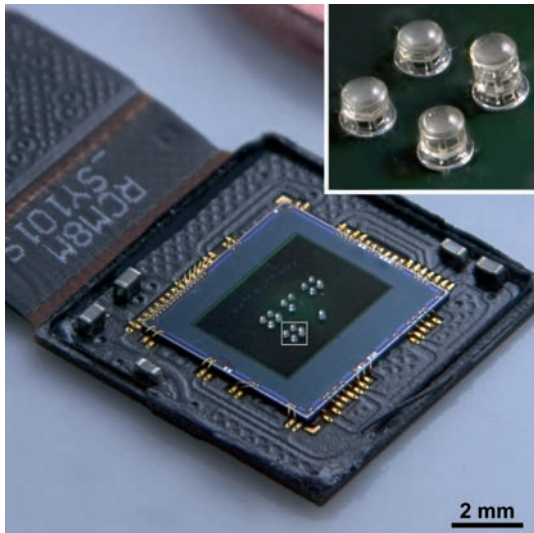


Fig. 2a: Miniaturized image sensor with increased resolution.

- the launch of the new release 3.0³ of the ITO open-source metrology software package ITOM⁴, and
- the implementation of a new principle for high-resolution lensless microscopy using the diffusing property of the random medium for imaging micro structures with diffraction-limited resolution⁵.

To ensure that ITO can comply with its mission under changing boundary conditions, we support the cooperative network SCoPE⁶ with many activities. On the one hand ITO is an active driver of the joint master course in Photonic Engineering that was established in spring 2013. On the other hand several joint research projects with different SCoPE members are in progress or on the way.



Fig. 2b: The Tilted Wave Interferometer TWI 60.

¹ Simon Thiele, Kathrin Arzenbacher, Timo Gissibl, Harald Giessen, Alois M. Herkommer: 3D-printed eagle eye: Compound microlens system for foveated imaging. *Science Advances* 3, e1602655, 3(2017)

² Mary Freebody: Great Strides in Optical Fabrication. *Photonics Spectra*, October 2016, pp. 42-45

³ <http://itom.bitbucket.org>

⁴ Marc Gronle, Wolfram Lyda, Marc Wilke; Christian Kohler, Wolfgang Osten: itom: an open source metrology, automation, and data evaluation software. *APPLIED OPTICS* Vol. 53, Issue: 14, Pages: 2974-2982, 2014 DOI: 10.1364/AO.53.002974

⁵ Alok Kumar Singh, Dinesh N Naik, Giancarlo Pedrini, Mitsuo Takeda, Wolfgang Osten: Exploiting scattering media for exploring 3D objects. *Light: Science & Applications* 6(2017), e16219; doi:10.1038/lssa.2016.219

⁶ Stuttgart Research Center for Photonic Engineering, <http://www.scope.uni-stuttgart.de/>

As a member of the Faculty of Mechanical Engineering, the Institute represents the University of Stuttgart in the field of Applied Optics in research and education. Together with our national and international partners, our research work focuses on the exploration of new optical measurement, imaging and design principles and their implementation in new components, sensors and sensor systems. Our overall research focus "Optical Metrology and Systems Design" is structured into nine main research directions:

- Active Metrology,
- Model-based Metrology,
- Remote Metrology,
- Resolution Enhanced Technologies,
- Computational Imaging,
- Sensor Fusion,
- Sensor Integration,
- Hybride Optics,
- Simulation Technologies, and
- Optical Systems Design.

The strong interaction between these directions gives the institute the required depth across the broad range of our activities in optics. The considerable number of research projects that are referred to in this report reflects again the success of this approach.

Besides our wide research activities, an ongoing strong commitment of ITO is directed to high-quality teaching on different levels (bachelor, master, PhD). Our consecutive bachelor-master course in medical technology – a joint and challenging project of the University of Stuttgart and the Eberhard Karls University Tübingen – is running very successful in both the bachelor and the master level. Since the beginning in 2010, ITO is one of the drivers of that course.

To cope with our ambitious and extensive approach to Applied Optics, a deep understanding of physics needs to be combined with practical engineering implementation. This is a daily challenge for all members of the staff. However, a good mixture of graduates in physics and engineering, a vital and innovative scientific climate, that considers the interdisciplinary cooperation with numerous national and international institutes, and a continuous observation of the technological and scientific progress are a good basis to meet these and future challenges.

Stuttgart, July 2017



Wolfgang Osten

Index

Institute structure

Team and structure	12
Staff of the Institute	14
Project partners	18
Studying optics.....	20
The research groups.....	22

Research projects

■ 3D-Surface Metrology

Topography measurement of packaged MEMS.....	26
<i>J. Krauter, M. Gronle, W. Osten</i>	
Single-shot white-light interferometer design.....	27
<i>R. Hahn, J. Krauter, K. Körner, M. Gronle, W. Osten</i>	
Wafer-level optics for an OCT system.....	28
<i>J. Krauter, M. Gronle, W. Osten</i>	
Simultaneous single-shot measurement of topography and refractive index of layered specimen.....	30
<i>T. Boettcher, M. Gronle, W. Osten</i>	
Adaptive chromatic confocal spectral interferometer	31
<i>D. Claus, M. Gronle, W. Osten</i>	
Dynamic referencing of coordinate measurement and tooling machines	32
<i>M. Gronle, T. Haist, W. Osten</i>	
Intelligent optical sensor for the 2D and 3D surface measurement and inspection.....	33
<i>M. Gronle, T. Haist, W. Osten</i>	
Comparison of various microscopic 3d measurement techniques for roughness and surface evaluation.....	34
<i>M. Gronle, T. Boettcher, K. Körner, W. Osten</i>	
Simulation of microscopic metal surfaces based on measured microgeometry.....	36
<i>H. Yang, T. Haist, M. Gronle, W. Osten</i>	
Open source measurement and evaluation software itom 3.0	38
<i>M. Gronle, H. Bieger, R. Hahn, J. Krauter, W. Osten</i>	

■	Active Optical Systems and Computational Imaging	
	Theoretical and experimental investigations concerning the influence of coherent noise on the resolution of data measured with triangulation sensors	40
	<i>S. Haberl, M. Gronle, T. Haist, W. Osten</i>	
	New setup for the characterization of image sensors with respect to fixed-pattern noise	42
	<i>T. Haist, J. Barth, Q. Duong-Ederer, W. Osten</i>	
	Versatile setup for testing phase retrieval methods	44
	<i>C. Lingel, T. Haist, W. Osten</i>	
	Post-processing for the compensation of chromatic aberrations in programmable microscopy	45
	<i>H. Pen, S. Gharbi, T. Haist, W. Osten</i>	
■	High Resolution Metrology and Simulation	
	Detection of grating asymmetries by phase-structured illumination	48
	<i>D. Buchta, S. Peterhänsel, M. L. Gödecke, K. Frenner, W. Osten</i>	
	Multiple-wavelength optical alignment tool	49
	<i>M. L. Gödecke, S. Peterhänsel, K. Frenner, W. Osten</i>	
	Wafer alignment on small targets with small pitches.....	50
	<i>C. M. Bett, M. L. Gödecke, D. Buchta, K. Frenner, W. Osten</i>	
	Design of a two-dimensional cascaded plasmonic superlens.....	51
	<i>L. Fu, H. Li, K. Frenner, W. Osten</i>	
	Nanofabrication of a cascaded plasmonic superlens	53
	<i>H. Li, L. Fu, K. Frenner, W. Osten</i>	
	Application of a speckle simulator for a machine-learning phase retrieval process	54
	<i>L. Fu, K. Frenner, W. Osten</i>	
	Nanopositioning- and measuring machine NPMM-200	55
	<i>K. Frenner, C. Pruß, W. Osten</i>	
	Detecting the depth of fluorescent light sources by structured illumination and shearing interferometry	57
	<i>J. Schindler, K. Frenner, W. Osten</i>	
■	Interferometry and Diffractive Optics	
	Next generation TWI	60
	<i>G. Baer, C. Pruß, A. Bielke, J. Schindler, A. Harsch, W. Osten</i>	
	Robust Radius metrology	62
	<i>C. Pruß, A. Wempe, J. Schindler, W. Osten</i>	

Measuring large convex surfaces with Tilted Wave Interferometry using stitching methods	63
<i>A. Harsch, J. Schindler, C. Pruß</i>	
Tilted-Wave-Interferometry: Improving accuracy by elimination of systematic errors	64
<i>J. Schindler, C. Pruß, W. Osten</i>	
Subwavelength diffractive optics for generation of cylindrical polarization states.	65
<i>CM. Mateo, O. Schwanke, L. Fu, C. Pruß, W. Osten</i>	
3D laser direct-writing for injection compression molding of diffractive-refractive elements	66
<i>S. Thiele, C. Pruß, M. Röder, D. Hera, T. Günther, A. Zimmermann, H. Kück, W. Osten</i>	
In situ fabrication of microstructures for encoder systems.....	67
<i>R. Hahn, C. Pruß, F. Schaal, W. Osten</i>	
Improved design of a diffractive zoom lens for interferometric measurements	68
<i>A. Bielke, C. Pruß, W. Osten</i>	
Microscope objective integrated optically addressable polarization shaping	69
<i>A. Bielke, C. Pruß, F. Schaal, W. Osten</i>	
■ Coherent Metrology	
Large field of view optical elastography for biological soft tissue investigation	72
<i>D. Claus, G. Pedrini, W. Osten</i>	
Residual stress analysis of ceramic coating by laser ablation and digital holography	74
<i>G. Pedrini, W. Osten</i>	
Nano-scale measurement of in-plane displacements of microscopic objects	76
<i>A. K. Singh, G. Pedrini, W. Osten</i>	
Combination of FEM-simulations and shearography for artwork inspection.....	77
<i>D. Buchta, G. Pedrini, W. Osten</i>	
Focus and perspective adaptive digital surgical microscope	78
<i>D. Claus, C. Reichert, A. Herkommer</i>	
Replacing conventional microscope objectives by a scattering plate: a comparative study	79
<i>A. K. Singh, G. Pedrini, M. Takeda, W. Osten</i>	
Spectrally resolved digital holography by using a white LED	80
<i>D. Claus, G. Pedrini, D. Buchta, W. Osten</i>	
Light field endoscopy and its parametric description	82
<i>J. Liu, D. Claus, A. Herkommer, W. Osten</i>	
Iterative phase retrieval based on variable wave-front curvature	83

D. Claus, G. Pedrini, W. Osten

Digital Holography for erosion monitoring inside the ITER Tokamak..... 84

G. Pedrini, I. Alekseenko, G. Jagannathan, G. Vayakis, W. Osten

■ **Optical Design and Simulation**

Design, simulation and 3D printing of complex micro-optics..... 88

S. Thiele, S. Ristok, H. Giessen, A. Herkommer

Compound microlens systems for foveated imaging89

S. Thiele, K. Arzenbacher, T. Gissibl, H. Giessen, A. Herkommer

Smartphone-microscope.....90

C. Reichert, D. Claus, A. Herkommer

Building kit for realization of optical systems91

C. Reichert, T. Haist, A. Herkommer

Design and measurements with the phase space analyzer 92

D. Rausch, A. Herkommer

Design of large field head mounted display systems..... 93

B. Chen, A. Herkommer

Publications 2015 – June 2017

Invited lectures on international conferences..... 94

Editorial work..... 97

Awards 97

W. Osten: Board Member 98

Membership of Editorial Boards 99

Reviewed papers..... 100

Conference proceedings and journals 105

Patents 110

Doctoral thesis, master & bachelor thesis and student research thesis 112

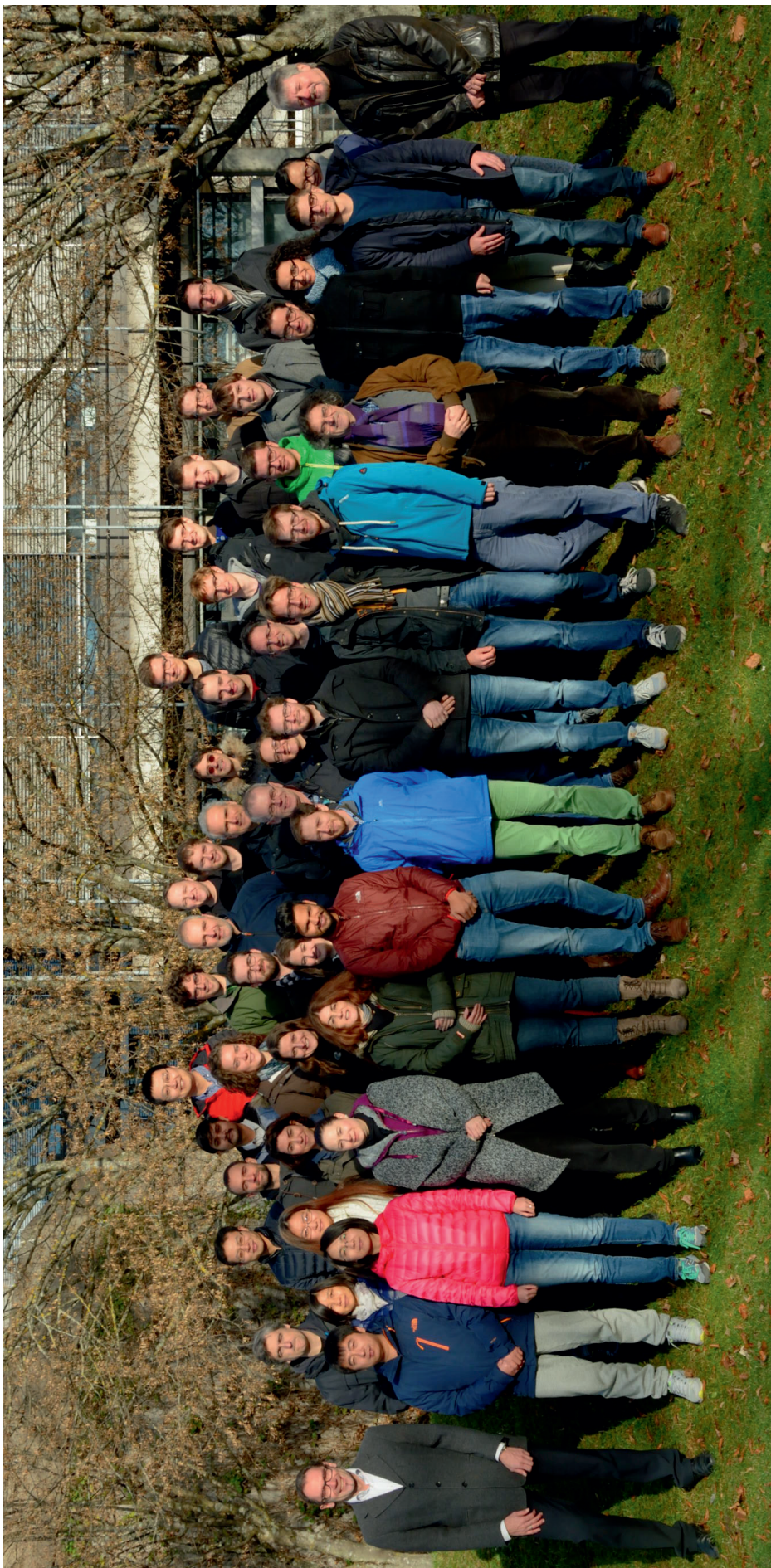
Colloquia & Conferences

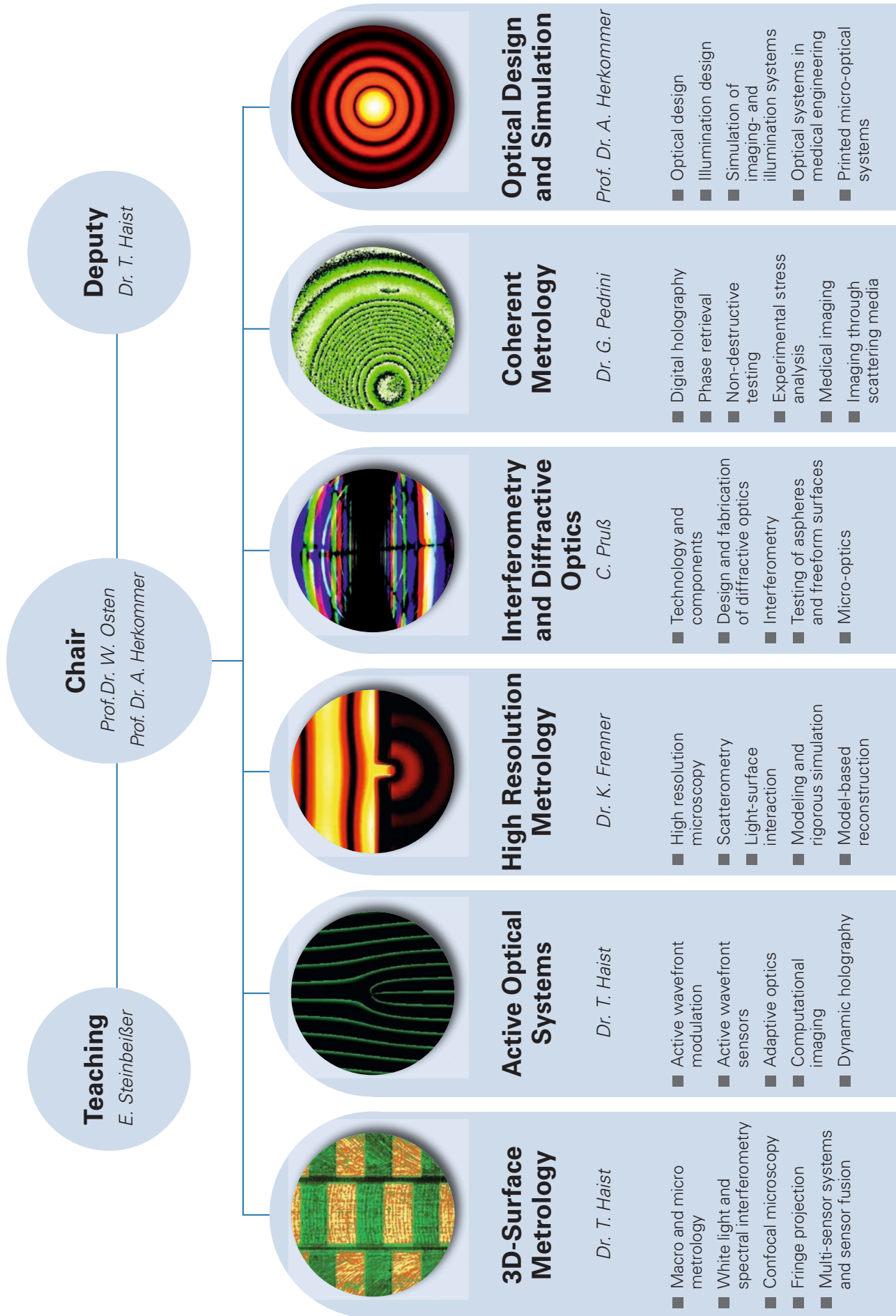
Stuttgart Scientific Symposium 2015
"Light of the future" 118

Optik-Kolloquium 2016120

Organized international conferences: 2015 – 2016 121

Team and structure





Administration, Software Engineering & Technical Support

Status quo: May 2017

Staff of the Institute

Status quo: March 2017

Director

Prof. Dr. Wolfgang Osten +49 (0) 711 685-66075 osten@ito.uni-stuttgart.de

Endowed Professorship for Optical Design and Simulation

Prof. Dr. Alois Herkommer +49 (0) 711 685-69871 herkommer@ito.uni-stuttgart.de

Administration and Secretary

Katja Costantino +49 (0) 711 685-69873 costantino@ito.uni-stuttgart.de

Christina Vogelmann +49 (0) 711 685-66074 vogelmann@ito.uni-stuttgart.de

Studies

Erich Steinbeißer +49 (0) 711 685-66068 steinbeisser@ito.uni-stuttgart.de

Research Assistants

3D-Surface metrology

Marc Gronle (leader) +49 (0) 711 685-69888 gronle@ito.uni-stuttgart.de

Tobias Boettcher +49 (0) 711 685-66656 boettcher@ito.uni-stuttgart.de

Dr. Klaus Körner +49 (0) 711 685-66082 koerner@ito.uni-stuttgart.de

Johann Krauter +49 (0) 711 685-69806 krauter@ito.uni-stuttgart.de

Haiyue Yang +49 (0) 711 685-66594 haiyue.yang@ito.uni-stuttgart.de

Florian Mauch left on 31.08.2014

Active Optical Systems

Dr. Tobias Haist (leader) +49 (0) 711 685-66069 haist@ito.uni-stuttgart.de

Quynh Duong-Ederer +49 (0) 711 685-69875 duong-ederer@ito.uni-stuttgart.de

Christian Lingel +49 (0) 711 685-66071 lingel@ito.uni-stuttgart.de

Malte Hasler left on 30.09.2015

Shihao Dong left on 15.05.2015

High resolution metrology and simulation

Karsten Frenner (leader) +49 (0) 711 685-66065 frenner@ito.uni-stuttgart.de
Claudia Bett +49 (0) 711 685-69804 bett@ito.uni-stuttgart.de
Liwei Fu +49 (0) 711 685-69833 fu@ito.uni-stuttgart.de
Maria Laura Gödecke +49 (0) 711 685-66623 goedecke@ito.uni-stuttgart.de
Huiyu Li +49 (0) 711 685-66846 huiyu.li@ito.uni-stuttgart.de
Sandy Peterhänsel left on 31.01.2016	
Valeriano Ferreras Paz left on 28.02.2015	
Holger Gilbergs left on 31.01.2015	
Philipp Schau left on 31.01.2015	

Interferometry and diffractive optics

Christof Pruß (leader) +49 (0) 711 685-66066 pruss@ito.uni-stuttgart.de
Alexander Bielke +49 (0) 711 685-69876 bielke@ito.uni-stuttgart.de
Robin Hahn +49 (0) 711 685-69879 hahn@ito.uni-stuttgart.de
Antonia Harsch +49 (0) 711 685-69870 harsch@ito.uni-stuttgart.de
Cherry May Mateo +49 (0) 711 685-69878 mateo@ito.uni-stuttgart.de
Johannes Schindler +49 (0) 711 685-60488 schindler@ito.uni-stuttgart.de
Thomas Schoder +49 (0) 711 685-66064 schoder@ito.uni-stuttgart.de
Oliver Schwanke +49 (0) 711 685-69877 schwanke@ito.uni-stuttgart.de
Frederik Schaal left on 31.12.2015	
Jan Beneke left on 30.06.2015	
Goran Baer left on 31.05.2015	

Coherent metrology

Dr. Giancarlo Pedrini (leader) +49 (0) 711 685-66078 pedrini@ito.uni-stuttgart.de
Dominic Buchta +49 (0) 711 685-66528 buchta@ito.uni-stuttgart.de
Dr. Daniel Claus +49 (0) 711 685-69890 claus@ito.uni-stuttgart.de
Alok Kumar Singh left on 31.12.2016	
Petra Schumacher left on 31.03.2015	
Marc Wilke left on 31.03.2015	

Optical Design and Simulation

Prof. Dr. Alois Herkommer (leader) . +49 (0) 711 685-69871 herkommer@ito.uni-stuttgart.de
Bo Chen +49 (0) 711 685-69885 chen@ito.uni-stuttgart.de
Denise Rausch +49 (0) 711 685-66648 rausch@ito.uni-stuttgart.de
Carsten Reichert..... +49 (0) 711 685-69805reichert@ito.uni-stuttgart.de
Simon Thiele..... +49 (0) 711 685-66609 thiele@ito.uni-stuttgart.de
Taimoor Talpur..... left on 31.12.2015

Software Engineering and Technicians

Heiko Bieger..... +49 (0) 711 685-66070bieger@ito.uni-stuttgart.de
Ralph Knoll..... +49 (0) 711 685-66067 knoll@ito.uni-stuttgart.de
Andreas Lorenz..... +49 (0) 711 685-66089 lorenz@ito.uni-stuttgart.de

Foreign Guests visiting the Institute: 2015 – June 2017

February 2015:

Elizabeth Rogan CEO OSA, Washington, USA
Dr. Fernando Mendoza-Santoyo CIO, Leon, Mexico
Dr. Elder de la Rosa Cruz CIO, Leon, Mexico
Dr. Eugene Arthurs..... CEO SPIE, Bellingham, USA
Prof. Toyohiko Yatagai..... Utsunomiya Univ., Utsunomiya, Japan
Prof. Dr. M. Takeda Utsunomiya Univ., Utsunomiya, Japan
Prof. Dr. Seppo Honkanen Univ. of Eastern Finland, Finland
Prof. Kazuyoshi Itoh Osaka University, Japan

March 2015:

Prof Yun Ma..... Nanjing University, China

May 2015:

Dr. Yu Fu Nanyang University, Singapore
Prof. Yoshio Hayasaki Utsunomiya Univ., Utsunomiya, Japan

November 2015:

Dr. Shoichi Furukava AsahiKASEI, Tokyo, Japan
Prof. Dr. Ting-Chung Poon..... Virginia Tech, Blacksburg, USA

January 2016:

Prof. Dr. Michael Unser..... EPFL, Lausanne, Suisse
Prof. Dr. Jamal Yagoobi Worcester Polytechnic Inst., Worcester, USA
Prof. Dr. Takashi Fukuda..... President of the University of Electro-Communication UEC,
Tokyo, Japan

February 2016:

Prof. Armondo Albertazzi..... Univ. Florianopolis UFSC, Florianopolis, Japan

March 2016:

Prof. Dr. Yasuo Kanematsu..... Osaka Univ., Japan

Dr. Teruyoshi Nobukawa Wakayama Univ., Japan

April 2016:

Dr. Xavier Colonna-Delega..... Zygo, Middlefield, USA

May 2016:

Dr. Jagannathan Govindarayan ITER Organization, St Paul Lez Durance Cedex, France

July 2016:

Dr. Jim Trolinger..... Metro Laser, Irvine, USA

Andrei Asimov TU Delft, Netherlands

Kanami Ikeda University of Electro-Communication UEC, Tokyo, Japan

November 2016:

Prof. Dr. Arie den Boef ASML Veldhoven, Netherlands

Dr. Stefan Keye ASML Veldhoven, Netherlands

Simon Huisman ASML Veldhoven, Netherlands

Alessandro Polo..... ASML Veldhoven, Netherlands

December 2016:

Dr. Ferenc Gyimesi..... Holometrox, Budapest, Hungary

February 2017:

Pieter Kappelhoff hitech, Den Haag, Netherland

Dr. Paul Montgomery..... UNISTRA, Strasbourg, France

March 2017:

Dr. Daniel Krekel..... Saint-Gobain, Sekurit, Herzogenrath

June 2017:

Prof. P. Almoró University Philippines, Manila, Philippines

Prof. Dr. Wei Wang Heriot Watt Univ., Edinburgh, GB

Dr. Yu Fu Nanyang University, Singapore

Prof. Dr. Qian Kemao..... Nanyang University, Singapore

Prof. Dr. Ping Jia President Changchun Institute of Optics,
Fine Mechanics and Physics (CIOMP), Changchun, China

Prof. Dr. Min Gu RMIT University, Australia

Prof. Dr. Yuhong Bai Changchun Inst. of Optics,
Fine Mechanics and Physics (CIOMP), Changchun, China

Dr. Po-Chi Sung Photomechanics Laboratory,
National Tsing Hua University, Taiwan

Project partners

Project collaboration with the following companies and organisations

(and many others):

Aesculap AG	Tuttlingen
Academy of Sciences of Moldova	Chisinau, Moldova
ASML Netherlands B.V.	Veldhoven, Netherlands
Carl Zeiss Meditec	Oberkochen
Carl Zeiss Microscopy	Jena
Carl Zeiss AG	Oberkochen
Carl Zeiss SMT AG	Oberkochen
Cascade Microtech GmbH	Thiendorf
Centre Spatial de Liege	Liege, Belgium
Centre Suisse d'Electronique et de Microtechnique	Zurich, Switzerland
Daimler AG	Stuttgart
DermaScan GmbH	Munich
ESA / ESTEC	Noordwijk, Netherlands
Fraunhofer ENAS	Chemnitz
Fraunhofer IAO	Stuttgart
Fraunhofer IOF	Jena
Fraunhofer IOSB	Karlsruhe
Fraunhofer IAP	Potsdam
Genotec GmbH	Waiblingen
Hahn-Schickard	Stuttgart
Holoeye AG	Berlin
IAE SB RAS	Novosibirsk, Russia
ILM	Ulm
IMS Chips	Stuttgart
International Thermonuclear Experimental Reactor, ITER	Cadarache, France
KARL STORZ GmbH & Co. KG	Tuttlingen
Laboratoire d'optique appliquée, IMT, EPFL	Neuchâtel, Switzerland
LaVision GmbH	Göttingen
Leica Microsystems CMS GmbH	Wetzlar
Mahr GmbH	Jena, Göttingen
Melexis N.V.	Ypern, Belgium
Nanoscribe GmbH	Eggenstein
Physikalisch Technische Bundesanstalt	Braunschweig

Polytec GmbH	Waldbronn
Robert Bosch GmbH	Gerlingen
Shenzhen University	China
Sick AG	Waldkirch
Sick Stegmann GmbH	Donaueschingen
Siemens AG	München
Staatliche Akademie der Bildenden Künste Stuttgart	Stuttgart
Stattice	Besancon, France
STVision GmbH	Haag a. d. Amper
Tampere University of Technology	Tampere, Finland
Technische Universität Wien	Wien, Austria
Trumpf GmbH + Co. KG	Ditzingen
Tsinghua University	Peking, China
Université de Franche-Comté	Besancon, France
University of Eastern Finland	Joensuu, Finland
VTT Technical Research Centre of Finland	Espoo, Finland
X-FAB Silicon Foundries	Erfurt

Studying optics

Traditionally our curriculum is primarily directed towards the students in upper-level diploma courses of **Mechanical Engineering, Cybernetic Engineering, Mechatronics, and Technology Management**. Since the academic year 2011/12 these courses are offered as master courses and an increasing number of master students is going to join our lectures.

This applies especially for the new master programme **“Micro-, Precision- and Photonics Engineering”** which enjoys great popularity also by students from other universities even from other countries.

Since the academic year 2009/10 we also offer our optics courses within the new bachelor and master program **“Medical Engineering”**, and since 2012 also within the new master program **“Photonic Engineering”**. We also welcome students from other courses, such as “Physics” and “Electrical Engineering” and “Information Technology”.

The following list should give you an overview about the lectures given at the ITO. Be aware that not all lectures are suitable for all courses and that most lectures are held in German language.

Core subjects in Bachelor and Master Courses (6 ECTS - Credit Points):

- **Fundamentals of Engineering Optics**
Lecture: Prof. Dr. W. Osten, C. Pruß
Exercise: A. Bielke, E. Steinbeißer
- **Optical Measurement Techniques and Procedures**
Lecture: Prof. Dr. W. Osten
Exercise: Dr. K. Körner, E. Steinbeißer
- **Optical Information Processing**
Lecture: Prof. Dr. W. Osten
Exercise: Dr. K. Frenner
- **Fundamentals of Optics** (only for B.Sc.)
Lecture: Prof. Dr. A. Herkommer
Exercise: D. Rausch
- **Optical Systems in Medical Engineering**
Lecture: Prof. Dr. A. Herkommer
Exercise: D. Rausch
- **Development of Optical Systems**
Lecture: Prof. Dr. A. Herkommer
Exercise: S. Thiele

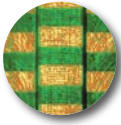
Elective subjects in Bachelor and Master Courses (3 ECTS - Credit Points):

- **Optical Phenomena in Nature and Everyday Life**
Lecture: Dr. T. Haist
- **Image Processing Systems for Industrial Applications**
Lecture: Dr. T. Haist
- **Optical Measurement** (only for B.Sc.)
Lecture: Dr. K. Körner, E. Steinbeißer
- **Polarization Optics and Nanostructured Films**
Lecture: Dr. K. Frenner
- **Introduction to Optical Design**
Lecture: Prof. Dr. A. Herkommer / Dr. Ch. Menke – in exchange
- **Advanced Optical Design**
Lecture: Prof. Dr. A. Herkommer / Dr. Ch. Menke – in exchange
- **Illumination Systems**
Lecture: Prof. Dr. A. Herkommer
- **Current Topics and Devices in Biomedical Optics** (only for B.Sc.)
Seminar: Prof. Dr. A. Herkommer

Additional studies:

- **project work and thesis within our fields of research**
(you will find a list of all student project works at the end of this annual report)
- **practical course "Optic-Laboratory"**
 - ➔ speckle measurement
 - ➔ holographic projection
 - ➔ digital microscopy
 - ➔ computer aided design of optical systems
 - ➔ measurement of the spectral power distribution
- **practical course "Optical Measurement Techniques"**
 - ➔ high contrast microscopy
 - ➔ digital holography
 - ➔ 2D-interferometry and measurement
 - ➔ quality inspection of photo-objectives with the MTF measuring system
 - ➔ ellipsometry
- **common lab for mechanical engineering (APMB)**

The research groups



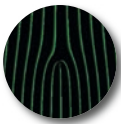
3D-Surface Metrology

The objective of the group is the analysis and the implementation of new principles for the acquisition of optical 3D-surface data of engineering and biological objects over a wide scale. Our main focus is on the enhancement of the metering capacity by a combination of physical models and optimized system design.

Current research activities are:

- 3D-measurement applying fringe projection and deflectometry (macroscopic and microscopic)
- adaptive techniques using spatial light modulators
- confocal microscopy
- white light interferometry
- spectral interferometry
- sensor fusion and data interpretation strategies

Contact: ofm@ito.uni-stuttgart.de



Active Optical Systems and Computational Imaging

The objective of our work is the development of flexible optical systems in order to enable new applications, especially within the field of scientific and industrial metrology. To achieve this goal, we make use of different modern light modulation technologies and computer-based methods. One focus of our work lies in the application of holographic methods based on liquid crystal displays and micromechanical systems for various applications ranging from optical tweezers to aberration control and testing of aspherical surfaces.

Main research areas:

- active wavefront modulation and sensors
- adaptive optics
- active wavefront sensors
- dynamic holography
- components, algorithms, and strategies
- waveoptical computing
- computational imaging

Contact: aos@ito.uni-stuttgart.de



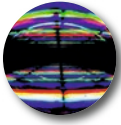
High Resolution Metrology and Simulation

The goal of this research group is the investigation of the interaction of light with 3d object structures in the micro and nano domain. Along with experimental research, one major aspect is the rigorous modelling and simulation as an integral part of the active metrology process. The analysis of all information channels of the electromagnetic field (intensity, phase, polarisation state of light) allows us to obtain sub-wavelength information about the structure.

Current research areas:

- modelling and rigorous simulation
- computational electromagnetics
- inverse problems
- high resolution microscopy
- scatterometry
- optical metamaterials
- superlenses

Contact: hms@ito.uni-stuttgart.de



Interferometry and Diffractive Optics

The goal of our research activity is to explore new measurement concepts using diffractive optics. One important application is the testing of optical surfaces, in particular, aspheric lenses. For this purpose we design and produce computer generated holograms (CGH). At the same time, we develop flexible measurement techniques for aspheres and freeform surfaces that aim to replace static null correctors. In addition to CGH for interferometry, our in house production facilities allow us to produce diffractive elements and micro-optics for a wide variety of applications such as imaging systems, UV-measurement systems, beam shaping applications and wavefront sensing.

Our research areas include:

- testing of aspheric and freeform surfaces
- design, fabrication and testing of hybrid refractive/diffractive systems
- interferometry and wavefront sensors
- tailored optics for metrology applications
- fabrication of diffractive elements and micro-optics

Contact: ide@ito.uni-stuttgart.de



Coherent Metrology

Our research objective is the analysis and application of methods based on coherent optics for the measurement of 3D-shape and deformation and to determine the material properties of technical objects and biological tissues. Aside from the quantitative measurements of form and deformation, methods for non destructive material testing are also analysed and applied.

Research areas include:

- holographic microscopy
- experimental stress analysis
- shape measurement
- holographic non-destructive testing
- endoscopy
- imaging through scattering media
- biomedical imaging and elasticity measurement of tissues

Contact: kom@ito.uni-stuttgart.de



Optical Design and Simulation

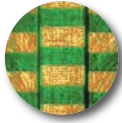
Focus of the group is the classical optical design of imaging and illumination systems, as well as ray-based and wave-optical system simulations. Main research targets are the development of novel tools for simulation and optimization and the design of innovative complex optical systems for industrial or medical purposes.

Current research topics are:

- imaging design
- illumination design
- optical simulations (ray-tracing and wave-optical)
- phase space methods in optical design and simulation
- complex surfaces in optical system design
- design and simulation of hybrid optical systems
- optical systems for biomedical applications

Contact: herkommer@ito.uni-stuttgart.de

3D-Surface Metrology



Topography measurement of packaged MEMS.....	26
<i>Supported by: BMBF</i>	
<i>Project: IRIS</i>	
<i>In cooperation with: Polytec GmbH, Robert Bosch GmbH, Cascade Microtech GmbH, Melexis GmbH, X-FAB MEMS Foundry GmbH, IMMS Institut für Mikroelektronik- und Mechatronik-Systeme gemeinnützige GmbH, Fraunhofer-Institut für Elektronische Nanosysteme ENAS</i>	
Single-shot white-light interferometer design.....	27
Wafer-level optics for an OCT system.....	28
<i>Supported by: EU (Call FP7-ICT-2011-8)</i>	
<i>Project: VIAMOS (Grant agreement no.: 318542)</i>	
<i>In cooperation with: Institut FEMTO-ST, VTT Technical Research Centre of Finland, Centre Suisse d'Electroique et de Microtechnique, Fraunhofer-Institut für Elektronische Nanosysteme ENAS, DermoScan GmbH, STATICE SAS, UFR Sciences Médicales et Pharmaceutiques, Centre Hospitalier Universitaire de Besancon, Centre National de la Recherche Scientifique</i>	
Simultaneous single-shot measurement of topography and refractive index of layered specimen.....	30
<i>Supported by: DFG German Science Foundation</i>	
<i>Project: Hochaufgelöste Single-Shot-Vermessung von semitransparenten Schichten mittels Chromatisch-Konfokaler Kohärenz-Tomographie (CCCT) (OS 111/47-1)</i>	
Adaptive chromatic confocal spectral interferometer	31
<i>Supported by: AdaScope (Landesstiftung Baden-Württemberg)</i>	
<i>In collaboration with: Fraunhofer IOSB in Karlsruhe</i>	
Dynamic referencing of coordinate measurement and tooling machines	32
<i>Supported by: DFG Os 111/42-1</i>	
<i>Project: DynRef</i>	
<i>In cooperation with: Institut für Systemdynamik (ISYS)</i>	
Intelligent optical sensor for the 2D and 3D surface measurement and inspection	33
<i>Supported by: Baden-Württemberg Stiftung</i>	
<i>Project: IOS23</i>	
<i>In cooperation with: IPVS, University of Stuttgart.</i>	
Comparison of various microscopic 3d measurement techniques for roughness and surface evaluation	34
<i>The project was supported and performed in cooperation with Walter Maschinenbau GmbH.</i>	
Simulation of microscopic metal surfaces based on measured microgeometry	36
<i>Supported by: Graduate School of Excellence advanced Manufacturing Engineering(GSaME), University of Stuttgart.</i>	
Open source measurement and evaluation software itom 3.0	38
<i>The core application of "itom" is released under the open source license LGPL.</i>	

Topography measurement of packaged MEMS

J. Krauter, M. Gronle, W. Osten

The fabrication of micro-electro-mechanical system (MEMS) is mainly driven by the consumer market and has grown almost exponentially over the last few decades [1]. For quality control, an electrical test is applied to 100% of the MEMS. However, if the test fails, it is not possible to localize the defect on the wafer since the MEMS structures are wrapped by a silicon cap wafer.

In the project IRIS, the ITO investigates the realization of optical topography measurement techniques of MEMS hidden by the silicon cap wafer. With the topography, the detection of bent or stuck MEMS fingers should be possible. A schematic cross-section of the MEMS is shown in fig. 1.

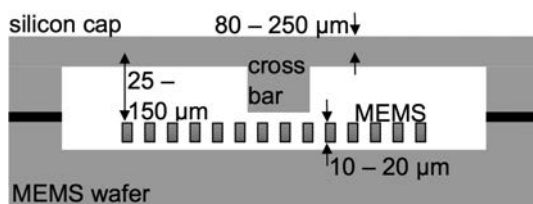


Fig. 1: Cross-section of the MEMS wafer.

Various techniques are known in the field of microsystem inspection [2]. The small dimensions of the MEMS require a resolution in the micrometer range. Low-coherence interferometry techniques (LCI) provide an axial resolution in the sub-wavelength range. A high lateral resolution is obtained with a Linnik interferometer, as depicted in fig. 2. The wavelength must be above $1.1 \mu\text{m}$ where silicon becomes transparent. In this setup, microscopic objective lenses are used with a numerical aperture of 0.65 and correction mechanics for spherical aberration caused by

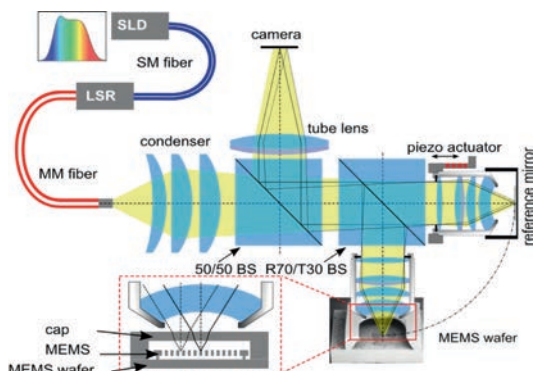


Fig. 2: Optical concept of the interferometer setup.

focusing through a slab of dielectric [3, 4].

A piezoactuator in the reference path is used for scanning the optical path difference and thus for detecting the LCI interferograms which are used for the calculation of the topography. Fig. 3(a) shows a first measurement and in fig. 3(b) a cross-section at some MEMS structures. The top surface of the fingers has a distance of about $45 \mu\text{m}$ to the background and the lateral structures are also resolved.

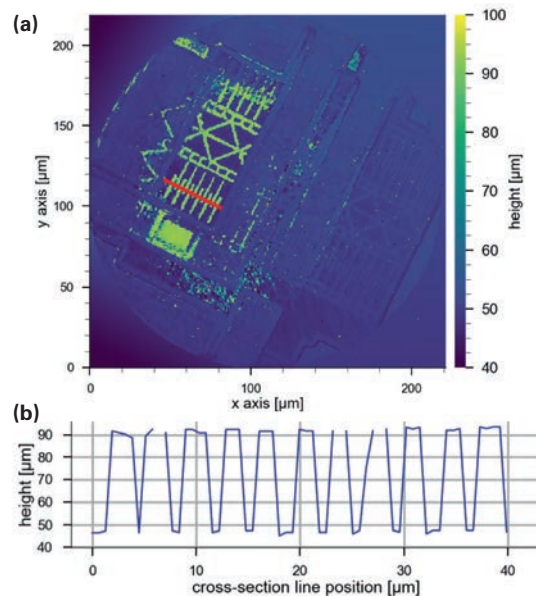


Fig. 3: (a) Topography measurement of MEMS with a cross-section in (b).

Supported by: BMBF – Project: IRIS

In cooperation with: Polytec GmbH, Robert Bosch GmbH, Cascade Microtech GmbH, Melexis GmbH, X-FAB MEMS Foundry GmbH, IMMS Institut für Mikroelektronik- und Mechatronik-Systeme gemeinsame GmbH, Fraunhofer-Institut für Elektronische Nanosysteme ENAS

References:

- [1] V. Lindroos, M. Tili, A. Lehto, and T. Motooka, Handbook of silicon based MEMS materials and Technologies. Oxford: Elsevier Science & Technology, 2010.
- [2] W. Osten, Optical inspection of microsystems. Boca Raton: CRC Press, 2007.
- [3] J. Krauter, M. Gronle and W. Osten, "Optical inspection of hidden MEMS structures" in Proc. of SPIE, 2017, vol. 10329-39.
- [4] J. Krauter, T. Boettcher, M. Gronle and W. Osten, "Low-coherence Interferometry for Industrial Applications", Proc. of AMA, 2017

Single-shot white-light interferometer design

R. Hahn, J. Krauter, K. Körner, M. Gronle, W. Osten

Nowadays, the fabrication of technical products faces the conflict of high-quality standards despite the increasing quantities. Therefore, fast and robust in-line inspection devices are needed. In addition to spectral interferometry, a well-known approach for high-resolution topography inspection is white-light interferometry (WLI). However, due to the need of a mechanical scan of the reference, the speed of signal acquisition is a strongly limiting factor for such devices. An improved version of WLI [1] is investigated based on a Linnik interferometer with reference path as shown in fig. 1.

This TFM introduces a constant lateral offset between the incident and reflected beam. This offset can be treated as a virtual field point leading to a tilted wavefront on the detector. The spatially modulated interferogram of the object and tilted reference wavefront can be observed along one axis of the camera (fig. 2). This is advantageous in comparison to the scanning WLI since the signal acquisition is done within one camera frame.

The geometry of the TFM shown in fig. 3 guarantees a stable frequency of the wavelets even if the mirror group is tilted or laterally displaced.

Due to this invariance and the single-shot approach, the device is dedicated especially for measurement tasks in rough and vibrating environments. By replacing the objective lenses with cylindrical lenses, the setup can be enlarged to a single-shot line sensor.

The current measurement range of the sensor is about $87\ \mu\text{m}$. With a more optimized TFM and a lower signal sampling, a measurement range greater than $500\ \mu\text{m}$ seems to be feasible. The interferometer is able to measure height differences smaller than $0.7\ \mu\text{m}$ and offers a positional standard deviation of less than $4\ \text{nm}$.

Limiting factors of the approach are the inhomogeneous illumination of the pupil plane and the low bandwidth of the light source. Especially, the inhomogeneous illumination leads to wrong height information if a phase precise evaluation [2] is applied. Once the illu-

mination is more homogeneous and the sensor is enlarged to a line sensor it turns out to be a powerful tool for in-line inspection tasks.

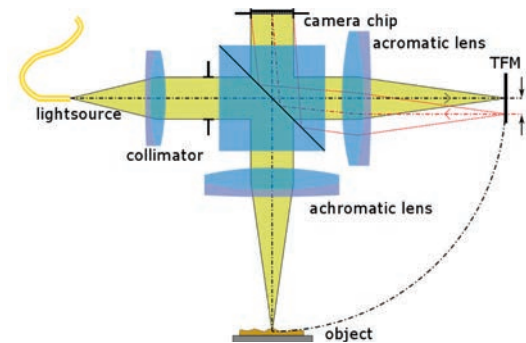


Fig. 1: Concept of the single-shot WLI. In the reference path a virtual field point is generated leading to a tilted wavefront in the observation plane.

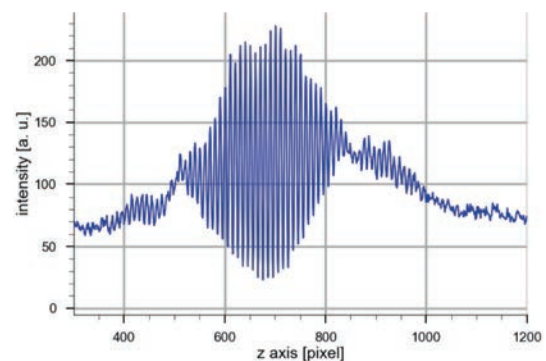


Fig. 2: Detected wavelet of one camera axis.

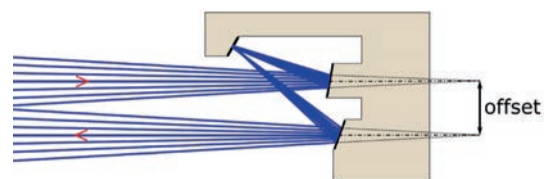


Fig. 3: Schematic drawing of the TFM. The Mirror has a size of $7 \times 7.5 \times 100\ \text{mm}$ and is milled out of monolithic copper part.

References:

- [1] Körner K, Berger R and Osten W, 2015, Method and arrangement for robust interferometry for detecting a feature of an object US Patent 8,934,104 B2.
- [2] Hahn R., Krauter J., Körner K., Gronle M., Osten W., "Single-shot low coherence pointwise interferometer with potential for in-line inspection", Measurement Science and Technology 28 (2017) 025009 (13pp).

Wafer-level optics for an OCT system

J. Krauter, M. Gronle, W. Osten

The European project VIAMOS proposes a new optical coherence tomography (OCT) system for skin cancer detection based on wafer-level optics. Wafer-level production leads to a reduction in the dimensions of the system, which improves handling and reduces system costs so that significantly more equipment can be distributed in clinics than current devices on the market which are large and expensive.

The basic detection concept of the system is the combination of swept-source OCT (SS-OCT) and phase shifting interferometry (PSI) in a miniaturized multi-channel system. A major part is the development of new micro-optics fabrication technologies, which are compatible with Micro-Opto-Electromechanical System technology (MOEMS). Each measurement channel is part of a 4 x 4 multi-channel objective lens in Mirau interferometer configuration as shown in fig. 1. The Mirau reference mirrors are mounted on a vertical scanner providing vertical displacement for the implementation of PSI.

The microlenses are made by glass melting in silicon cavities. First, the cavities of the silicon wafer are etched by deep reactive ion etching (DRIE). A glass wafer of Borofloat®33 is then anodically bonded to the cavity wafer. In a furnace with a temperature between 600 and 700°C the glass melts and after reaching the wanted lens-sag height it must be abruptly cooled down [1]. After polishing of the backside, a micro-lens array of plano-convex lenses is obtained. By bonding two of such microlens wafer together to a lens doublet, the imaging performance can be increased especially for off-axis field points [2]. A cross-section of the final micro-lens doublet array is shown in fig. 2.

The entire 4 x 4 Mirau micro-interferometer array consists of such a microlens wafer that is bonded to a reference mirror wafer, a spacer wafer and a beamsplitter wafer. The reference mirror wafer has vertical comb drive structures that implement PSI detection, resulting in an "active" Mirau interferometer in each measurement channel. A sta-

ble phase shift is introduced by a sinusoidal displacement in the range of hundreds of nm at a frequency of 500 Hz [3].

The overall project objective was the development of the introduced micro-optics OCT system, in which the ITO has designed the optical imaging and illumination system for the micro-optics [4]. In parallel, the ITO has built a similar on-bench OCT system for the proof of concept (Mockup) demonstration of the microsystem functionality [5]. This laboratory setup is operated with the same signal generation and evaluation in the same wavelength range but consists of bulk optics. In SS-OCT the signal detection happens in the Fourier-domain, which Fourier-transform represents the axial object structure (A-Scan). Since the signal is a real-valued spectral interferogram, the A-Scan after the transformation results in an object structure that is mirrored around a DC-peak. PSI techniques resolve the complex conjugate ambiguity and remove so the DC- and non-interferometric image artifacts. With this setup, a suppression ratio of the complex conjugate term of 36 dB and a system sensitivity greater than 96 dB was demonstrated [6]. In fig. 3 the measurement of an onion slide shows the feasibility to measure biological specimens. Here three layers are visible in a range of 200 µm. The imaging depth in this setup is limited due to the numerical aperture of 0.1.

The final VIAMOS microsystem functionality was demonstrated by imaging a varnish onto a painting [7] as shown in fig. 4.

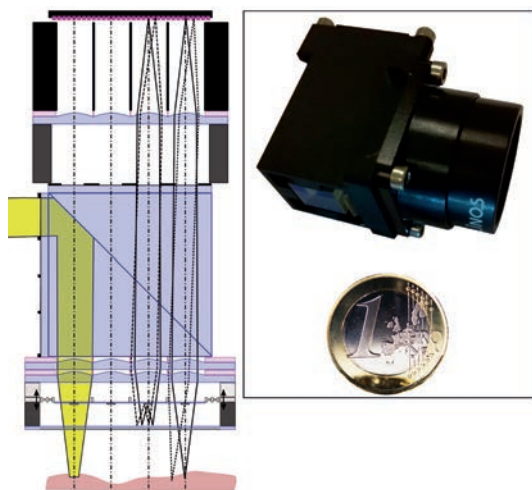


Fig. 1: Optical layout and photograph of the VIAMOS OCT system.

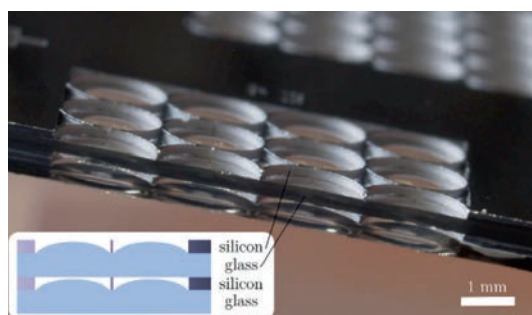


Fig. 2: Cross-section of the micro-lens doublet wafer.

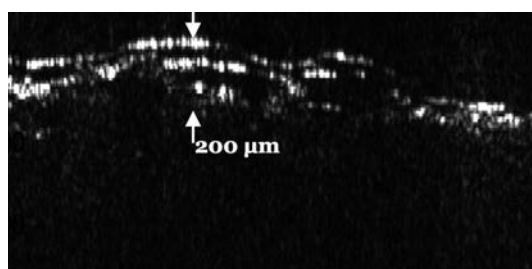


Fig. 3: B-Scan of an onion slide obtained by the on-bench OCT system.

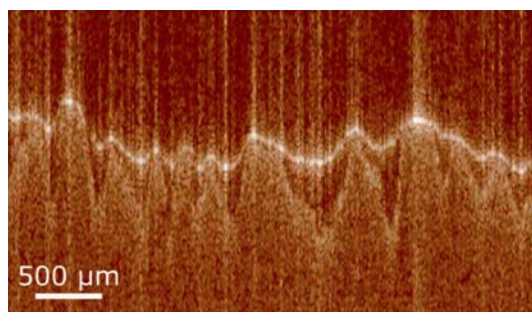


Fig. 4: B-Scan of a layer of varnish onto a painting obtained by the VIAMOS micro-system.

Supported by: EU (Call FP7-ICT-2011-8)

Project: VIAMOS (Grant agreement no.: 318542)

In cooperation with: Institut FEMTO-ST, VTT Technical Research Centre of Finland, Centre Suisse d'Electroique et de Microtechnique, Fraunhofer-Institut für Elektronische Nanosysteme ENAS, DermoScan GmbH, STATICE SAS, UFR Sciences Médicales et Pharmaceutiques, Centre Hospitalier Universitaire de Besancon, Centre National de la Recherche Scientifique

References:

- [1] Albero, J.; et. al. "Dense arrays of millimeter-sized glass lenses fabricated at wafer-level," *Optics Express* 23 (9), 11702–11712, 2015.
- [2] Albero, J.; et. al. "Wafer-level fabrication of multi-element glass lenses: lens doublet with improved optical performances," *Optics Letters* 41 (1) 96–99, 2016.
- [3] Lullin, J.; et. al. "An electrostatic vertical microscanner for phase modulating array-type Mirau microinterferometry," *J. Micromechanics Microengineering* 25 (11), 115013, 2015.
- [4] Krauter, J.; et. al., "Optical design of a Vertically Integrated Array-type Mirau-based OCT System," *Proc. of SPIE* 9132 (91320L), 2014.
- [5] Krauter J.; et. al. "Full-field swept-source optical coherence tomography with phase-shifting techniques for skin cancer detection," *Proc. of SPIE* 9529 (952913), 2015.
- [6] Krauter, J.; et. al. "Performance analysis of a full-field and full-range swept-source OCT system," *Proc. of SPIE* 9576 (957609), 2015.
- [7] Perrin, S. "Development and characterization of an optical coherence tomography micro-system," Université de Franche-Comté, 2016.

Simultaneous single-shot measurement of topography and refractive index of layered specimen

T. Boettcher, M. Gronle, W. Osten

In precision manufacturing, the workpiece usually has to be cleaned before inspection, since contaminations like machining fluids distort the measurement of the specimen's topography, especially if an unknown refractive index of the contamination layer cannot be corrected. Similar situations occur in measurements of varnish layers or thin materials. There are some systems reported that enable simultaneous measurements of a layer's refractive index and its thickness without prior knowledge, mostly based on confocal microscopy and/or spectral interferometry. However, all of them require transparent specimens or sophisticated signal modeling, lack single-shot capability, or use very complex experimental setups.

By combining chromatic confocal microscopy and an interferometric scheme very similar to Fourier domain OCT, we gained a new measurement method, we call Chromatic Confocal Coherence Tomography (CCCT). With this, we aim for single-shot simultaneous measurements of refractive index and thickness/layer topography of specimens featuring semi-transparent layers, which may also be located on top of opaque objects.

The basic idea of this concept is to make use of the fact, that the refractive index of a layer effects the thickness measurement in different ways when using confocal or interferometric schemes respectively. Interferometric measurements overestimate the geometric thickness d by the refractive index n , as they measure the optical thickness d_{wave} :

$$d_{wave} = d \cdot n \quad (1)$$

On the other hand, confocal systems gain the value d_{conf} , an underestimation of d by n and a correction factor depending on the numerical aperture NA of the used objective, as can be seen from Fig.1:

$$d_{conf} = \frac{d}{n} \cdot \frac{\sqrt{1-NA^2}}{\sqrt{1-\left(\frac{NA}{n}\right)^2}} \quad (2)$$

The combination of eq. (1) and (2) gives a fourth-order polynomial, which has only one real-valued positive solution. Hence, it is possible to evaluate both, layer thickness and refractive index simultaneously, if confocal and interferometric information is available.

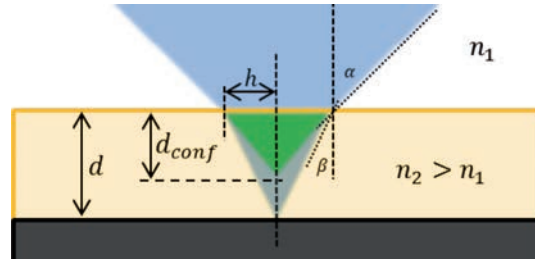


Fig. 1: Refraction at semi-transparent surface. Confocal schemes underestimate the actual layer thickness.

Experimentally, we achieve a single-shot simultaneous measurement by using a CCCT setup [1], providing decoupled confocal and interferometric channels resulting in a signal as shown in Fig.2.

First proof-of-concept measurements were conducted on a range of fused silica and diamond samples of different thicknesses. Although we still identified some potential for improvements, the results were quite promising with derivations of less than 3% with respect to the nominal values of thickness and refractive index [2].

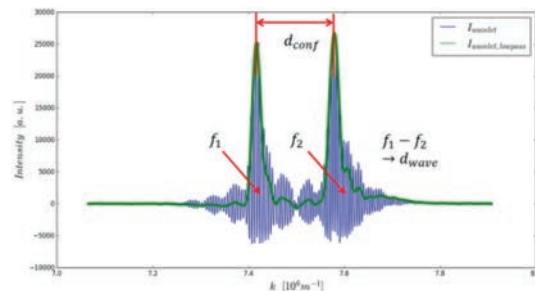


Fig. 2: CCCT signal of a 50µm fused silica sample. The distance of the two envelope peaks is corresponds to the thickness measured by the confocal channel, while the difference of the peaks' respective wavelet frequencies is the interferometrically measured thickness.

Supported by: DFG German Science Foundation
Project: Hochaufgelöste Single-Shot-Vermessung von semitransparenten Schichten mittels Chromatisch-Konfokaler Kohärenz-Tomographie (CCCT) (OS 111/47-1)

References:

- [1] Boettcher, T.; Lyda, W.; Gronle, M.; Mauch, F.; Osten, W. „Robust signal evaluation for Chromatic Confocal Spectral Interferometry“, Proc. SPIE 8788, 2013.
- [2] Boettcher, T.; Gronle, M.; Osten, W. „Multi-layer topography measurement using a new hybrid singleshot technique: Chromatic Confocal Coherence Tomography (CCCT)“, Opt. Ex., 25(9), 2017.

Adaptive chromatic confocal spectral interferometer

D. Claus, M. Gronle, W. Osten

Optically based methods such as white light interference microscopy or confocal microscopy are increasingly applied in surface metrology due to their contactless measurement principle combined with high lateral and axial resolution. Both methods rely on a mechanical scan in order to obtain depth information of the object under investigation.

Chromatic confocal microscopy (CCM) in combination with a short-coherent light source (broad spectrum) and a spectrometer offers a non-scanning approach to access depth information of an object point. Likewise, a swept source can be employed, which offers the advantage of reduced acquisition time. This is due to the fact that the wavelength can be selected to obtain an in-focus object point. By means of chromatic confocal spectral interferometry (CCSI), the axial resolution can be increased while maintaining the same field of view. However, in order to cover the entire field of view, the object has to be scanned by either an x-y stage attached to the object or orthogonal galvanic mirror pairs. Some applications may require a more flexible approach where only certain object points of interest are scanned. This can be realized via the application of fast-switching optical elements such as a digital mirror device (DMD), which is particularly well suited for CCSI since it does not exhibit chromatic dispersion effects as in the case of a LCoS. Therefore, a swept source CCSI sensor in combination with a DMD for scanning the field of view has been developed. The challenge of the proposed system in comparison to a point CCSI sensor exists in delivering a diffraction-limited resolution over the entire field of view and over the entire wavelength range (depth range). Based on the optomechanical design a setup has been configured, shown in fig. 1. A collimated laser beam emitted from the swept source (820 nm–870 nm with 0.05 nm spectral resolution) hits the DMD, only the on-state pixels are imaged on the object, while the light from the off-state pixels is deflected and does not enter the entrance pupil of the object illumination system. The on-state light enters a Linnik interferometer with a diffractive element mounted in front of the microscope objective (Olympus LCPLN20XIR Objective) to enable chromatic depth separation. The field of view of our system is $1.6 \times 1.6 \text{ mm}^2$ with

a lateral resolution is $1.25 \mu\text{m}$, the depth scan ranges from $-23 \mu\text{m}$ for 820 nm to $23 \mu\text{m}$ for 870 nm. A typical scan over the entire wavelength range is shown in Fig. 2 for an object point at a certain depth position. The depth position has then been changed via the application of a piezo mounted mirror so that the relationship between wavelength applied at the swept source and the z-position could be established. The experimental findings are shown in Fig. 3, which indicate that a good agreement between the experimental and theoretical findings has been obtained.

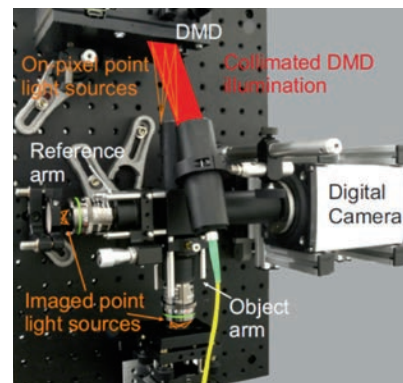


Fig. 1: Linnik based CCSI setup with illumination and imaging optics.

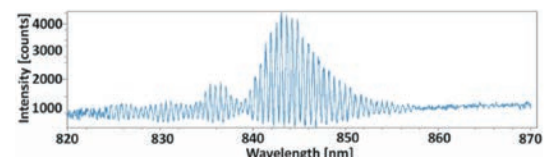


Fig. 2: CCSI Signal for a single pixel on the digital camera while scanning the different wavelength (x-axis).

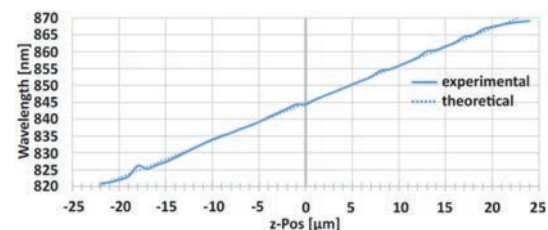


Fig. 3: z-position obtained from centre of gravity of coherence envelope, as shown in Fig. 2 for only one position.

Supported by: AdaScope
(Landesstiftung Baden-Württemberg)
In collaboration with: Fraunhofer IOSB in Karlsruhe

References:

- [1] Claus, D.; Böttcher, T.; Osten, W. "Hybrid optical design for a wide field chromatic field chromatic confocal scanning interferometry", DGAO Proceedings Dresden, 2017.

Dynamic referencing of coordinate measurement and tooling machines

M. Gronle, T. Haist, W. Osten

For the high precision control and positioning of coordinate measurement and tooling machines it is usually not sufficient to only measure the individual positions of all axes. Especially for the case of dynamic movements, inaccuracies will occur. On the one hand, static positioning errors are induced by manufacturing imperfections or adjustment errors. These can be corrected using calibration routines. On the other hand, dynamic and kinetic errors mainly occur due to fast movements and generate bending moments or dumping of the axes.

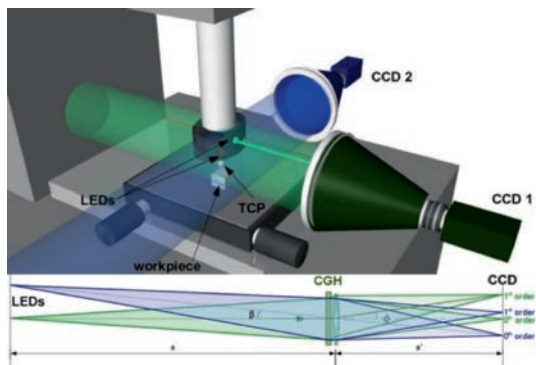


Fig. 1: Scheme of the holographic multipoint tracking sensor.

The goal of the project “DynRef”, that has been worked out in cooperation with the Institute of System Dynamics (ISYS), is the development of a high-precision controller for low positioning errors under fast and dynamic movements. However, this controller can only be operated if precise position information of the tool or sensor of the device is available. A simple, low-cost but also accurate optical sensor concept is depicted in fig. 1. The objective is a fast tracking of a LED marker, attached to any moving body. The spot of this LED is then observed by a default industrial camera. However, by applying a center of gravity evaluation, subpixel precision in the range of 1/10 to 1/100 of a pixel can be obtained. In order to highly increase this accuracy, a hologram is placed in front of the sensor, such that the spot of one LED is divided into 16 single spots on one sensor. In fig. 2, the horizontal position of the center of gravity of three exemplary sub-spots is depicted, where the LED has been moved by up to 100 mm. Hereby, the real position of the marker is contained in every spot position whereas the

noise as one limiting part of the overall precision follows a statistical independent distribution. By taking the mean value of all spot positions, noise as well as erroneous sinusoidal effects, due to the pixelated detector, is filtered out, such that the overall signal to noise ratio can be highly increased with respect to one single spot detection. In the depicted example, the RMS-error after averaging over 14 spots is 0.0028 px in contrast to a value of 0.010 px of a single spot evaluation. This improvement is close to the theoretical value of the square root of the number of averaged values.

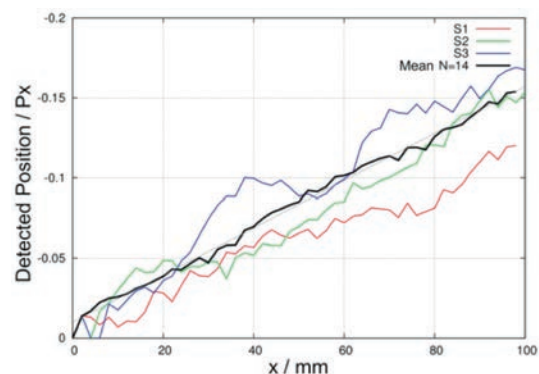


Fig. 2: Position measurement of three exemplary sub-spots and the averaged value over all 14 spots.

Supported by: DFG Os 111/42-1

Project: DynRef

In cooperation with: Institut für Systemdynamik (ISYS)

References:

- [1] Haist, T.; Dong, S.; Arnold, T.; Gronle, M.; Osten, W. “Multi-image position detection”, *Opt. Express* 22(12), 14450-63 (2014).
- [2] Haist, T.; Gronle, M.; Bui, D.A.; Osten, W. “Holografische Mehrpunktgenerierung zur Positionsanalyse”, *TM – Techn. Mess.* 82(5), 273-279 (2015).
- [3] Haist, T.; Gronle, M.; Bui, D.A.; Jiang, B.; Pruß, C.; Schaal, F.; Osten, W. „Towards one trillion positions”, *Proc. SPIE 9530*, 9530-03 (2015).
- [4] Haist, T.; Gronle, M.; Arnold, T.; Bui, D.A.; Osten, W. “Verbesserung von Positions-bestimmungen mittels holografischer Mehrpunktgenerierung”, in: *Forum Bildverarbeitung 2014*, F. Puente León, M. Heizmann (Hrsgb.), KIT Scientific Publishing, 239-247 (2014).

Intelligent optical sensor for the 2D and 3D surface measurement and inspection

M. Gronle, T. Haist, W. Osten

The objective of this project is the realization of a new and cheap sensor system for a precise, fast and flexible 2D and 3D inspection of technical objects. The system, whose optical scheme is depicted in fig. 2, is based on a triangulation sensor whereas the illumination contains two different optical measurement principals:

On the one hand, the geometry of the object, whose ideal model is considered to be known before the measurement, is verified by projecting object-adapted fringes onto the specimen using a LCOS-based projection system and a green LED (fig. 1). The fringe pattern is then analyzed by a new realization of a cheap telecentric lens. This fringe projection mode is visualized in the scheme in fig. 2 by the blue projection and green detection path.

On the other hand, coherent light from a secondary laser source (532 nm) is modulated by the same LCOS such that single spots can be projected with high precision at desired locations of the object (red path of fig. 2). Their positions are then evaluated by the same telecentric objective. Using this mode, precise height measurements of distinct parts of the object under inspection are possible. In order to avoid disturbing speckle due to the coherence illumination, the incident wavefront is slightly varied such that averaging over several images will reduce the impact of the statistically uncorrelated speckles.

The hybrid telecentric objective lens is a cost-effective realization of a double telecentric imaging system for large object fields. Two small off-the-shelf lenses and one large diffractive optical front element (DOE) are used in combination to achieve a small telecentricity error. Due to this DOE, its spectral bandwidth is rather limited, inducing chromatic aberrations especially when using the LED illumination. To overcome this problem, a special camera is developed by the institute of parallel and distributed systems (IPVS) of the University of Stuttgart. It is equipped with a special FPGA board that allows executing an online deconvolution of the aberrated images to remove these chromatic errors.

The overall objective of this project is to realize a fast inspection of parts with a measurement field of up to 100 x 100 mm² and a resolution of 100 µm using the fringe projection mode.

Supported by: Baden-Württemberg Stiftung

Project: IOS23

In cooperation with: IPVS, University of Stuttgart.

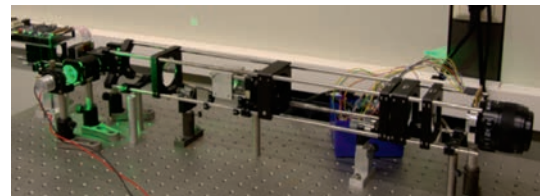


Fig. 1: Optical setup of the illumination of the fringe projection mode.

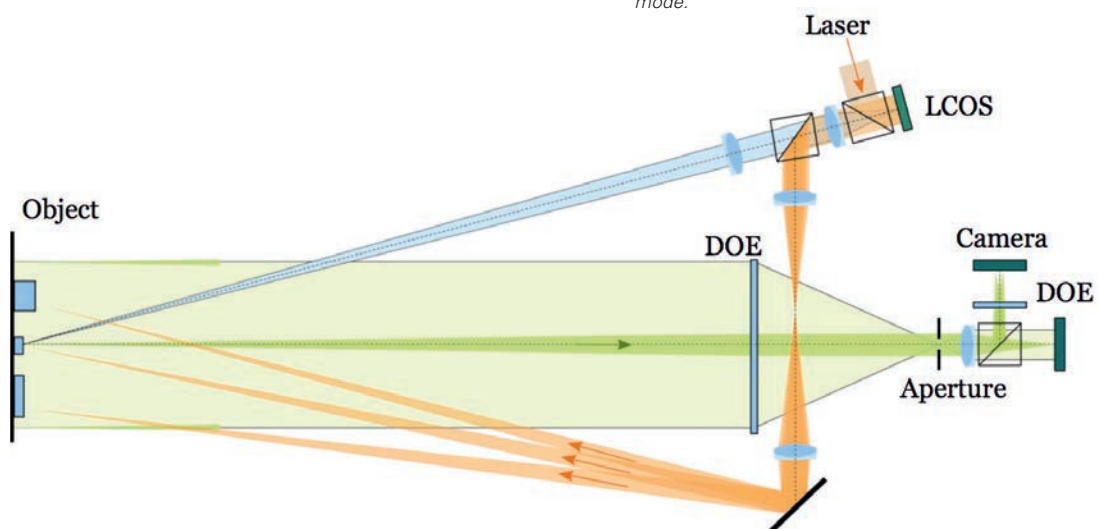


Fig. 2: Scheme of the optical setup: The object-adapted fringes are projected via the blue path, precise multi-point measurements are generated by the red path and all projections are recorded and analyzed by a telecentric objective (green path).

Comparison of various microscopic 3d measurement techniques for roughness and surface evaluation

M. Gronle, T. Boettcher, K. Körner, W. Osten

With respect to tactile sensors or AFM-based techniques, optical measurement techniques show the great advantage of high measurement productivity. This holds also for pointwise measuring devices like chromatic confocal sensors with fast linear stages. However, the benefit is clearer visible in case of area-measuring 3d sensors like confocal microscopy, white-light interferometry (WLI) or focus variation microscopy. The high measurement productivity of optical measurement techniques is indispensable for in-line manufacturing. For high-tech products with special surface profiles, traceable surface properties like the line roughness parameters R_a , R_q and R_z are strong sales arguments.

For a round-robin comparison of state of the art measurement sensors, the surface of different fine-processed samples was firstly evaluated by means of different optical devices for measurement of topography, and secondly by an AFM-based microscope as well as a tactile sensor for reference. In all cases, the above mentioned relevant roughness parameters were calculated.

For a correct evaluation according to the standard DIN EN ISO 4288, an estimate of the expected roughness parameters and its surface characteristics have to be known in advance. From this the required measurement length and cut-off wavelength can be derived. Furthermore, the standard DIN EN ISO 3274 defines the maximal sampling distance of the profile measurement. For instance a roughness of $R_a = 0.3 \mu\text{m}$ yields a

measurement length of 4.0 mm and a maximal sampling distance of $0.5 \mu\text{m}$. Appropriate optical profile measurement techniques and commercially available devices have been chosen that fit these requirements. Hereby, both the axial resolution as well as the sampling distance is no limiting factor. However, the required measurement length of few millimeters often requires stitching of separately acquired measurement fields (if area-measuring sensors are used). In an example, up to 17 single measurements are required for a 50x objective. For the round-robin test, sensors of the following classes have been used: scanning confocal microscopy with a numerical aperture (NA) of 0.8, WLI with an NA of 0.55 limited by the Mirau-lens und focus variation microscopes (NA 0.8 or 0.9).

Fig. 1 shows exemplary topography measurements of one test specimen acquired with different optical sensors that are commercially on the market. The measurement systems are hereby based on the previously described measurement principles. As far as possible, only the raw, unfiltered topography information is exported from the devices. The data processing, visualization, and roughness evaluation are afterward done using the open source software *itom*. All measurements have been analyzed by identical methods under consideration of the standards DIN EN ISO 4288 and DIN EN ISO 3274.

The results have also been compared to the reference values, obtained by a tactile as well as an AFM-based sensor system. The

sample under test has a Ra value of $0.32\ \mu\text{m}$ (tactile) and $0.33\ \mu\text{m}$ (AFM). The results of the single optical sensors lie within a similar range ($\pm 10\%$ of the reference value), but obviously, the measured topography representation looks very different. As an example, the density of valid data points obtained by the original data sets varies from sensor to sensor (e.g. see the results from the confocal microscope 1 in comparison to the focus variation 2). Furthermore, the lateral resolution of the measurement results seems to be quite different as it can, for instance, be seen

from the measurements of focus variation 1 with respect to WLI 1 or WLI 2. Although the focus variation sensor was equipped with the highest numerical aperture, its resulting lateral resolution appears to be much lower than the one from the white-light interferometer. All in all, it can be seen that clearly different topographies (amplitude values) might lead to very similar roughness results.

As a consequence, roughness parameters derived from partly incorrect surface profiles have to be assessed more carefully.

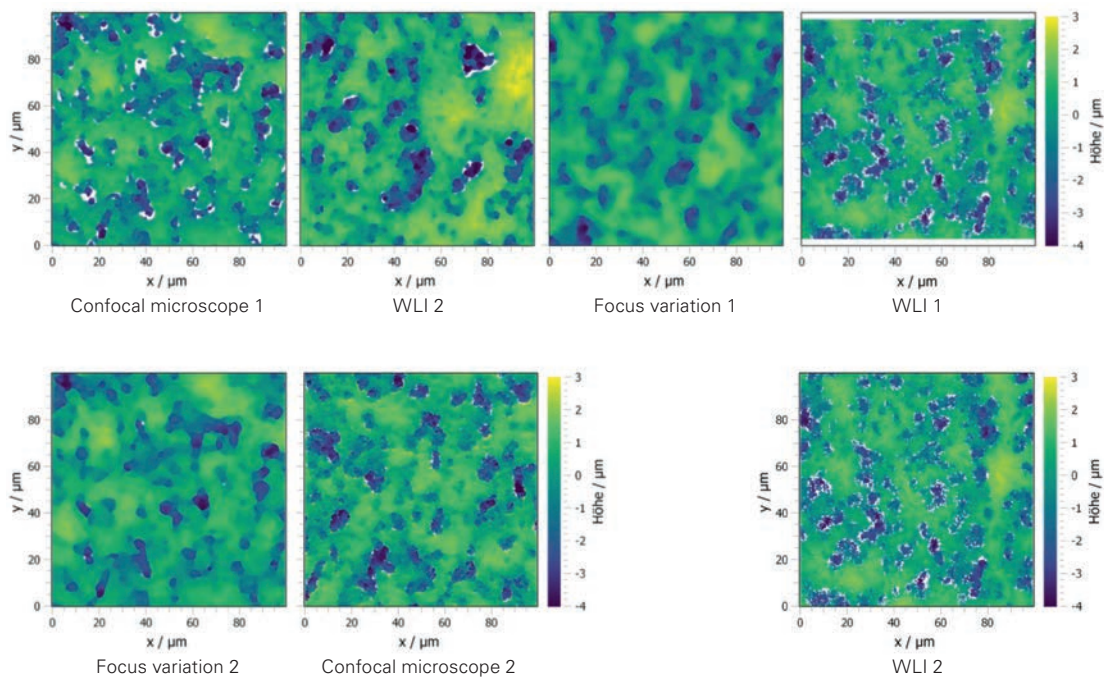


Fig. 1: Topography measurements of one specimen using different optical sensor systems.

The project was supported and performed in cooperation with Walter Maschinenbau GmbH.

Simulation of microscopic metal surfaces based on measured microgeometry

H. Yang, T. Haist, M. Gronle, W. Osten

One challenging part of the development of machine vision processes for automated visual inspection is the lack of sufficient training data of images of expected defects under various illumination conditions and view directions. Additionally, the amount of required training data increases with the number of different objects and surface variations.

To overcome this problem, it is possible to adjust and optimize inspection systems based on virtual, synthesized images instead of the real ones. However, if one compares the creation of such synthesized images with virtual scenes created for human eyes, it is necessary to provide very realistic images for image processing algorithms instead of “nice” visualizations only. Therefore, it should render the whole scene in an accurate way according to the physical phenomenon. The crucial issue of the synthesized image is dealing with the scattering properties of the rough surfaces. Therefore, the most common BRDF method, which is widely used in computer graphics, is not the suitable tool for simulating microscopic metal surfaces, since it does not provide any concrete information in the interesting area.

The goal of the work is find out an efficient and accurate rendering method for synthesizing the appearance of microscopic metal surfaces, which can be used as training data for surface inspection systems. The wave

optical methods, such as RCWA, FDTD..., provide the rigorous results, but their computational effort is quite high. Therefore, we applied and compared ray tracing and two scalar diffraction approximation methods, thin element approximation and local plane interface approximation method. In the simulation, the geometry of the metal surfaces are using the data, which are measured by a microlens and Nipkow Spinning disk confocal microscope.

In raytracing method, each microfacet is treated as a tilted flat mirror surface and the reflectance at each microfacet is calculated by applying Fresnel equations [1]. Fig. 1 indicates the high similarity between the simulated image and realistic image by using ray tracing method.

In scalar diffraction approximation methods, they can provide accurate diffraction pattern, only if the sample is thin enough. When the sample contains high deviation of the surface roughness, these methods are not valid any more [2].

Further work will focus on the rigorous wave-optical method combined with the angular spectrum method for synthesizing the images of arbitrary metal surfaces in the microscale range. Also it is planned to simulate the BRDF [3] of the surfaces based on the measured microgeometry.

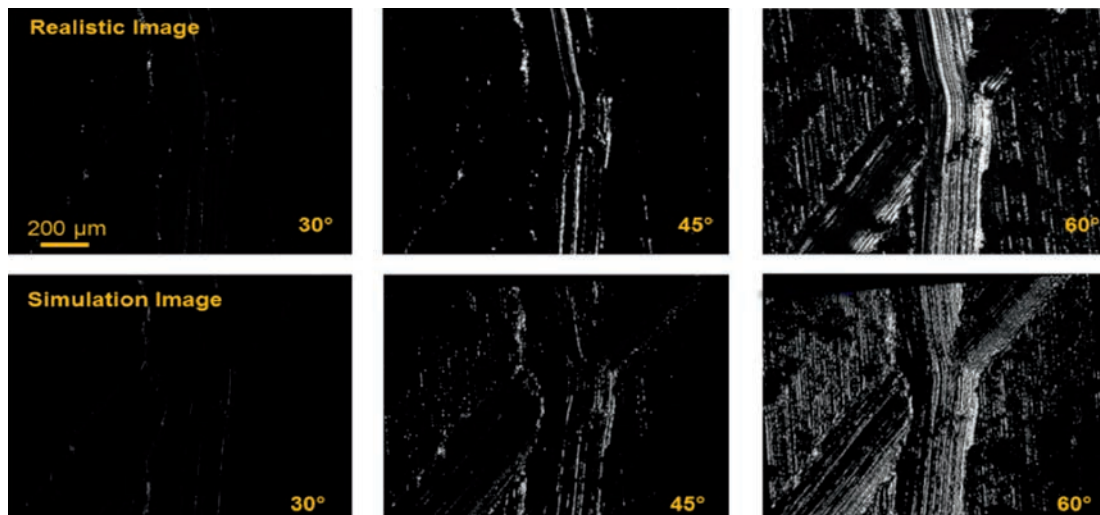


Fig. 1: Real image captured by camera and simulation results for scratch on stainless steel under three different incident angles with 30°, 45° and 60°.

Supported by: Graduate School of Excellence advanced Manufacturing Engineering (GSaME), University of Stuttgart.

References:

- [1] Yang, H.; Haist, T.; Gronle, M.; Osten, W. „Realistic simulation of camera images of micro-scale defects for automated defect inspection“, In Forum Bildverarbeitung 2016, page 63. KIT Scientific Publishing, 2016.
- [2] Yang, H.; Haist, T.; Gronle, M.; Osten, W. „Simulation of microscopic metal surfaces based on measured microgeometry“, tm - Technisches Messen, Vol.2, Pages 6, 2017.
- [3] Yang, H.; Haist, T.; Gronle, M.; Osten, W. „Simulated BRDF based on measured surface topography of metal“, SPIE Metrology, Paper 10334-4, 2017.

Open source measurement and evaluation software itom 3.0

M. Gronle, H. Bieger, R. Hahn, J. Krauter, W. Osten

itom is an open source software suite for operating measurements systems, laboratory automation, and data evaluation. Its development has been started at ITO in 2011 in order to provide a software that can easily be used to control optical setups, create and execute data evaluation algorithms in Python and/or C++, communicate with hardware components or easily create individual user interfaces.

The software (fig. 1) has been designed considering various requirements: On the one side, it should be used by non-experienced users to easily create an experimental setup in a lab and

If desired, users can also build their individual user interfaces with a huge set of different widgets including the itom specific plots and figures. While the design process is done in a WYSIWYG design tool, the interaction is added via Python methods. This allows creating modern and complex windows and dialogs in order to simply the operation of systems.

In the period under report, the functionality of itom has been continuously extended to provide a user-friendly software interface as well as a flexible and fast development and operating tool. Until now, more than 70 different plugins for various hardware components and algorithms have been created and published. For instance, the unified camera interface allows operating cameras from PointGrey, Ximea, Allied Vision, SVS Vistek, PCO, QImaging, Andor or IDS Imaging among others. Additionally generic plugins for DirectShow, GenICam or Microsoft MediaFoundation provide an access to a high number of other cameras.

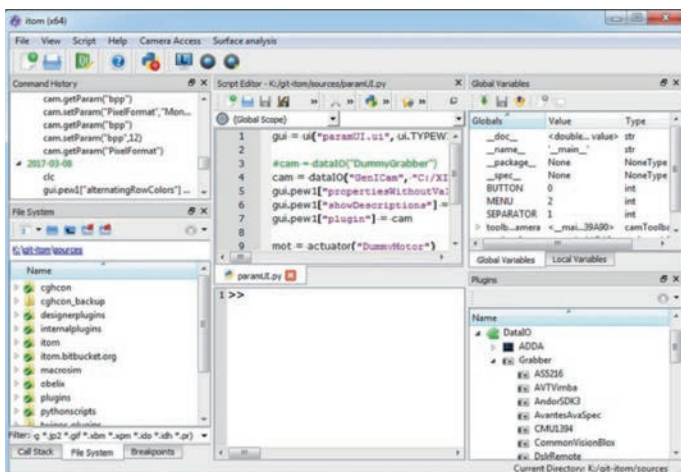


Fig. 1: Screenshot of the main window of itom.

control cameras, displays or actuators. On the other side, the software has to be able to operate high-speed and complex measurement systems. While the rapid prototyping is provided by the fully integrated Python scripting language, performant algorithms, and hardware connections can be added via a unified plugin interface. Hardware and software plugins are written in C++ and can integrate arbitrary 3rd party components as well as CUDA or other parallelization techniques.

Besides the operation of hardware systems, itom can also be used for data evaluation purposes. Therefore it provides many algorithm plugins, can benefit from the wide range of Python packages and allows plotting data in multiple dimensions. These plots (fig. 2) are mainly adapted to the evaluation of measurement data.

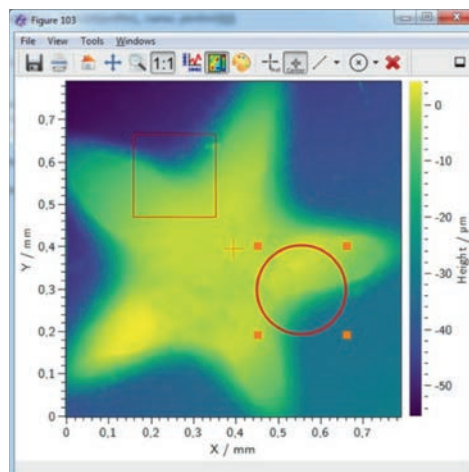


Fig. 2: The 2d plot of itom shows the topology of a euro coin.

The core application of **"itom"** is released under the open source license LGPL. The sources as well as setups for Windows can be freely downloaded under

<http://itom.bitbucket.org>.

References:

- [1] Gronle, M.; Lyda, W.; Wilke, M.; Kohler, C.; Osten, W. "itom: an open source metrology, automation, and data evaluation software", *Appl. Opt.* 53, 2974-2982 (2014).

Active Optical Systems and Computational Imaging



Theoretical and experimental investigations concerning the influence of coherent noise on the resolution of data measured with triangulation sensors	40
--	----

Supported by: Landesstiftung Baden-Württemberg

Project: IOS23

In cooperation with: IPVS, University of Stuttgart.

New setup for the characterization of image sensors with respect to fixed-pattern noise	42
--	----

Versatile setup for testing phase retrieval methods	44
---	----

Post-processing for the compensation of chromatic aberrations in programmable microscopy	45
---	----

Theoretical and experimental investigations concerning the influence of coherent noise on the resolution of data measured with triangulation sensors

S. Haberl, M. Gronle, T. Haist, W. Osten

Active triangulation on rough surfaces is fundamentally limited by speckle noise. Especially for laser-based methods speckles will lead to a strong uncertainty in height measurements. Dorsch and Häusler clearly explained and analyzed the (conventional) situation where the numerical aperture of the illumination of the surface under test is lower than for the imaging onto the image sensor [1]. This situation is common for typical systems using scanning lasers points or scanning lines ("Lichtschnitt"). The other option is to use a comparatively lower numerical aperture for the imaging.

For all such speckle-limited measurement systems the typical approach is use some kind of temporal averaging to finally reduce the speckles. To this end we investigated the use of dynamic computer-generated holograms written into a spatial light modulator (here: Holoeye TN-LCD, 800 x 600 pixels). By this approach it becomes possible to directly program the wavefront of the illuminating spot of a triangulation sensor. Also, the position of the spot can be very accurately changed. Different patterns have been tested by simulation and experiment.

It turned out that for the conventional geometry (numerical aperture of illumination low) the speckle-based uncertainty can only be reduced by a small amount (approximately 20 to 30 %). However, for the case with the low numerical aperture of the imaging strong improvement is possible by using a micromovement of the illuminating spot (within the area of the diffraction limit of the imaging). This indeed is expected because different microstructures are illuminated leading to

different (uncorrelated) speckles. This way, the statistical measurement uncertainty has been reduced by a factor of three using the average of ten recordings.

Apart from micromovement, different other wavefront changes in the Fourier plane have been investigated. Zernike polynomials as well as doughnut wavefronts with different integer and non-integer phase dislocations are also possible.

Fig. 1 shows the setup used for testing the improved triangulation. Fig. 2 shows measurement curves for the linear axial translation of a plane object using a piezo stage. Obviously, the micromovement method with ten times averaging considerably improves the statistical measurement uncertainty. In the future the method might be used also in combination with a rotating static computer-generated hologram. Additional errors due to the discretization of the image sensor might be eliminated using a multipoint imaging optics [2].

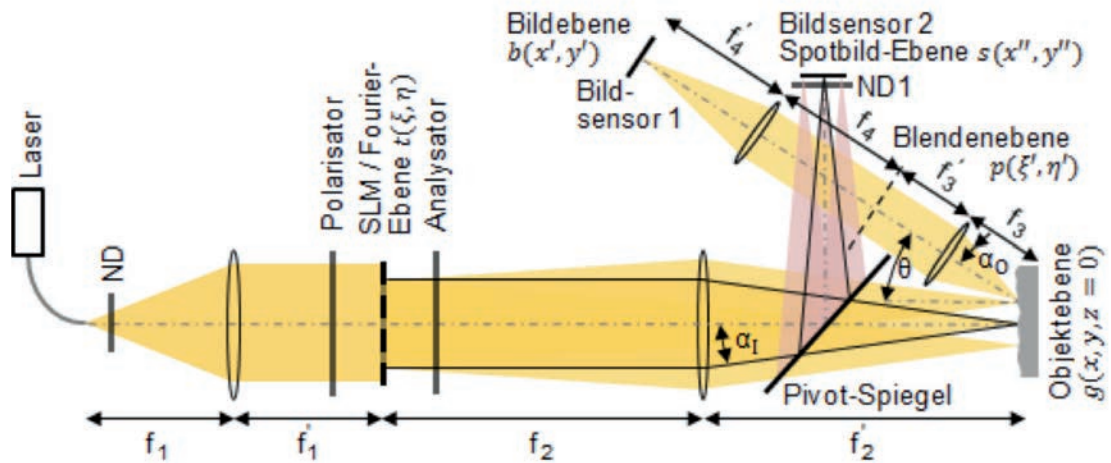


Fig. 1: Experimental setup for testing the reduction of statistical measurement uncertainties.

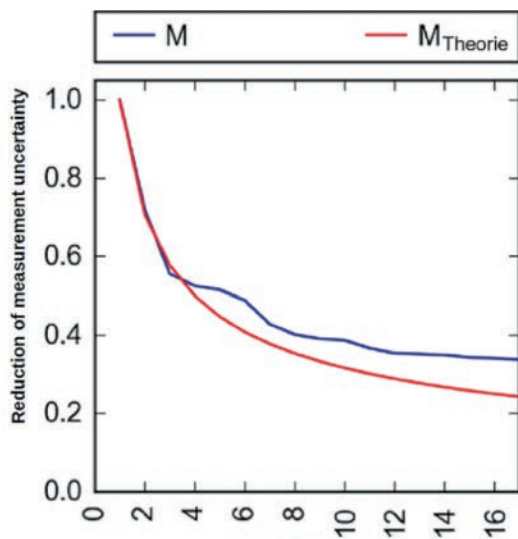


Fig. 2: Reduction of measurement uncertainty of triangulation spot for axial displacement of the test surface with conventional imaging and under different amounts of averaging using micromovements.

Supported by: Landesstiftung Baden-Württemberg
Project: IOS23
In cooperation with: IPVS, University of Stuttgart.

References:

- [1] Dorsch, R. G.; Häusler, G.; Herrmann, J. M. "Laser triangulation: fundamental uncertainty in distance measurement." *Applied Optics* 33.7 (1994): 1306-1314.
- [2] Haberl, S. „Untersuchungen zur Reduktion von Speckle-Rauschen durch räumliche Lichtmodulation in der optischen Messtechnik“, Masterarbeit Institut für Technische Optik, Universität Stuttgart 2017.

New setup for the characterization of image sensors with respect to fixed-pattern noise

T. Haist, J. Barth, Q. Duong-Ederer, W. Osten

Fixed-pattern noise is – especially for CMOS-based sensors – one of the main noise contributions for image sensors. Whereas time dependent noise, e.g. dark current noise, photon noise, read-out noise, can be always reduced by averaging over many frames, the spatial noise contributions are not so simple to eliminate. Especially at high light levels, the so-called photo-response non-uniformity (PRNU) considerably limits the achievable signal-to-noise ratio and, therefore, the achievable measurement accuracy for different image-sensor based measurement techniques. At low-light levels, on the other hand, dark signal non-uniformity (DSNU) is the major contribution.

Of course, the sensor manufacturers already include dedicated circuits and look-up tables to individually correct the responses of the respective pixels. However, since the behavior depends on a lot of factors (e.g. wavelength, exposure time, temperature etc.), complete calibration for all applications is not possible.

We realized a setup for measuring PRNU and DSNU based on a Fourier geometry with a rotating diffusor. Compared to the standard characterization setup as proposed in the leading standard EMVA1288 [1], a better light efficiency is achieved. Also problems due to possible straylight/reflections on the sensor housing is reduced and sensor-sided telecentricity is achieved.

The setup is depicted in fig. 1. The rotating diffusor is located in a Fourier plane of the sensor. Therefore, imperfections of the diffusor (dirt, scratches etc.) will be distributed evenly on the whole sensor and, therefore, will not disturb the measurement.

Within the measurement procedure (implemented in ITOM) every frame is recorded 100 times to average out temporal noise contributions. A very stable fiber-coupled thermal light source has been used in combination with different 10 nm bandpass filters to measure the behavior of three sensors (PCO edge 3.1 scientific CMOS), Point Grey GS3-U3-23S6M-C (Sony IMX 174) and Ximea XiQ MQ013MG – E2). All sensors achieved quite good results for PRNU with the PCO edge and the Sony sensor achieving results below 0.3 %. For the DSNU, as expected, the scientific CMOS sensor of the PCO edge resulted in exceptionally high quality with DSNU values below the measurement uncertainty of our measurement setup.

Temperature dependence of DSNU for the non-cooled sensor was as expected (strongly increasing DSNU) with temperature. Also, as expected, especially for small F-numbers pollution of the cover plate of the sensor increases the PRNU.

Fig. 2 shows a typical output of the characterization software where the PRNU is shown for every column of the image sensor. In addition, maximum and minimum values for the deviations are shown and a histogram of the deviations are rendered in the background.

Versatile setup for testing phase retrieval methods

C. Lingel, T. Haist, W. Osten

Meanwhile there is a bunch of different phase retrieval approaches available. In this project we have developed a benchmark system and a corresponding optical setup for testing the performance of different phase retrieval methods. Therefore, we are using a spatial light modulator (SLM) in the optical path for adaptively changing the characteristics of the setup. Doing so, we are able to use the setup for testing different phase retrieval methods and their parameters without any mechanical changes. Thereby, the user is supported with respect to the task-dependent selection of the most suitable phase retrieval method.

Usually, for measuring the phase of an object, an interferometric measurement setup is utilized. Beside interferometry of holography which need some reference wave for determining the phase, there are also methods which do not have the necessity of a second interfering wave. These phase retrieval methods often use multiple images and a corresponding algorithm for calculating the phase.

Because there are many different phase retrieval methods and their performance strongly depend on the phase object itself and some method specific parameters it is important to compare different methods for a given object. Therefore, we introduced a benchmark system, for objective judging of the methods [1]. Next to the pure simulation based benchmark, a practical implementation is important to verify the simulation results. Thus, we built a microscopic setup including an SLM for easy and fast parameter changing, see fig. 1. We insert a rotating diffuser in the illumination path for speckle reduction and by moving the laser in z-direction we can control the grade of coherence. After the phase object we image it via a microscopic objective and a tube lens onto on half of the SLM in the intermediate image plane. There we can manipulate the object using for example some phase masks. After that the object is imaged onto the camera by a telescope where the second half of the SLM is placed in the Fourier plane, where we can correct aberrations or introduce some defocus by writing in some Zernike polynomials.

In fig. 2 an example measurement result is depicted. There we used the transport of intensity equation (TIE) method for retrieving the

phase of a phase USAF target [2]. This method is based on the intensity measurements of different defocused images and the main parameters which have to be adjusted are the Δz between the defocused images and the number of the images. The different z positions of the images can be achieved by writing different defocus holograms in the SLM and so we can run the measurement with many different parameters for finding the optimal settings. In this case we used 43 defocused images with $\Delta z = 2 \mu\text{m}$.

In conclusion, we developed a SLM based adaptive phase retrieval setup which is suitable to measure phase objects with different methods and parameters by proper hologram settings.

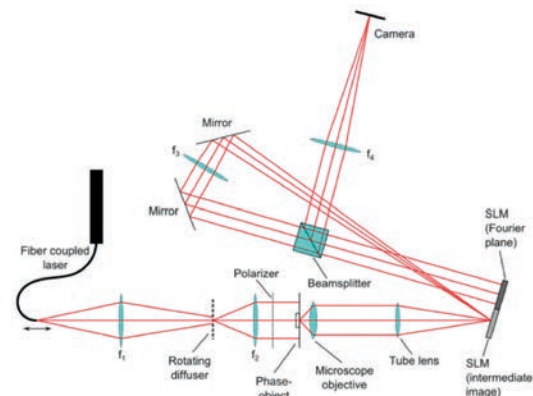


Fig. 1: Microscopic Setup for adaptive phase retrieval. The SLM is separated and one side is placed at the intermediate image plane and the other side is in the Fourier plane.

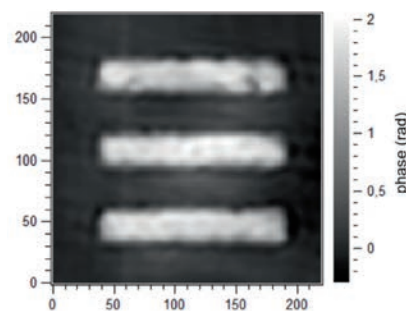


Fig. 2: TIE measurement of 3 phase bars of a phase USAF target. The nominal phase of the structure is $\pi/2 = 1.57 \text{ rad}$.

References:

- [1] Lingel, C.; Hasler, M.; Haist, T.; Pedrini, G.; Osten, W. "A benchmark system for the evaluation of selected phase retrieval methods", Proc. SPIE 9132, Optical Micro- and Nanometrology V, 91320R (2014).
- [2] Lingel, C., Haist, T.; Osten, W. "Spatial-light-modulator-based adaptive optical system for the use of multiple phase retrieval methods," Appl. Opt. 55, 10329-10334 (2016).

Post-processing for the compensation of chromatic aberrations in programmable microscopy

H. Pen, S. Gharbi, T. Haist, W. Osten

Spatial light modulator (SLM) based microscopy [1] traditionally is performed using coherent illumination. However, problems due to speckles and other interference-based disturbances often lead to noisy images. Incoherent illumination avoids such problems. Spatial incoherence in combination with monochromaticity is hard to achieve at reasonable optical power. Therefore, often temporal averaging e.g. using rotating diffusers is employed. LEDs achieve a limited spatial and temporal coherence and are in principle good choices for microscopy. When used in combination with a diffractive optical elements and a carrier frequency (which is necessary to separate unwanted diffraction orders due to the non-ideal modulation characteristic of the SLM from the desired diffraction order) strong chromatic aberrations will occur.

The chromatic aberration will be always perpendicular to the grating structure. Therefore, it is possible to change the orientation of the PSF shape by rotating the carrier frequency grating. Then, by postprocessing it becomes possible to combine several images obtained with different orientations in order to compute one sharp image with strongly reduced overall chromatic aberrations. To

this end for every pixel position it is decided which image of the acquired image stack yields locally the sharpest image. This pixel is selected to be locally used within the final image. For the decision different metrics might be used. Currently we employ a simple local standard deviation metric to decide about the local sharpness.

The setup (fig. 1) uses a Holoeye Pluto modulator in combination with green light (535 nm) and a Vistek CCD image sensor. Instead of a microscope objective lens a conventional achromat with a focal length of 30 mm is used in order to achieve a long working distance. The aberrations due to the achromat are corrected by proper addressing of the SLM (modulation of the carrier frequency by the conjugate of the aberration).

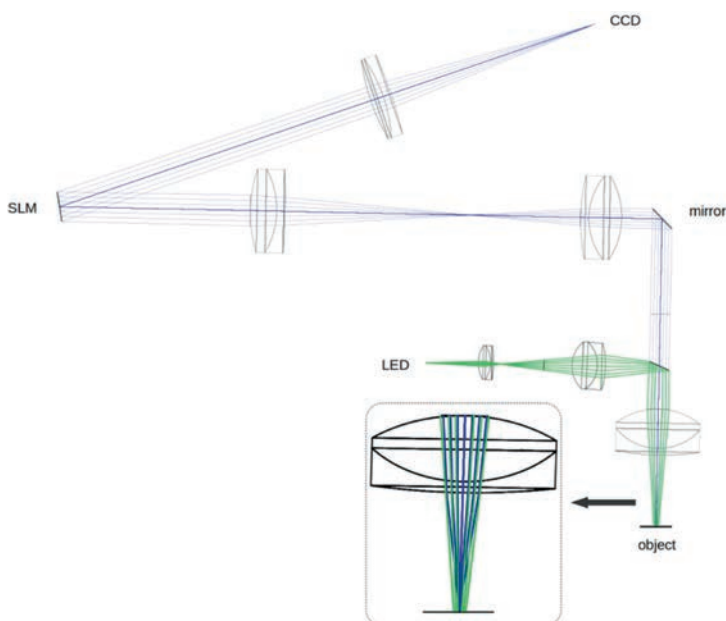


Fig. 1: Setup with achromat lens for programmable microscopy.

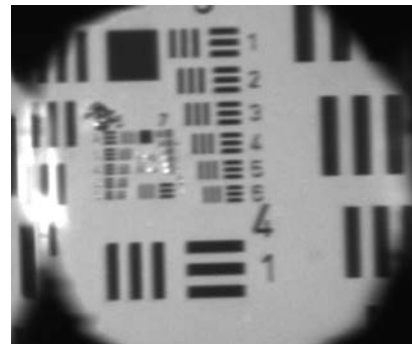


Fig. 2: Chromatic aberration (here in horizontal direction) due to LED illumination

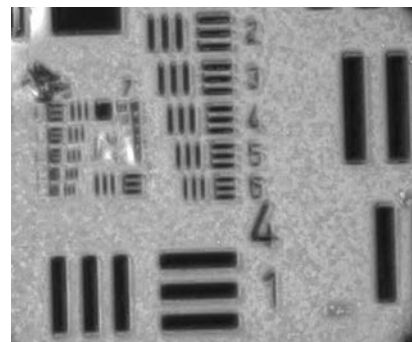


Fig. 3: Combination of 7 images to improve resolution.

References:

- [1] Haist, T.; et al. "Programmable microscopy." In Javidi, Bahram, Enrique Tajahuerce, and Pedro Andres, eds. Multi-dimensional imaging. John Wiley & Sons, 2014. Multi-Dimensional Imaging (2014): 153-173.

High Resolution Metrology and Simulation



Detection of grating asymmetries by phase-structured illumination	48
<i>Supported by: ASML</i>	
<i>Project: NANOSI – Detecting nano-sized asymmetries in silicon trenches using phase-sensitive structured illumination</i>	
<i>In cooperation with: ASML</i>	
Multiple-wavelength optical alignment tool	49
<i>Supported by: ASML</i>	
<i>Project: ALIGN – Multiple-wavelength optical alignment tool</i>	
<i>In cooperation with: ASML</i>	
Wafer alignment on small targets with small pitches.....	50
<i>Supported by: ASML Veldhoven</i>	
<i>Project: Wafer alignment on μDBO targets</i>	
<i>In cooperation with: ASML Veldhoven</i>	
Design of a two-dimensional cascaded plasmonic superlens.....	51
<i>Supported by: DFG under the project OS111/40-1</i>	
Nanofabrication of a cascaded plasmonic superlens	53
<i>Supported by: China Scholarship Council (CSC) and DFG through the project OS111/40-1</i>	
Application of a speckle simulator for a machine-learning phase retrieval process	54
Nanopositioning- and measuring machine NPMM-200	55
<i>Supported by DFG German Science Foundation</i>	
<i>Project: Nanopositionier- und Messmaschine (Os 111/44-1)</i>	
<i>In cooperation with: TU-Ilmenau</i>	
Detecting the depth of fluorescent light sources by structured illumination and shearing interferometry	57
<i>Supported by: Landesstiftung Baden-Württemberg, Project: FluoTis</i>	

Detection of grating asymmetries by phase-structured illumination

D. Buchta, S. Peterhänsel, M. L. Gödecke, K. Frenner, W. Osten

In order to improve the process-control robustness in semiconductor device manufacturing, it is necessary to characterize grating asymmetries on the nanometer scale. Model-based scatterometry is the state-of-the-art optical metrology tool for wafer inspection. We study the combination of classical scatterometry with coherent, phase-only structured illumination. By means of rigorous simulations, it has already been shown that the resulting phase profile in the far-field image plane is an excellent indicator for any kind of grating asymmetry, such as overlay error in double-patterning gratings [1] or profiles with asymmetric sidewall angles [2]. It is possible to determine both the absolute value and the sign of an asymmetry.

Within a joint research project, ASML and ITO were aiming at an experimental verification of the promising simulation results. A schematic drawing of the implemented setup is shown in fig. 1. A step phase plate generates a phase offset of π between the two halves of the entrance pupil of the microscope objective (numerical aperture of 0.8). The spot-on-wafer is imaged onto the detector and coherently superposed with a tilted, unstructured reference beam, thus creating a phase-sensitive digital hologram. The intensity and phase distributions can be retrieved by applying Fourier analysis.

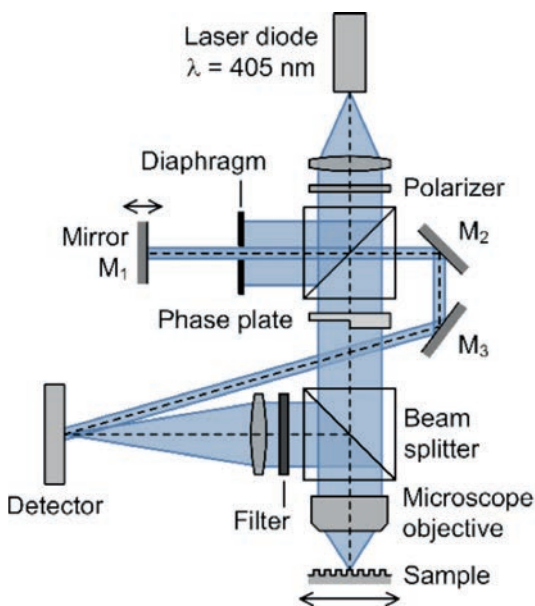


Fig. 1: Schematic drawing of the experimental setup [3]. The phase profile in the far-field image plane is reconstructed by off-axis digital holography.

Fig. 2 depicts exemplary intensity and phase cuts, taken at different lateral focus positions. The phase-structuring creates two distinct spots in the focal plane. In the dark center between the two spots, the phase profile features a steep phase jump of π . The gray areas mark regions of low intensity, which should not be used for phase evaluation. In the remaining regions, we observe a good qualitative agreement between measurement and simulation. Even the strong dependence on the lateral focus position is well approximated. We are hence optimistic that it will be possible to reconstruct the underlying grating asymmetries. To this end, the measured signal has to be compared to a library of simulated signals with different types and degrees of asymmetry.

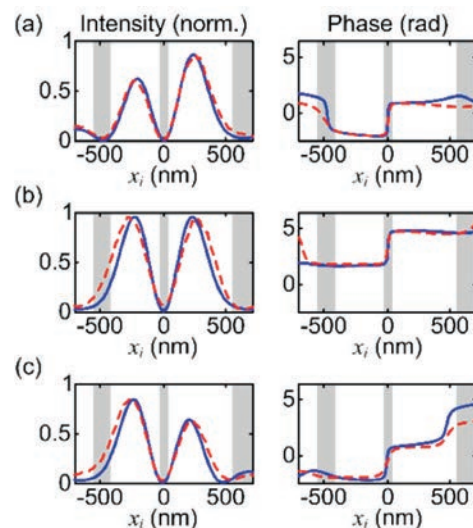


Fig. 2: Comparison between simulation (solid blue curves) and measurement (dashed red curves) [3]. The lateral focus position varies from (a) to (c).

Supported by: ASML

Project: NANOSI – Detecting nano-sized asymmetries in silicon trenches using phase-sensitive structured illumination

In cooperation with: ASML

References:

- [1] Peterhänsel, S.; et al. "Detection of overlay error in double patterning gratings using phase-structured illumination", *Opt. Express* 23(19), 24246-24256, 2015.
- [2] Peterhänsel, S.; et al. "Phase-structured illumination as a tool to detect nanometer asymmetries", *J. Micro/Nanolith. MEMS MOEMS* 15(4), 044005, 2016.
- [3] Gödecke, M. L.; et al. "Detection of grating asymmetries by phase-structured illumination", *Proc. SPIE* 10449, 104490C, 2017.

Multiple-wavelength optical alignment tool

M. L. Gödecke, S. Peterhänsel, K. Frenner, W. Osten

State-of-the-art integrated circuits consist of dozens of individual layers stacked on top of each other. Furthermore, multiple-patterning techniques are often used to enhance the feature density. The device performance depends on the accurate alignment of each pattern with respect to underlying or neighboring product patterns. A placement accuracy in the nanometer range requires measurements of the wafer position with sub-nanometer precision [1]. Due to fabrication tolerances, the alignment targets may feature asymmetric grating profiles. If not properly taken into account, such asymmetries result in placement errors larger than the targeted accuracy. Therefore, it would be beneficial if the optical alignment sensor was capable of characterizing (or calibrating for) grating asymmetries. Furthermore, the measurements should be carried out with multiple wavelengths in parallel, thus improving both the process robustness and the measurement speed.

Within a joint research project, ASML and ITO were investigating different pupil-based alignment-sensor designs by means of rigorous simulations. Fig. 1 shows an exemplary setup based on coherent scanning Fourier scatterometry, extended by a Mach-Zehnder-/Linnik-type reference arm and a 180°-rotational shearing element

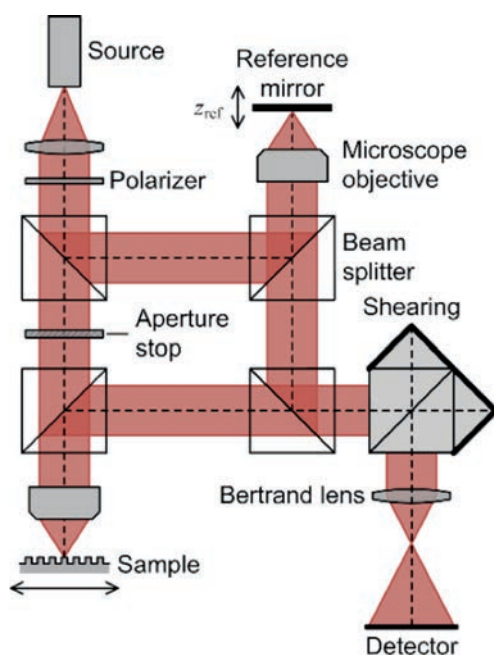


Fig. 1: Schematic drawing of an exemplary interferometric alignment-sensor design. The intensity signal is detected in the angle-resolved pupil plane.

in front of the detector. The spatially-structured aperture stop in the object arm separates the higher diffraction orders from the dominant 0th order, which ensures a high contrast of the alignment signal (present only in the higher orders). The unstructured reference beam is shifted in phase and coherently superposed with the object beam. The wavelength separation can be realized by a single-shot hyperspectral-imaging approach [2].

Fig. 2 (a) depicts the dependence of the detected alignment position x_{align} on the pupil coordinate NA_x for different sidewall-angle (SWA) configurations (at $\lambda = 700$ nm). The symmetric profile yields the ideal value of $x_{align} = 0$ for all NA_x -values. Asymmetric configurations can be uniquely identified (both absolute value and sign). An additional shift of the reference mirror along the optical axis (in z_{ref} -direction) significantly increases the signal strength, see fig. 2 (b). The common zero crossing of all curves at one specific NA_x -coordinate is particularly interesting, as it allows for a SWA-independent measurement.

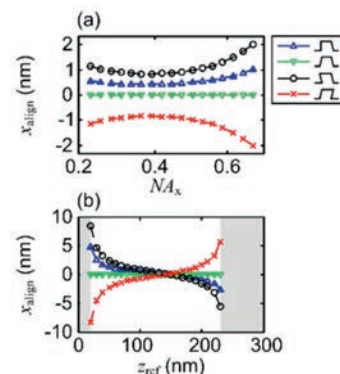


Fig. 2: Alignment position x_{align} for different SWA-configurations. (a) Angular dependence on NA_x at $z_{ref} = 70$ nm. (b) Dependence on z_{ref} at $NA_x = 0.6$.

Supported by: ASML
Project: ALIGN – Multiple-wavelength optical alignment tool
In cooperation with: ASML

References:

- [1] Den Boef, A. J. "Optical wafer metrology sensors for process-robust CD and overlay control in semiconductor device manufacturing", Surf. Topogr.: Metrol. Prop. 4, 023001, 2016.
- [2] Hagen, N. "Snapshot advantage: a review of the light collection improvement for parallel high-dimensional measurement systems", Opt. Eng. 51(11), 111702, 2012.
- [3] Gödecke, M. L.; et al. "Robust determination of asymmetric side wall angles by means of coherent scanning Fourier scatterometry", Proc. SPIE 9890, 98900M, 2016.

Wafer alignment on small targets with small pitches

C. M. Bett, M. L. Gödecke, D. Buchta, K. Frenner, W. Osten

Multiple patterning is commonly used in the semiconductor industry to fabricate small structures in the nm regime. For an accurate fabrication, mask and wafer alignment is of the utmost importance. State-of-the-art interferometric alignment measurements are often carried out by measuring the signal of higher diffraction orders while scanning over a grating, see report “Multiple wavelength optical alignment tool”. By shrinking the size of the grating markers to a few lines with small pitch, the space requirements of the markers could be drastically reduced down to a few μm^2 . Moreover, there already exist such small gratings on the wafer these days, in form of so-called μDBO -gratings used for overlay measurements. In a joint research project with ASML, we have investigated two possible sensor designs – one pupil- the other image-plane based - for small-sized alignment targets (7-10 lines) with small pitches (down to 400 nm).

The measurement of small-sized targets is challenging, as neighboring structures can easily influence the alignment signal. Additionally, an illumination spot smaller than the target size is necessary to provide an adequate photon efficiency. This implies the illumination of extended pupil patches where optical aberrations heavily influence the alignment signal. Therefore, the robustness of the alignment signal was analysed in detail by rigorous simulations for different illumination and detection settings. The settings were optimized until an alignment error in the sub-nanometer range could be reached.

Some of the abovementioned aspects such as e.g. the influence of the finite target size on the alignment signal, were experimentally verified by a proof-of-concept setup.

Moreover, hyperspectral imaging solutions were investigated and integrated into the setup for the pupil plane sensor. By measuring many different wavelengths simultaneously, the sensor is much less sensitive to partly absorbing layers within the layer stack of the sample. A schematic drawing of one hyperspectral imaging solution is given in fig. 1. It is based on the spectrograph tiger [1,2] using a microlens array and a prism to simultaneously record the spatial as well as the spectral information. With the help of a prototype setup, we were able to measure alignment signals single-shot for different wavelengths, see fig. 1.

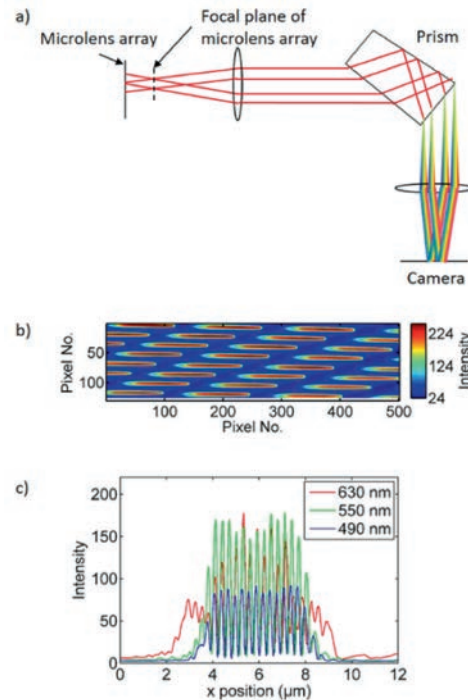


Fig. 1: Hyperspectral imaging solution: a) schematic drawing of hyperspectral setup. The focal plane of the microlens array is imaged onto the detector via a 4f-imaging system. In between, the spectral information is separated by a prism. b) Detector image of hyperspectral sensor (false-color). By rotating the microlens array, the different spectra do not overlap [2]. c) Hyperspectral alignment signal on finite target. The spot size increases for longer wavelengths leading to an enhanced influence of the grating edge. Pitch 600 nm, 8 lines.

Currently, one of the sensor designs is going to be miniaturized within the follow-up joint research project, with the aim of integrating it into the nano-positioning and -measuring machine NPMM-200 (available at ITO from September 2017 onwards). It offers a resolution of 0.08 nm and a positioning reproducibility smaller than 4 nm in a total measurement range of $200 \times 200 \times 20 \text{ mm}^3$ (see report “Nanopositioning and measuring machine”) which allows for a comprehensive demonstration of the sensor’s practical performance as an alignment and positioning tool.

Supported by: ASML Veldhoven
Project: Wafer alignment on μDBO targets
In cooperation with: ASML Veldhoven

References:

- [1] Bacon, R. et al, Astron. Astrophys. Suppl. Ser. 113, 347-357 (1995).
- [2] Körner, K. et al, Patent DE102006007172B4.

Design of a two-dimensional cascaded plasmonic superlens

L. Fu, H. Li, K. Frenner, W. Osten

To achieve a direct far field imaging for subwavelength structure, a cascaded plasmonic superlens was suggested [1]. Recently, the expected imaging capability was demonstrated experimentally [2]. However, there are two limitations with this design. Since one component of the cascaded lens is a two-layer 1D periodic grating, subwavelength imaging is optimally achieved only when the object (two slits in a thick Cr layer) is aligned with the grating. Furthermore, it works only for p-polarized light with the electric field perpendicular to the grating for exciting surface plasmons. In this paper an alternative plasmonic superlens is suggested based on our previous design [1], the imaging property of which will be improved concerning the two problems. As shown in fig. 1(a), the superlens is still composed of two parts, i.e.; a grating assisted Fabry-Perot cavity (FPC) and a planar plasmonic lens (PPL). To enable 2D imaging, 1D gratings are replaced by circular gratings for the FPC structure and 1D slits are replaced by circular slits in the PPL. To further overcome the alignment problem, the center of the lens is replaced by two-layer flat metallic films. Through the excitation of surface plasmons via the periodic gratings, and their interaction and hybridization with the FP cavity modes [3], a flat optical dispersion versus spatial frequency, which is desired for subwavelength imaging, can be obtained. Similarly, to magnify the near field image behind

the FPC, a PPL which provides a hyperbolic phase compensation, is cascaded to it.

Imaging property of the lens for 2D imaging is calculated using COMSOL Multiphysics, which solves Maxwell's equations using a finite-element method. However, direct simulation of this lens using a 3D model turns out to be very difficult due to the presence of nanometer structure features in a large-sized structure. Under this circumstance, 3D simulations for circular symmetric structures can be approximated by 2D simulation, as is often done for spheres through simulating cylinders.

A 2D COMSOL model was built in the xz -plane as shown in fig. 1(b) by using perfect matched layers to surround the simulation domain. The lens size along the x -axis is $26 \mu\text{m}$ and the minimum mesh is of 2 nm . An electric point dipole oscillating at 640 nm wavelength along the x -axis is used as a point source. In addition, the dipole and the FPC are embedded in a dielectric with a refractive index of $n=1.41$ (as will be fabricated) and the field distribution behind the PPL is calculated in air. Using the structural parameters given in fig. 1(b), near-field distribution behind the PPL was calculated. Assuming that the object is observed under an objective with $\text{NA} = 1$, far field imaging can be derived using forward and backward Fourier transformations. Figs. 2(a) and (b) show virtual images for one dipole and for two incoherent dipoles above the lens, respectively. An elongated focus with 580 nm full width

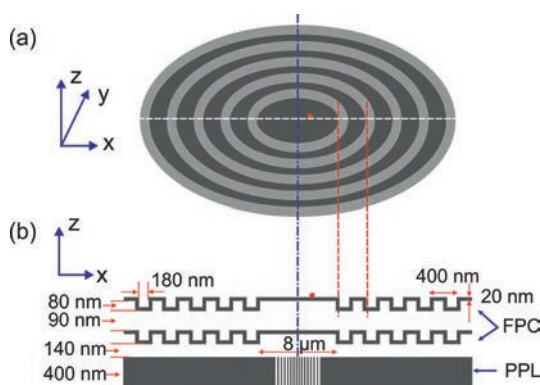


Fig. 1: Schematic of a 2D cascaded plasmonic superlens in Silver (not in scale). (a) Top view of the FPC and PPL structure. (b) Cross-sectional view along the white dashed line in (a). Slit width from left to right (along the center) in the PPL is 88, 64, 57.5, 47.5, 42, 34, 42, 47.5, 57.5, 64, and 88 nm, respectively.

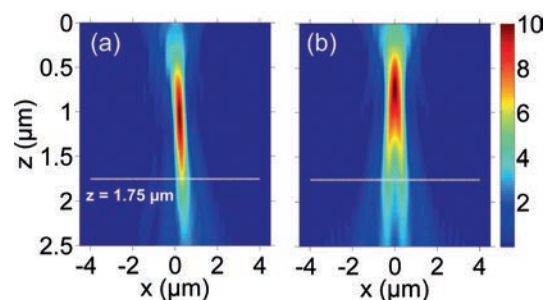


Fig. 2: (a) A virtual image in the xz -plane above the cascaded superlens when one point dipole is located at 120 nm with respect to the lens center ($x=0$). (b) The image obtained from the superlens when two dipoles with a distance of 240 nm are excited incoherently.

at half maximum (FWHM) is obtained. We see from fig. 2(b) that the image for two dipoles with a distance of 240 nm can be well resolved.

Fig. 3(a) plots the image fields from fig. 2 along the x-axis at $z=1.75 \mu\text{m}$ for one and two dipoles, respectively. The image contrast for two dipoles is around 0.65, which is well below the Rayleigh criterion. To further investigate the imaging property of the superlens, image shift as a function of dipole position is plotted in fig. 2(a). Also the plots for imaging with the FPC structure alone (no PPL) and with the PPL alone (no FPC) are shown. The FPC structure alone can transfer the waves from the dipole directly to the other side of the structure with an almost linear image shift with the dipole. Nevertheless, the slope of the curve is unit due to the lacking of phase compensation mechanism for image magnification. Imaging can also be obtained with only PPL alone. However, the near field interaction between the dipole and

the nano-slits is so strong that no linear relationship is manifested on the image-object curve, as can be seen from fig. 3(b). Once the two components are combined together, a linear image shift with the dipole is demonstrated. The slope from the linear fit results in a magnification a factor of 2, which plays a critical role for the resolving power of our plasmonic superlens (higher than 240 nm at 640 nm wavelength).

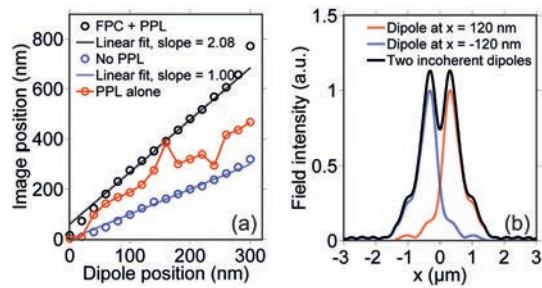


Fig. 3: (a) Field plot from one and two dipoles, respectively at $z=1.75 \mu\text{m}$ (along the dashed lines in fig. 2). (b) Image shift with the position of one dipole along the x-axis for three different cases.

Supported by: DFG under the project OS111/40-1

References:

- [1] Fu, L.; Schau, P.; Frenner, K.; Osten, W., Proc. SPIE 9526, 95260Z (2015).
- [2] Li, H.; Fu, L.; Frenner, K.; Osten, W., submitted to SPIE, Optical Metrology, June, 2017 München.
- [3] Fu, L.; Schau, P.; Frenner, K.; Osten, W.; Weiss, T.; Schweizer, H.; Giessen, H., Phys. Rev. B 84, 1–6 (2011).

Nanofabrication of a cascaded plasmonic superlens

H. Li, L. Fu, K. Frenner, W. Osten

For the direct imaging with subwavelength resolution, a cascaded plasmonic superlens for far field subwavelength imaging was suggested [1]. Schematic of the structure is shown in fig. 1(a), which is composed of two parts: a double layer meander cavity structure (DLMC) to couple and to support the propagation of evanescent waves and a planar plasmonic lens (PPL) to transfer waves into free space with magnification. A double-slit in Cr was used as a test object and placed underneath the cascaded structure.

Here we report about the fabrication of a superlens and demonstrate its imaging capability. Fabrication procedures of each part were first conducted separately to optimize the parameters and their optical properties were measured to ensure that they behave as designed. Then the whole cascaded lens was assembled through a layer-by-layer stacking technique. A cross section of the fabricated structure was cut by a focused ion beam (FIB) milling machine (Helios NanoLab DualBeam from FEI). The SEM image in fig. 1(b) shows the shape and relative position among the three parts of the structure. Fig. 1(c) shows the simulation results along the xz-plane calculated using fabrication parameters.

The imaging property of the cascaded structure was then measured by a microscope with $NA = 1.3$. The structure is illustrated from the bottom side by a collimated laser beam with a wavelength of 640 nm. Taking the field $1.5 \mu\text{m}$ above the back side of the double-slit as the position of image plane (red dashed line shown in fig. 1(c)), a far-field image of the double slits with a distance of 800 nm was captured by a CCD camera in the image plane and is shown in fig. 1(d). The measured distance of the double slits is about 1680 nm, indicating a magnification factor of 2.1. The distortion of the image shown in fig. 1(d) was induced by non-parallel alignment between the double-slit and the DLMC grating structure during the fabrication, which can be avoided in practical applications when the object is a point source. The intensity distribution drew from the measured image along the red arrow line was compared with simulation to further validate the obtained image. We can see that the intensity distributions agree with each other very well as illustrated in fig. 1(e).

In summary, the experimental results show

that our cascaded plasmonic superlens can be realized using existing nano-fabrication facility at our institute. The captured image displays that the cascaded structure possesses the capability to image an object with a magnification factor in the far field. Furthermore, a very good agreement between the measured and calculated fields was obtained due to the well-controlled nano-fabrication procedure. These results pave the way for further investigating the resolving capability of the superlens beyond the diffraction limit.

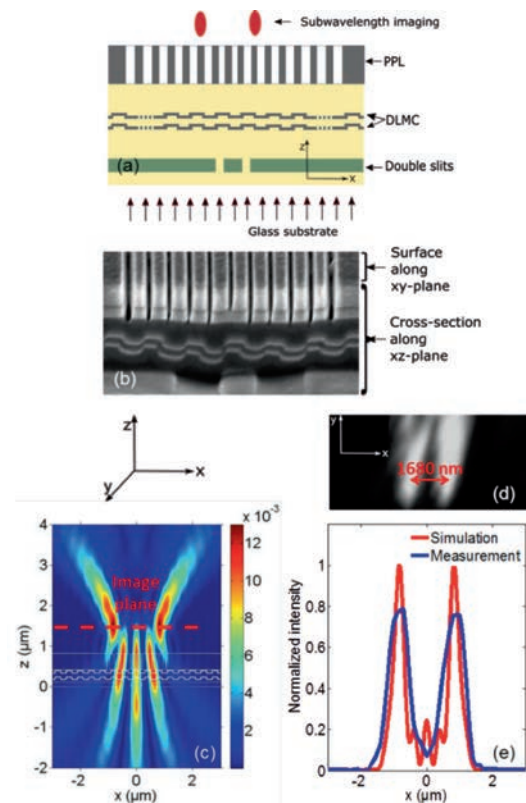


Fig. 1: (a) Schematic of a cascaded plasmonic superlens; (b) Cross section of a test fabricated cascaded structure; (c) Simulation field distribution in the xz-plane; (d) Images of the double-slit in the xy-plane captured by CCD camera at a position along the dashed line shown in (c); (e) Comparison between simulation and measurement results.

Supported by: China Scholarship Council (CSC) and DFG through the project OS111/40-1

References:

- [1] Fu, L.; Schau, P.; Frenner, K.; Osten, W., SPIE Optical Metrology, 95260Z (2015).
- [2] Li, H.; Fu, L.; Frenner, K.; and Osten, W., SPIE Optical Metrology, accepted (2017).

Application of a speckle simulator for a machine-learning phase retrieval process

L. Fu, K. Frenner, W. Osten

Via analyzing speckle fields in optical metrology, profound information of surface under inspection can be obtained. To calculate speckle fields scattered from rough surfaces rigorously, a speckle simulator based on surface integral equation method using higher order boundary element was developed [1]. In this report we demonstrate a possible application of the speckle simulator for a machine-learning trained phase-retrieval process [2].

Specklegrams produced in an interferometric speckle imaging system are made up of pixels whose intensities are proportional to the phase of the corresponding speckle wrapped onto a range of $-\pi$ to $+\pi$. Through phase-unwrapping process, shape and features, vibration modes, or strain components of the object under study can be extracted. However, specklegrams are inherently noisy and reliable phase unwrapping remains a key challenging task.

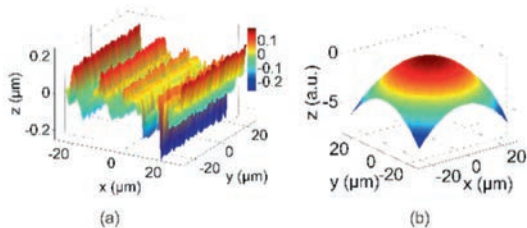


Fig. 1: Numerically generated rough surface ($50 \times 50 \mu\text{m}^2$) with a correlation length of $1 \mu\text{m}$ in the x -direction and 1 mm in the y -direction. The RMS along the x -direction is $0.3 \mu\text{m}$ and along the y -direction is 1.5 nm . (b) A surface deformation with a Gaussian beam distribution is applied to the rough surface shown in (a).

Statistical pattern recognition techniques known as machine learning are receiving substantial attentions. A promising potential has been demonstrated in predicting the location of phase discontinuities through the application of a neural network by training a 10×10 pixel kernel [3]. However, to train the machine learning system, a large number of examples, to which the solution is known beforehand are needed. In further, the examples have to be as varied as possible to generalize the learned information. A speckle simulator can ideally be employed for this aim.

In this report we investigate the feasibility of generating correlation speckles using

the speckle simulator. We assume a rough surface of an aluminum plate (fig. 1(a)) which is illuminated by a plane wave at 520 nm wavelength and an incident angle of 30° . The surface was meshed by 400 higher order quadrilateral elements, each with ten edges. Reflected speckle fields of different E-field components 500 mm above the surface are calculated. Then a surface deformation with a Gaussian displacement and an amplitude smaller than $\lambda/10$ (fig. 1(b)) was created. Speckle correlation interferogram was then calculated and obvious correlation fringe from the field component of E_x was obtained, as is shown in fig. 2(b) [4]. It turns out that for numerical simulation the absolute deformation amplitude is not in question.

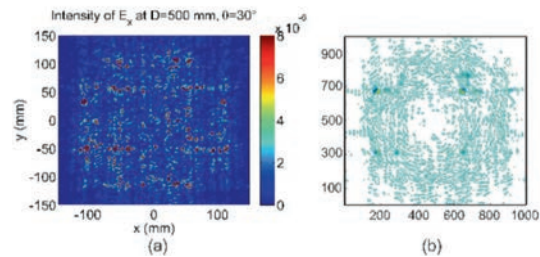


Fig. 2: (a) Generated speckle field E_x 500 mm above the surface at an incident angle of 30° and at 520 nm wavelength. (b) Calculated correlation speckle.

The results are consistent with those expected in both theoretical and experimental works. To continue this study for which large number of training examples are required, increased simulation speeds would be crucial. In addition, an increased simulation area will bring the training examples to be as faithful as possible. Both aspects can be accomplished by implementing the fast multiple method and further by the multilevel fast-multiple method. The computation cost via these algorithms can be reduced from $O(N^3)$ to $O(N^{3/2})$ and further to $O(N \log N)$ [5].

References:

- [1] Fu, L.; Frenner, K.; Osten, W. *Opt. Lett.* 39, 4104 (2014).
- [2] Sawaf, F.; Groves, R. M., *Appl. Opt.* 53, 5439–5447 (2014).
- [3] Sawaf, F.; Grove, R. M.; *Opt. Eng.* 52, 101907 (2013).
- [4] Sawaf, F.; Private Communication.
- [5] Song, J. M.; Chew, W. C.; *Microw. Opt. Tech. Lett.* 10, 14–19 (1995).

Nanopositioning- and measuring machine NPMM-200

K. Frenner, C. Pruß, W. Osten

Nanopositioning and measuring machines (NPMM) enable positioning, measuring, probing and manipulating of objects with nanometer precision on extended surfaces. The NPMM-200 will be implemented and applied as an integrative part of the ITO infrastructure including sophisticated devices for high resolution imaging, measurement and materials processing. With the installation of such a high performance nano measuring and positioning device the gap that is still existing in the processing and measurement chain will be closed and manifold new applications and collaborations with national and international partners become possible. The NPMM will be used for sophisticated measurements, manipulation, processing and positioning tasks in the framework of nano- and microsystem- technology.

High resolution and fast detection of local properties like imperfections, faults or deviations from design can be adapted to extended optical components and systems much more flexible with a multi-scale measurement strategy and sensor fusion than probing with individual sensors. Sensor fusion combines high precision absolute shape measurement

with additional information on the nanoscopic scale below the resolution limit of optical systems using e.g. plasmonic near-field sensors and optical metamaterials. Selection of suitable sensors in such a multisensor system and determination of their parameters can be performed automatically by an assistance system. Key element in the final finishing step of high precision fabrication, where the error of the optical surface is reduced to the 10 nm level (rms) or below, is the absolute measurement. Such a high precision characterization of optical functional surfaces like e.g. aspheres, free forms, DOEs and hybride elements can be improved by combining optical full field methods with NPMM-200 measurements. Atomic impurities in solids like Diamond or SiC must be positioned with a spatial accuracy of better than 10 nm in order to show quantum correlations. Additional control and communication structures processed on different length scales have to be combined to quantum circuits and quantum processors. These control structures consist of superconducting rings, their position can be determined using the NPMM-200. Integration of such an expensive and unique device will be realized at ITO within a remote

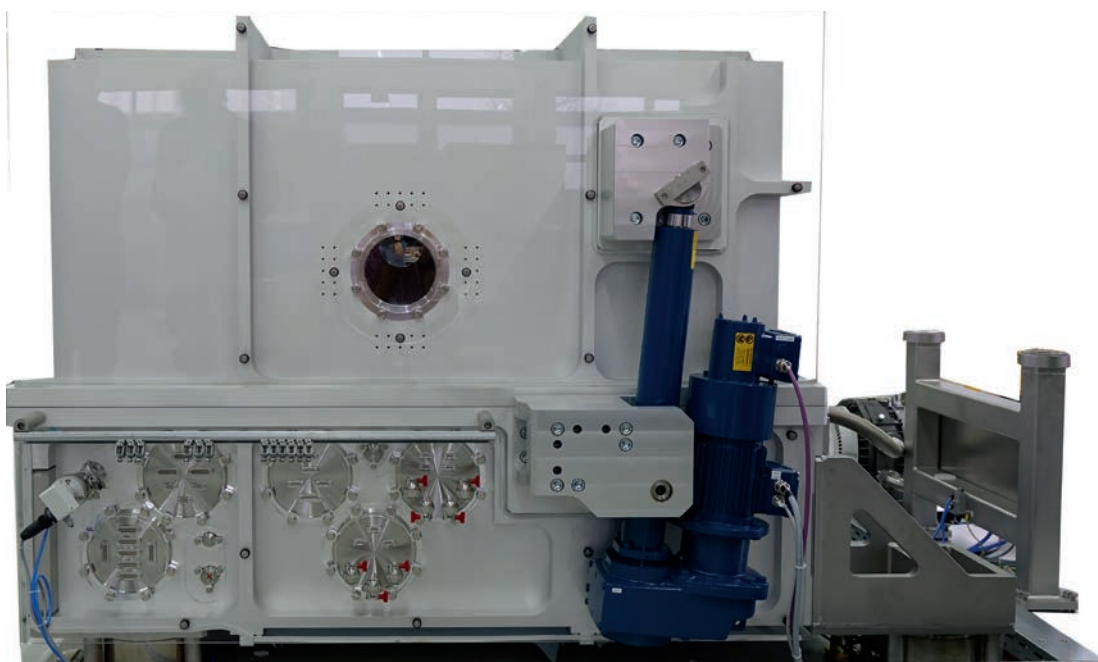


Fig. 1: Housing of the new NPMM-200

laboratory concept. Based on such a concept and referring to a systematic access procedure, the NPMM could be applied by remote users. The implementation of a virtual nano-processing and nano-measurement center is objective of these investigations.

The performance of the NPMM-200 was impressively demonstrated by TU Ilmenau. There are numerous exemplary measurements like depth standard measurements, diffractive structures on curved surfaces, step height to 15 mm reference objects, measurements of high precision mirrors, integration of grippers and various sensors [1,2].

The performance characteristics of NPMM-200 allows for positioning on large (200x200 mm) areas with topography differences of up to 25 mm in relatively high speed (30 mm/s) with improved resolution (0.08 nm) and with a high reproducibility of up to 1 nm.

To achieve these performance parameters, the use of modern homodyne interferometers in vacuum is required. Such modern interferometers are characterized by the use of two-beam and three-beam interferometers. Therefore only one laser is required for each measuring axis. This minimizes frequency differences in 6D-measurements. The stability of the laser is better than 10^{-9} .

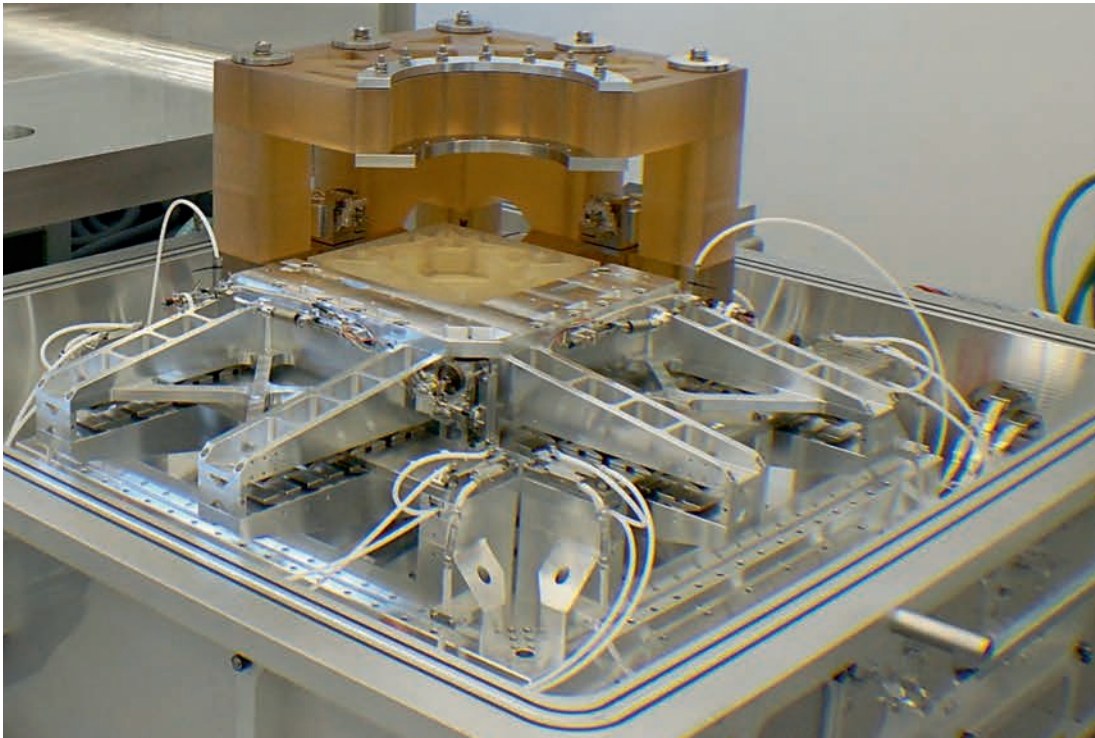


Fig. 2: Central parts of the NPMM-200

Supported by DFG German Science Foundation
Project: Nanopositionier- und Messmaschine
(Os 111/44-1)
In cooperation with: TU-Ilmenau

References:

- [1] Hoffmann, J.; Weckenmann, A.: Traceable profilometry with a 3D Nanopositioning Unit and zero indicating Sensors in compensation method, Journal of Physics: Conference Series 13 (2005) 228–231
- [2] Jäger, G.; et al. : Nanomeasuring and nanopositioning engineering, Measurement 43 (2010) 1099–1105

Detecting the depth of fluorescent light sources by structured illumination and shearing interferometry

J. Schindler, K. Frenner, W. Osten

Non-invasive diagnostics can strongly profit from optical methods like optical coherence tomography or confocal fluorescence microscopy. Yet, many biological materials like skin are strongly scattering and limit the penetration depth in which structures can be resolved. It is even more difficult to retrieve information about the vertical position, i.e. the depth of a light source within a material.

A novel method has been developed which tackles this problem by a combination of structured illumination and detection based on lateral shearing interferometry. The setup is depicted in fig. 1. The structured illumination is realized by separating two beams in a Sagnac interferometer and in the pupil plane of the microscope leading to two intersecting beams. This yields a coarse restriction of the illuminated volume and an interference pattern of allowing a local addressing of the excitation of the fluorescence. The detection is based on lateral shearing interferometry realized in a Michelson interferometer. This enables an interferometric evaluation of the recorded signal: Due to the balanced paths in the interferometer even the short coherence length of fluorescent light in the range of $10\ \mu\text{m}$ is sufficient and no spatial coherence is needed as interference takes place between the object wave of a single point and a laterally shifted copy of itself. Depth information can be obtained by evaluating the curvature of the recorded phase which is directly related to the defocusing of the light source. The measurement principle is illustrated in fig. 2: With an increasing distance of the fluorescent light source to the focus of the microscope objective, the fringe spacing increases which indicates a decreased curvature of the wave fronts. A quantitative comparison is shown in fig. 3. The sample consists of fluorescent inclusions in a material with a scattering coefficient comparable to dental enamel. The comparison with the nominal values shows an agreement with relative deviations in the range of 10 %.

Further optimization of the setup can be obtained by using fluorophores in the infrared region, where the effects of scattering are less pronounced or working at higher numerical apertures for increased depth resolution.

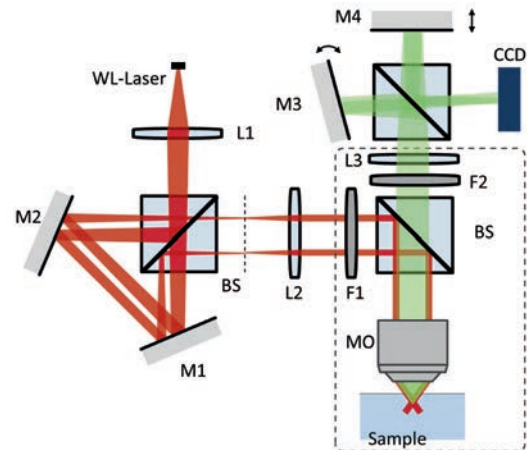


Fig. 1: Experimental setup with structured illumination (red) and detection (green) attached to a microscope (dashed) in epi-illumination.

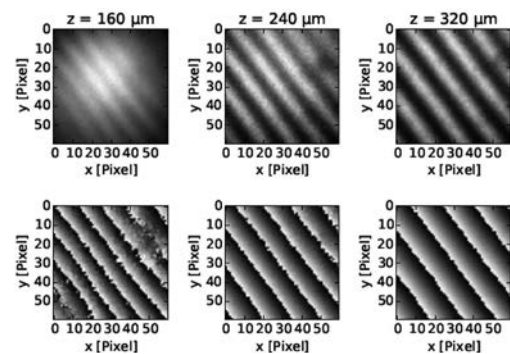


Fig. 2: Recorded intensities and phase signals for a fluorescent particle in different vertical positions.

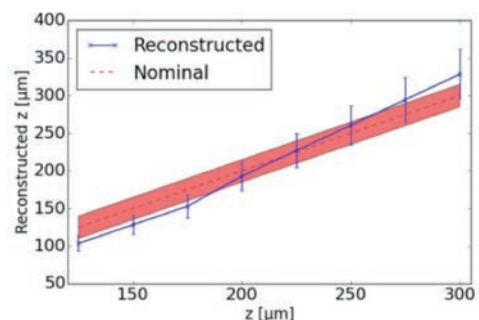


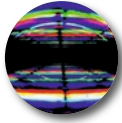
Fig. 3: Reconstruction of the depth of fluorescent inclusions of rhodamine 6G in a scattering material.

Supported by: Landesstiftung Baden-Württemberg, Project: FluoTis.

References:

- [1] Schindler, J.; Schau, P.; Brodhag, N.; Frenner, K.; Osten, W. "Retrieving the axial position of fluorescent light emitting spots by shearing interferometry", J. Biomed. Opt. 21(12), 125009 (Dec 28, 2016).

Interferometry and Diffractive Optics



Next generation TWI	60
<i>Supported by: DFG, AiF, EU</i>	
<i>Projects: AutoCalib (Os111/45-1), TWI-Stitch (IGF-Projekt: 18592 N), EMPIR Freeform</i>	
<i>In cooperation with: Mahr GmbH and PTB.</i>	
Robust Radius metrology	62
<i>Supported by: EU</i>	
<i>Project: EMPIR Freeform</i>	
<i>In cooperation with: PTB.</i>	
Measuring large convex surfaces with Tilted Wave Interferometry using stitching methods	63
<i>Supported by: AiF within the programme for sponsorship by Industrial Joint Research (IGF) of the German Federal Ministry of Economic Affairs and Energy based on an enactment of the German Parliament via the Forschungsvereinigung Feinmechanik, Optik und Medizintechnik e.V. FOM</i>	
<i>Project: TWI-Stitch (IGF 18592 N)</i>	
<i>In cooperation with: Technische Hochschule Deggendorf.</i>	
Tilted-Wave-Interferometry: Improving accuracy by elimination of systematic errors	64
<i>Supported by: DFG German Science Foundation</i>	
<i>Project: Ein selbst-kalibrierendes Verfahren zur Vermessung von Asphären und Freiformflächen (OS 111/45-1)</i>	
Subwavelength diffractive optics for generation of cylindrical polarization states.	65
<i>Supported by: AiF</i>	
<i>Project: SUBWELL (IGF 18728 N)</i>	
<i>In cooperation with: IFSW, University Stuttgart, within the programme for sponsorship by Industrial Joint Research (IGF) of the German Federal Ministry of Economic Affairs and Energy based on an enactment of the German Parliament.</i>	
3D laser direct-writing for injection compression molding of diffractive-refractive elements	66
<i>Supported by: AiF</i>	
<i>Project: HOLEOS</i>	
<i>In cooperation with: Hahn-Schickard, Stuttgart, within the programme for sponsorship by Industrial Joint Research (IGF) of the German Federal Ministry of Economic Affairs and Energy based on an enactment of the German Parliament.</i>	
In situ fabrication of microstructures for encoder systems	67
<i>Supported by: BMBF</i>	
<i>Project: "PhotoEnco – Photonisch strukturierbare Werkstoffe und photonische Prozesse für die individualisierte Herstellung von Encodermaßverkörperungen und deren Abtasperipherien"(13N10854)</i>	
<i>In cooperation with: Sick Stegmann, Allresist, Acsys, STVision</i>	
Improved design of a diffractive zoom lens for interferometric measurements	68
<i>Supported by: BMBF</i>	
<i>Project: ETIK (FKZ 16N12258)</i>	
<i>In cooperation with: Zeiss SMT AG</i>	
Microscope objective integrated optically addressable polarization shaping	69
<i>Supported by: DFG</i>	
<i>Project: OS111/35-1</i>	
<i>In cooperation with: IHFG (University Stuttgart), University Potsdam, Fraunhofer IOF, Jena.</i>	
<i>This project is part of the DFG priority programme 1337 "Active micro optics"</i>	

Next generation TWI

G. Baer, C. Pruß, A. Bielke, J. Schindler, A. Harsch, W. Osten

Tilted wave interferometry (TWI) was invented to provide optics manufacturers with an asphere and freeform metrology solution for specular surfaces. The wish list in this application is challenging:

- high flexibility that allows to measure aspheres but also freeform surfaces
- interferometric accuracy
- areal measurements with high lateral resolution
- high measurement speed \ll 1 min
- traceable to the SI unit system.

The main challenges for such metrology systems are vignetting, i.e. the potential loss of measurement light at the curved specular surfaces, and calibration, i.e. the separation of the instrument's systematic error from the measurement signal.

The key aspects of the solution that TWI provides are on one hand a new illumination scheme that ensures that the measurement light returns to the detector even if the surface under test has a deviation from the best fitting sphere of several hundred micrometers. The other key point is the calibration approach that takes the standard 2D interferometer calibration to a 4D volume calibration. 4D refers to two position coordinates plus two coordinates for the angle of incidence. This approach takes care of the so called retrace error, an error that occurs, when the test setup deviates from the so called null test, where the test rays hit the surface under test under normal incidence. The volume calibration models the interferometer in a so called black box model, where the aberrations are described with a set of polynomials. The polynomial coefficients are determined comparing the response of the model with experimental calibration measurement results. It could be shown that the convergence of the solution of this inverse problem strongly depends on the boundary conditions set e.g. by the calibration positions used. With a suitable choice of calibration positions, we achieve a stable convergence in real life conditions, including positioning errors, lens aberrations and noise.

Together with our industrial partner Mahr the TWI principle is now being commercialized. After its first presentation to the optical community 2015 on the occasion of the International Year of Light celebration at ITO's 30th optics colloquium in Stuttgart's "Haus der Wirtschaft", the TWI60 received major attention on 2016's OPTATEC fair in Frankfurt.

The potential of this successful principle has not come to an end. The TWI calibration approach allows not only to calibrate TWI interferometers, but also other optical systems such as non-nulltest interferometers, e.g. sub-Nyquist interferometers.



Fig. 1: TWI 60 on the OPTATEC fair June 2016.

The next generation currently under investigation aims to further increase the setup stability. The transition to a more common path design, where the reference surface is integrated into the test arm as is known from Fizeau interferometers [6]. The benefit of this arrangement has been shown by simulations, also by our partner PTB [9].

*Supported by: DFG, AiF, EU
Projects: AutoCalib (Os111/45-1),
TWI-Stitch (IGF-Projekt: 18592 N), EMPIR Freeform
In cooperation with: Mahr GmbH and PTB.*

References:

- [1] Liesener, J.; Garbusi, E.; Pruß, C.; Osten, W. "Verfahren und Messvorrichtung zur Vermessung einer optisch glatten Oberfläche," DPMA Patent DE 10 2006 057 606.3 (2006).
- [2] Garbusi, E.; Pruß, C.; Osten, W. "Interferometer for precise and flexible asphere testing," Opt. Lett. 33(2008)2973–2975.
- [3] Baer, G.; Schindler, J.; Pruß, C.; Osten, W. „Calibration of a non-null test interferometer for the measurement of aspheres and free-form surfaces”, Opt. Express 22 (2014) 25, pp. 31200-31211.
- [4] Baer, G.; Pruß, C.; Osten, W. „Verfahren zur Kalibrierung eines Messgerätes”, Patent Application DPMA 10 2014 209 040.7 (2014).
- [5] Baer, G.; Osten, W. „Justage einer zu prüfenden optischen Fläche in einer Prüfvorrichtung”, DPMA Patent DE 10 2011 102 196.9 (2011).
- [6] Baer, G.; Pruß, C.; Osten, W. „Verkippte Objektwellen nutzendes und ein Fizeau-Interferometerobjektiv aufweisendes Interferometer”, Patent Application DPMA 102015222366.3 (2015).
- [7] Baer, G.; Schindler, J.; Pruß, C.; Siepmann, J.; Osten, W. "Fast and Flexible Non-Null Testing of Aspheres and Free-Form Surfaces with the Tilted-Wave-Interferometer", International Journal of Optomechatronics Vol. 8 , Iss. 4 (2014).
- [8] Fortmeier, I.; Stavridis, M.; Wiegmann, A.; Schulz, M.; Osten, W.; Elster, C. "Analytical Jacobian and its application to tilted-wave interferometry," Opt. Express 22, 21313-21325 (2014).
- [9] Fortmeier, I.; Stavridis, M.; Wiegmann, A.; Schulz, M.; Osten, W.; Elster, C. "Evaluation of absolute form measurements using a tilted-wave interferometer," Opt. Express 24, 3393-3404 (2016).
- [10] Pruß, C.; Schindler, J.; Baer, G.; Osten, W. "Measuring aspheres quickly - Tilted Wave Interferometry", Opt. Eng. (submitted) (2017).

Robust Radius metrology

C. Pruß, A. Wempe, J. Schindler, W. Osten

Shape testing of optical surfaces like lenses or mirrors includes irregularities of the surface that directly would add aberrations to an optical system but also the global shape that defines the optical functionality. A spherical surface is described by only four parameters: its location in space plus the radius of curvature. Increasing tolerance requirements dictate decreasing measurement uncertainties, plus the boundary condition that the low uncertainty must be kept even in close to production environments.

Areal interferometry in its embodiment as Fizeau or Twyman-Green interferometer is a standard choice for high precision surface inspection. Much has been done to bring this high resolution metrology method even to harsher environments. One shot metrology approaches like the carrier frequency evaluation method or based on geometric phase shifting help to mitigate the effects of air turbulences and vibrations that are omnipresent, e.g. when testing large surfaces. One shot methods freeze the fringes and with it the errors due to these dynamic effects. Due to the statistic nature of the disturbances, averaging out these effects is the method of choice for measuring in harsh environments or highest accuracies.

The measurement of the absolute radius, however, involves – due to the differential nature of interferometry – at least two measurements: One in the so called cat's eye position, where the surface under test is at the focal position of the transmission sphere of the interferometer and another one at the so called null test position, where the rays of the test arm hit the surface under normal incidence. The distance between these two positions is the radius of the surface, typically measured with a distance measuring interferometer (DMI).

In non-stable environments the time between these two measurements is a source of uncertainty, since a drift in the setup over the measurement time introduces an error.

To decrease this uncertainty we introduce a drift compensation scheme based on the assumption that the drift primarily behaves linearly over time in the relevant time span. In our case, this time span is of the order of

several minutes. The drifts can most probably be accounted to temperature dependent variations of the setup, so this assumption seems justified.

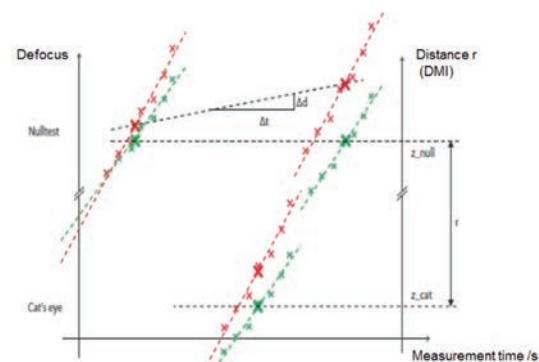


Fig. 1: Principle of the radius measurement drift compensation. The null test position z_{null} and the cat's eye position z_{cat} are found using measurements at a series of small z -steps around the respective position. From two subsequently detected positions in either null test or cat's eye the linear part of the drift can be estimated.

The approach was tested on an automated test setup based on a standard interferometer (ALI200 from Schneider Optikmaschinen equipped with a Trioptics μ Phase2HR interferometer and a SIOS SP2000 DMI). The results in figure 2 give an indication on the high reproducibility that was obtained even in a standard lab environment.

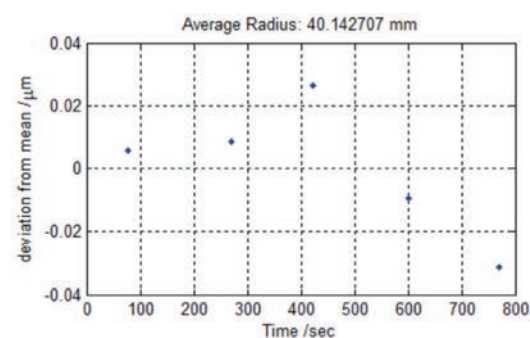


Fig. 2: Radius measurements on a 40 mm reference sphere.

Supported by: EU
Project: EMPIR Freeform
In cooperation with: PTB.

Measuring large convex surfaces with Tilted Wave Interferometry using stitching methods

A. Harsch, J. Schindler, C. Pruß

The production of aspheric lenses and freeform optics has increased over the last years since they offer a high degree of freedom in optical design. They are produced in an iterative production process during which it is necessary to monitor their form closely. The quality of high precision optics, especially of aspheres and freeforms, is highly depending on the repeatability and accuracy of measurement results. The Tilted Wave Interferometer (TWI), which was invented at ITO for the purpose of fast and accurate measurements of aspheres and freeforms, is able cover strong asphericity without using compensation optics like CGHs or scanning the specimen and is not limited to rotationally symmetric designs [1].

At present there are no satisfactory metrology tools available for aspheres with large diameters like optics for astronomical telescopes or high energy applications. Generally, large specimen can be measured by capturing smaller sub-apertures and stitching them together after the data acquisition. By combining stitching technologies and tilted wave interferometry, it becomes possible to measure large convex aspherical surfaces with high lateral resolution in a fast, non-contact measurement without any restrictions to the measurable diameter.

Our partner at TH Deggendorf developed a Stitching Software adapted to a standard Fizeau Interferometer with competitive results [2]. This expertise will be expanded to realize a Stitching Software tailored to the needs of the Tilted Wave Interferometer. The fundamental difference between the two interferometers is the much more complex calibration of the TWI, which is necessary for the flexibility of the device. Thereby it is possible to measure the specimen with a low number of sub-apertures.

Three benchmarking specimen with diameters between 150 mm and 450 mm have been defined and are manufactured at THD. Their radii vary between -1700 mm and 4500 mm while their asphericities reach values up to 780 μm .

The gathered knowledge in this project will be of great interest to optic manufacturers since it will provide a highly flexible and accurate tool suitable for measuring large convex aspheres.

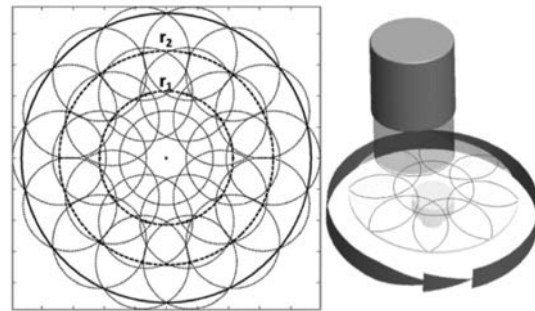


Fig. 1: Stitching pattern of a surface under test [2].

Supported by: AiF within the programme for sponsorship by Industrial Joint Research (IGF) of the German Federal Ministry of Economic Affairs and Energy based on an enactment of the German Parliament via the Forschungsvereinigung Feinmechanik, Optik und Medizintechnik e.V. FOM
Project: TWI-Stitch (IGF 18592 N)
In cooperation with:
Technische Hochschule Deggendorf.

References:

- [1] Liesener, J. et al. "Verfahren und Messvorrichtung zur Vermessung einer optisch glatten Oberfläche," DPMA: DE 102006057606.3. (2006).
- [2] Maurer, R.; Schneider, F.; Wuensche, C.; Rascher, R.: Calculation of the reference surface error by analyzing a multiple set of sub-measurements, Proc. SPIE 8838; <http://dx.doi.org/10.1117/12.2024003> (2013).

Tilted-Wave-Interferometry: Improving accuracy by elimination of systematic errors

J. Schindler, C. Pruß, W. Osten

A key factor for the success of the Tilted-Wave-Interferometer has been the development of sophisticated calibration algorithms [1].

Still, it is possible to further eliminate calibration errors. The measurement setup is designed for configurations far away from the null test providing the flexibility to measure a given specimen in a certain range of positions and orientations. One can exploit this freedom for schemes consisting of measurements in several different positions. The fundamental principle is that the surface under test (SUT) remains unchanged between the different measurements. Hence, redundancies occur and can be used in order to eliminate calibration errors.

Fig. 1 presents a simulation example of a system with some calibration errors: The top row shows the measurement results in two different rotations around the z-axis. An astigmatic error component is present. This could e.g. arise from a calibration with remaining errors in the reference sphere. The figure in the bottom right shows the ability to eliminate this part of the error by considering measurement configuration in different rotations around the z-axis leading to a decrease of the reconstruction error from 15 nm to 10 nm. Symmetries play an important role. E.g., rotationally symmetric calibration errors cannot be eliminated in this configuration.

A second approach is based on small translations or rotations. One can exploit the fact that either the calibration errors or the SUT remain approximately constant over a certain range of positions in the test space, depending on their gradients. Fig. 2 shows the different signal components that need to be distinguished: Both calibration error and phase difference due to the figure error are of the same magnitude. The difference between two laterally sheared positions shows a systematic behaviour: In the central patches, the change of the calibration error dominates whereas the outer show much larger contribution from the actual figure error. A model describing the calibration errors for each patch needs to be employed in order to take advantage of this kind of separation of signal components and is described in [2].

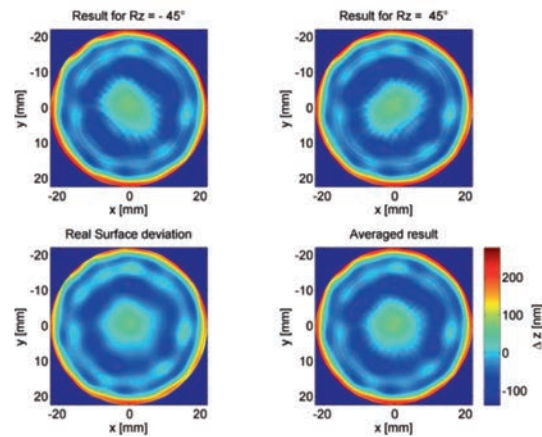


Fig. 1: Reconstructed surface errors in rotated positions (top row), true results (bottom left) and averaged result.

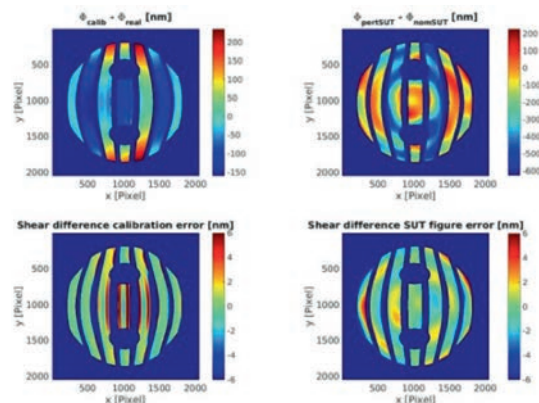


Fig. 2: Phase differences between OPL for calibrated and real QP polynomial (top left) and perturbed and nominal SUT (top right). The bottom row shows the difference of the above quantities for two positions shifted about 20 μm .

Supported by: DFG German Science Foundation
Project: Ein selbst-kalibrierendes Verfahren zur Vermessung von Asphären und Freiformflächen (OS 111/45-1)

References:

- [1] Baer, G.; Schindler, J.; Pruß, C.; Osten, W. "Calibration of a non-null test interferometer for the measurement of aspheres and free-form surfaces", *Opt. Express* 22 (2014) 25.
- [2] Schindler, J.; Bielke, A.; Pruß, C.; Osten, W. "Increasing the accuracy of Tilted-Wave-Interferometry by elimination of systematic errors", *SPIE Optical Metrology*, 2017.

Subwavelength diffractive optics for generation of cylindrical polarization states

CM. Mateo, O. Schwanke, L. Fu, C. Pruß, W. Osten

The race to the realization of efficient, simple, cost-effective and novel diffractive optical elements (DOE) for processing or forming cylindrical waves has just started. One particular example of such DOE is a polarizer that filters out azimuthal polarization distribution from an unpolarized or circularly polarized incident beam while allowing the radially polarized distribution to pass through. This has gained a lot of interest because of its several foreseen applications for example, in laser material processing. Such DOE already exist; however, the fabrication process to manufacture them still requires improvement in the context of simplicity and cost while not compromising the DOE's performance.

Within the SubWell project, the fusion of novel DOE conceptual designs and straightforward, cost-effective corresponding fabrication processes is studied. Three design variants were provided by the Institut für Strahlwerkzeuge (IFSW). Depending on the design, the DOE components can be used in terms of either the internal or external resonances in laser operation. The first design is the grating waveguide output coupler (GWOC) which is used inside the resonator and aims to select radially polarized distribution. The second design is a broadband intra-cavity grating mirror that converts the polarization and is based on sub- λ lattice structures. The third design is a transmissive polarization converter with a lattice periodicity that is much smaller than the wavelength of light.

These designs are implemented in Institut für Technische Optik (ITO) in which laser lithography and plasma etching techniques are utilized. In the first design, the circular grating lines were written using a direct laser writing technique on a resist-coated wedged fused silica (FS) substrate and then patterned by inductively-coupled plasma (ICP) etching. Alternating layers of Ta_2O_5 and SiO_2 were then deposited on the etched FS substrate with an antireflection (AR) coating at the backside. Table 1 shows the clean intensity distribution (LG01/ doughnut mode) of a beam was extracted out of the 1st generation of GWOCs [1].

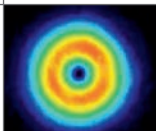
Design	Grating period (nm)	Etch depth (nm)	Intensity profile of the extracted beam
Grating waveguide output coupler	900	30	

Table 1: Grating parameters for the 1st generation of GWOCs. A clean and perfectly uniform LG01 (doughnut mode) intensity distribution was extracted out of the 1st generation of GWOCs [1].

Scanning beam interference lithography (SBIL) will be used to realize the structures with relatively small periodicities of the second design.

To implement the third design which is the transmissive extra-cavity polarization converter, a new interference-lithographic method, the so-called Scanning Mask Interference Lithography Exposure (SMILE) has been developed and tested successfully in ITO. The motivation behind this development is to reach the requirements set by the design which demands a grating period of 300 nm and an etch depth of 1 μ m. Figure 1 shows the schematic of the lattice design, the actual setup and an element after photoresist (PR) patterning. With this setup, the required complex lattice structure was written in a few exposure steps at a wavelength of 405 nm.

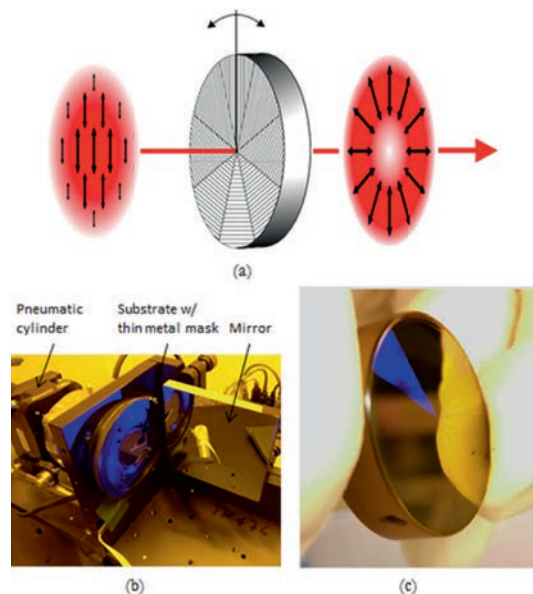


Fig. 1: (a) Schematic of the designed extra-cavity polarization converter utilizing the form-birefringence with Ta_2O_5 grating. (b) SMILE setup used to fabricate the (c) sector structure with linear gratings.

Supported by: AiF

Project: SUBWELL (IGF 18728 N)

In cooperation with: IFSW, University Stuttgart, with-in the programme for sponsorship by Industrial Joint Research (IGF) of the German Federal Ministry of Economic Affairs and Energy based on an enactment of the German Parliament.

References:

- [1] Eckerle, M., Dietrich, T., Schaal, F., Pruß, C., Osten, W., Ahmed, M.A.; Graf, T. "Novel thin-disk oscillator concept for the generation of radially polarized femtosecond laser pulses", Opt. Lett. 41, 1680 (2016).

3D laser direct-writing for injection compression molding of diffractive-refractive elements

S. Thiele, C. Pruß, M. Röder, D. Hera, T. Günther, A. Zimmermann, H. Kück, W. Osten

The success of diffractive optical elements (DOE) is strongly depending on capabilities in their fabrication. Traditionally, laser- or e-beam-based lithography processes are employed to generate high resolution binary and multi-level diffractive structures. Typically, the standard substrates are flat and allow for a plentitude of replication methods such as injection molding, hot embossing, roll-to-roll fabrication and others. However, extending the application of DOE to curved substrates as required for efficient optical designs imposes technical challenges.

Compared to direct tool fabrication by ultra-precision micromachining, laser direct-writing (LDW) offers significant advantages when it comes to resolution and design flexibility [1]. LDW can overcome short-comings of ultra-precision diamond turning regarding structure size, shapes and orientation, which

with high lateral resolutions down to the sub-micrometer level [2].

LDW is the first step in the process chain as displayed in fig. 1. Since the final application of the mass replicated hybrid refractive-diffractive lenses is working in the near infrared, comparably high DOE modulation depths in the region of $1.6 \mu\text{m}$ become necessary. Together with periods down to $5 \mu\text{m}$ this leads to challenging aspect ratios. An iterative optimization process ensured that the required modulation depth could be reached across most of the lens surface.

The resulting curved photoresist master was used to create a stamper by using Ni electroplating. The structure could be transferred onto the metal stamper with nanometer accuracy.

By means of injection compression molding, the DOE structure was then transferred into a thermoplastic transparent material. The molded element reveals a homogeneous density distribution and low birefringence.

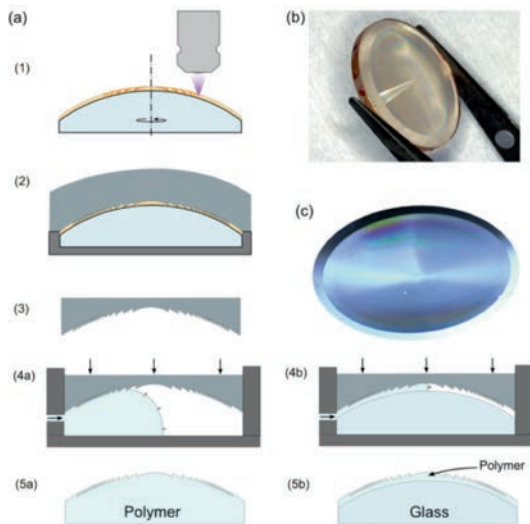


Fig. 1: (a) Process chain: (1) LDW, (2) Ni electroplating, (3) stamper fabrication, (4a) monolithic injection stamping, (4b) hybrid injection stamping, (5a) monolithic element, (5b) hybrid element. (b) Master in photoresist. (c) Stamper after electroplating. [3]

are restricted by the tool radius and the feasible tool paths. The method was optimized to allow for writing of continuous diffractive profiles in a grayscale photoresist process on curved substrates with surface angles of up to 15° . In particular, the LDW method excels in writing non-rotationally symmetric DOE

Supported by: AiF

Project: HOLEOS

In cooperation with: Hahn-Schickard, Stuttgart, within the programme for sponsorship by Industrial Joint Research (IGF) of the German Federal Ministry of Economic Affairs and Energy based on an enactment of the German Parliament.

References:

- [1] Häfner, M.; Reichle, R.; Pruß, C.; Osten, W. "Laser direct writing of high resolution structures on curved substrates: evaluation of the writing precision", Proc. Fringe 2009, Springer, Heidelberg.
- [2] Hopp, D.; Pruß, C.; Osten, W.; Seybold, J.; Fritz, K.-P.; Botzemann, T.; Mayer, V.; Kück, H. "Diffractive incremental and absolute coding principle for optical rotary sensors", Appl. Opt. 50(26), pp. 5169-5177 (2011).
- [3] Röder, M.; Hera, D.; Thiele, S.; Pruß, C.; Günther, T.; Osten, W.; Zimmermann, A. "3D laser direct-writing based master fabrication for injection compression molding of diffractive-refractive elements", Conference Abstract EOSAM 2016, not officially published, no external copyright claims.

Parts of this paper were directly taken from [3].

In situ fabrication of microstructures for encoder systems

R. Hahn, C. Pruß, F. Schaal, W. Osten

The progress in automation and the increasing requirements on precision in the fabrication of novel technical products are leading to increasing demands on mechanical movements and therefore the feedback systems, e.g. shaft encoders. Minimal encoder errors and at the same time the flexibility to adapt to customer's needs are getting more and more important. To satisfy those needs, the BMBF project PhotoEnco under the leadership of Sick Stegmann GmbH explores a radically new fabrication approach for high-resolution customized encoders: Instead of the traditional assembly of prefabricated encoder discs, new photonic technologies are used to define the angular scales in one of the last steps within the assembled system.

There are many different types of encoders. In optical encoders, the signal is typically generated with an encoder disc in combination with a read-out grating. The encoder disc is fabricated in a lithographic process and afterwards mounted into the encoder. If the rotational axis of the encoder disc is not perfectly aligned to the encoder axis, the device will detect wrong angular positions. The in-situ fabrication of the encoder disc developed within the project will avoid such errors.

Therefore a circular laser direct writing system (CLWS), which writes the needed structures while the already mounted encoder disc is rotating around its axis, will be developed. To obtain the required contrast without any chemical post exposure processing new photoresists must be developed. The necessary chemical substances are developed by Allresist GmbH, while their processing and characterization is accomplished at ITO. Beside the use of photoresist, ACSYS GmbH evaluates, whether laser chrome ablation is a feasible alternative for encoder disc production in a CLWS.

The first modulation principle evaluated was refractive index variation based on a negative resist. After illumination and a followed post exposure bake, the resist changes its refractive index in the illuminated areas. Fig. 1 shows a microscopic image of a linear grating written into the resist. In an interferometer, an index variation of 0.008 was measured. This index variation can be used for the generation of diffractive elements, which also can be used for contrast generation in shaft encoders.

Another examined resist evaporates, when it is processed with high optical intensities at 532 nm. The first experiments showed different states

of evaporation. In lower power regions, there is a kind of "blow-up" detectable, where the resist forms hills. We have shown a remarkable resolution of these structures of < 500 nm, yet the maximum achievable height was limited to ~ 100 nm, see fig. 2. When the power is high enough, the material evaporates as expected, see fig. 3. Like the first resist, this resist changes the phase of the incoming light and is therefore suited for the fabrication of diffractive encoder structures.

Other resists developed by Allresist irreversibly change their optical density when heated above a temperature threshold. These resists are good candidates for the generation of apertures usable for the fabrication of encoder discs as well as for many other technical devices.

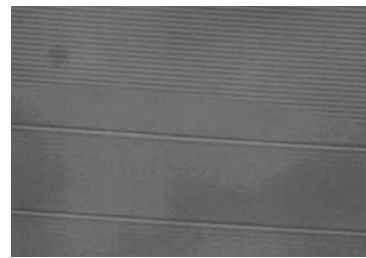


Fig. 1: Linear grayscale grating written in a refractive index changing resist.

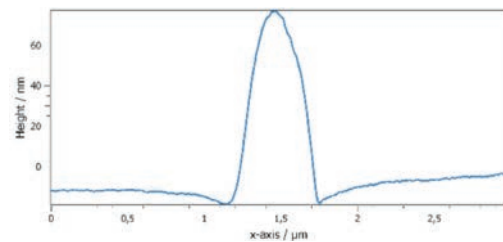


Fig. 2: Resist topography of a laser induced structure.

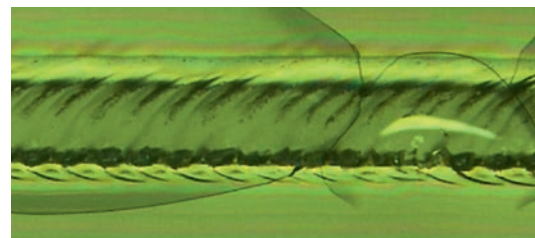


Fig. 3: Ablated resist structure. Line width: $50 \mu\text{m}$.

Supported by: BMBF
 Project: "PhotoEnco – Photonisch strukturierbare Werkstoffe und photonische Prozesse für die individualisierte Herstellung von Encodermaßverkörperungen und deren Abtasperipherien"(13N10854)
 In cooperation with:
 Sick Stegmann, Allresist, Acsys, STVision

Microscope objective integrated optically addressable polarization shaping

A. Bielke, C. Pruß, F. Schaal, W. Osten

Compared to electrically addressed spatial light modulators (e.g. LCOS-SLMs) optically addressed spatial polarization modulators can generate high resolution patterns without pixel artefacts. This results in improved efficiency, less stray light and no spurious diffraction orders.

The principle of operation is based on a photochrome material. Birefringent properties of the material are changed by illumination with red light. The spatial shaping of the light field is achieved by structured illumination of the thin photochrome material layer.

To use the optically addressed material, an optical addressing module is needed. These are usually spacious and have fixed illumination patterns.

To overcome these restrictions we created a compact optical addressing module based on 200 independently switchable VCSEL light sources and a hybrid diffractive/refractive beam shaping optics. It has a diameter of less than 30 mm and can be mounted inside a microscope objective (figure 1).



Fig. 1: Microscope with objective integrated spatial polarization shaping system.

The packing density relies on a VCSEL array (emission at 650 nm wavelength). Therefore it was necessary to develop a new fast and reversible optical addressable material [1]. Red light illumination of the material induces a spatial birefringence change $\Delta n(x,y)$ in the system of up to 0.2 .

The optically addressed layer is placed in the pupil of the microscope objective. Therefore the system can be used for manipulation of the imaging.

One application is tuneable phase contrast.

By tuning the VCSEL currents the illumination patterns can be altered. This can be used to optimize the phase contrast parameters for the specimen and enhance the desired contrast (figure 2).

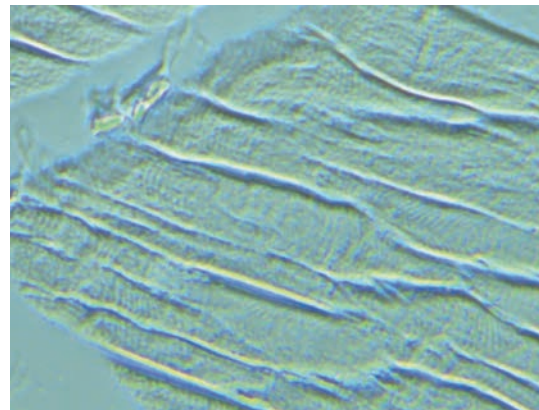


Fig. 2: Tuneable phase contrast image of rabbit taste bud cells.

The system might be also used for other purposes e.g. spatially tuned polarized illumination patterns for material analysis or all optically tuneable systems.

Supported by: DFG

Project: OS111/35-1

In cooperation with: IHFG (University Stuttgart), University Potsdam, Fraunhofer IOF, Jena.

This project is part of the DFG priority programme 1337 "Active micro optics"

References:

- [1] Schaal, F.; Rutloh, M.; Weidenfeld, S.; Osten, W. (2015). Chapter 8 Spatially Tunable Polarization Devices. *Tunable Micro-optics*, p.197, Cambridge University Press.
- [2] Schaal, F. et al.: Proc. of the International Workshop on Photonics Polymer for Innovation, JST, Japan, 2016

Coherent Metrology



Large field of view optical elastography for biological soft tissue investigation 72

*Supported by: Jointly founded project IoC105 (state of Baden-Württemberg, Aesculap AG and the Universities of Tübingen and Stuttgart under the Scope of the Industry on Campus initiative)
In cooperation with: the Institute for Materials Testing, Materials Science and Strength of Materials (IMWF) and the Institute for system dynamics (ISYS) at the University of Stuttgart, and the clinics for urology and gynaecology at the Eberhard Karls University in Tübingen*

Residual stress analysis of ceramic coating by laser ablation and digital holography.....74

*Supported by: DFG German Science Foundation
Project: Ermittlung von Eigenspannungen in beschichteten Oberflächen (OS 111/37-1).
In cooperation with: IFKB, Universität Stuttgart, Prof. R. Gadow and IMW, Universität Stuttgart, Prof. S. Schmauder.*

Nano-scale measurement of in-plane displacements of microscopic objects 76

*Supported by: DFG German Science Foundation
Project: Remote Laboratory for Optical Micro Metrology (OS 111/39)
and the Sino-German Center under grant GZ-760.
In cooperation with: Shenzhen University, China, Prof. Xiang Peng.*

Combination of FEM-simulations and shearography for artwork inspection..... 77

*Supported by: DFG German Science Foundation
Project: Die materielle Veränderung von Kunst durch Transporte (OS 111/34-2)
In cooperation with: Staatliche Akademie der Bildenden Künste Stuttgart, Prof. Christoph Krekel*

Focus and perspective adaptive digital surgical microscope 78

*Supported by: IoC215 (state of Baden-Württemberg, Carl Zeiss Meditec and the Universities of Tübingen and Stuttgart)
In cooperation with: the department of Technische Informatik at the Eberhard Karls Universität Tübingen and Carl Zeiss Vision Lab in Tübingen*

Replacing conventional microscope objectives by a scattering plate: a comparative study 79

Spectrally resolved digital holography by using a white LED 80

*Supported by: European Commission, H2020
Project: HOLO (TWINN 687328)*

Light field endoscopy and its parametric description 82

Supported by: Jingdan Liu acknowledges the financial support from the China Scholarship Council (CSC, No. 201506030010).

Iterative phase retrieval based on variable wave-front curvature 83

*Supported by: Jointly funded project IoC105 (state of Baden-Württemberg, Aesculap AG and the Universities of Tübingen and Stuttgart under the Scope of the Industry on Campus initiative)
In cooperation with: the Institute for Materials Testing, Materials Science and Strength of Materials (IMWF) and the Institute for system dynamics (ISYS) at the University of Stuttgart, and the clinics for urology and gynaecology at the Eberhard Karls University in Tübingen.*

Digital Holography for erosion monitoring inside the ITER Tokamak..... 84

Supported by: International Thermonuclear Experimental Reactor (ITER)

Large field of view optical elastography for biological soft tissue investigation

D. Claus, G. Pedrini, W. Osten

In minimally invasive surgery the haptic feedback, which represents an important tool for the localization of abnormalities, is no longer available. Elastography is an imaging technique, which results in quantitative elastic parameters. It can hence be used to replace the lost sense of touch, as to enable tissue localization and discrimination. For the implementation of optical elastography, we have chosen digital image correlation based on a spectrally engineered illumination source, that enables imaging of biological surface markers (blood vessels) with high contrast. In digital image correlation, two images (loaded and unloaded) are recorded. The displacement introduced by loading is calculated using locally defined cross-correlation within a small window. Our window is 65x65 pixels with 50% overlap between consecutive windows.

The mechanical loading is generated using a rolling indenter shown in fig. 2, which enables the investigation of large organs (size of the kidney) with reduced measurement time compared to a scanning approach. Furthermore, the rolling indentation results in strain contrast improvement and an increase in detection accuracy based on averaging approach, as demonstrated in [1].

From the displacement measurements the strain distribution, representing a quantitative elastic parameter, can be calculated. However, other elastic parameters such as stress, shear modulus cannot be obtained from the measurements. An under-defined inverse problem has to be solved to access these parameters. This is commonly accomplished using a well-defined forward problem that is implemented in a finite element model (FEM), which starts with the desired parameters of interest (input) and results in the measurable parameters (output). In an iterative manner, adjustment of input parameters, a good match between experimental and simulated data can be ensured and in that manner, other elastic parameters are retrieved, as schematically depicted in fig. 2. The amount of necessary iterations can further be reduced via the application of a priori knowledge.

In our case, only one iteration was necessary to obtain a good match between measured and simulated strain, see fig. 3. Our simulation is based on the implementation of a 3D hyperelastic model into an FE environment (Arruda-Boyce model).

Not only the uniaxial 3D distribution of strain, stress and shear modulus but all the different corresponding tensor components are retrieved for different indenter position. The results of which are presented in [1].

The application of digital image correlation was also demonstrated for a biological sample (kidney). The strong absorption of blood vessels in green light compared to the surrounding tissue could be used to generate traceable surface markers. The strain map obtained, as shown in fig. 4.

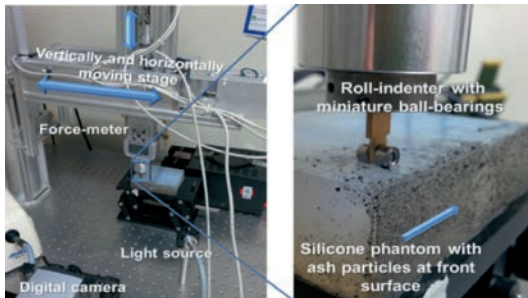


Fig. 1: Roll-indenter with silicone phantoms

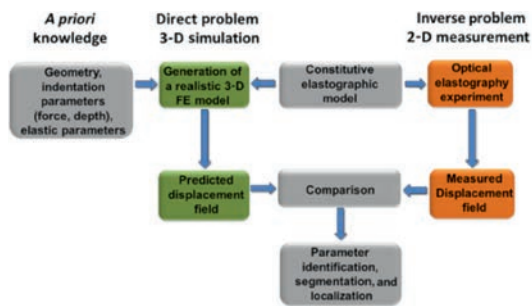


Fig. 2: Parameter-identification based on the comparison between the outcome of the FE-model (solution of direct problem) and experimentally measured values (displacement field and strain map).

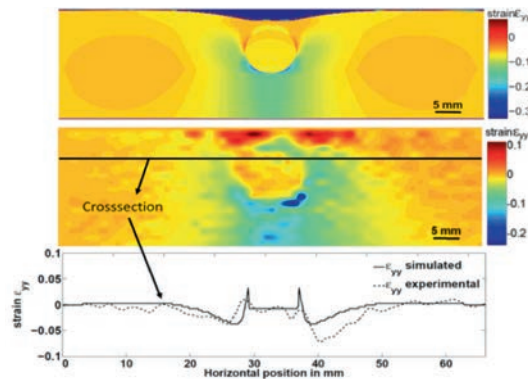


Fig. 3: Comparison between FE Simulation (top) and experimentally obtained strain map (bottom) with cross-section plot, highlighted by dark line in experimental data .

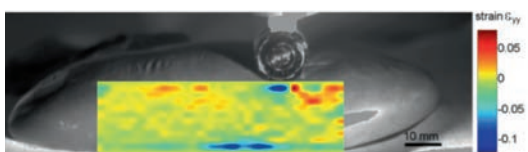


Fig. 4: Strain map obtained from porcine kidney.

Supported by: Jointly founded project IoC105 (state of Baden-Württemberg, Aesculap AG and the Universities of Tübingen and Stuttgart under the Scope of the Industry on Campus initiative)

In cooperation with: the Institute for Materials Testing, Materials Science and Strength of Materials (IMWF) and the Institute for system dynamics (ISYS) at the University of Stuttgart, and the clinics for urology and gynaecology at the Eberhard Karls University in Tübingen

References:

- [1] Claus, D.; et al. "Large-field-of-view optical elastography using digital image correlation for biological soft tissue investigation", J. Med. Imag. 4(1), 014505, 2017.

Residual stress analysis of ceramic coating by laser ablation and digital holography

G. Pedrini, W. Osten

Ceramic coatings are commonly used to improve the wear or heat resistance of many technical components, but due to their deposition process, e.g. plasma or high velocity oxygen fuel spraying, rather high residual stresses can build up within the coating and underneath. The reason for that are differences in the coatings and substrates expansion coefficients, inhomogeneous temperature distribution during the process and the quenching of splats. The mechanical hole drilling technique can be used for the detection of residual stresses in coatings. The residual stresses are locally relieved due to the material removal process, which leads to a deformation of the surface around the hole. These deformations, measured as relaxed strains through strain gauges rosettes, in combination with appropriate calibration data (separately determined by simulation for the layer composite), allows the quantitative determination of the residual stress depth profile. The disadvantage of the strain gauges is that they can only be used on flat and relatively smooth surfaces, where the rosette is applied.

We propose an approach (see fig. 1) to avoid the mechanical drilling operation and the application of strain gauges, where a pulsed laser is used for the object machining (ablation process) leading to 3D residual deformation by stress relaxation which are measured by an optical system based on digital holographic interferometry. The residual stresses at different depth of the coating are calculated from the deformations obtained after incremental loading, the profile (shape, depth) of the machined surface and the material parameters. Figure 2 (a) shows a milled horizontal bar obtained after 64000 laser pulses, the depth of the machined structure is 130 μm . Figures 2 (b-g) show the wrapped phase and the corresponding 3D deformations produced by the milling. Figure 3 shows the results of the residual stress calculations by using conventional mechanical incremental hole drilling with strain gauges and the proposed method with laser ablation and digital holography. The coating used for the investigations had a thickness of 200 μm .

The results obtained by the conventional hole drilling and the proposed methods show the same qualitative behaviour but of course there are differences between the two curves. The mechanical incremental hole drilling determination alone cannot validate the results. I.e. X-Ray diffraction measurements near the surface proved high residual stresses around -600 MPa. The inaccuracies are due to the non-ideal geometry produced by laser ablation that produce errors in the calculation of the residual stresses in particular for the very first step.

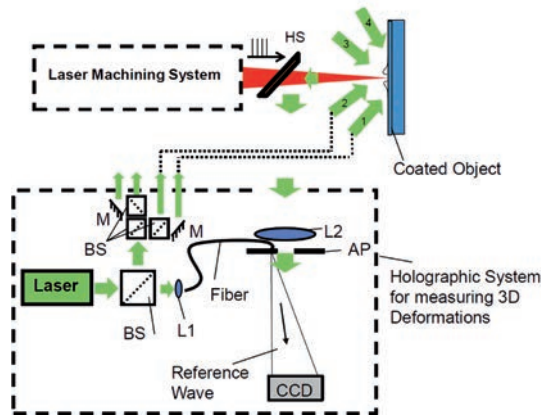


Fig. 1: Setup for laser machining and measurement of the 3D object deformation by digital holography. HS: harmonic separator.

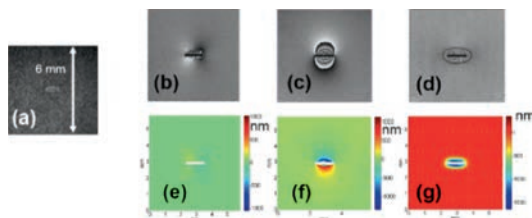


Fig. 2: Image of the bar shaped machined structure after 64000 laser pulses (a). Phase modulo 2π (wrapped phases) and calculated displacements along the x (b, e), y (c, f) and z (d, g).

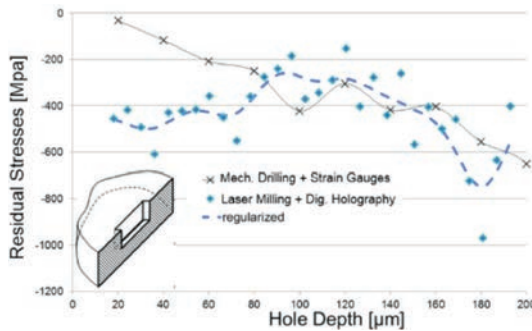


Fig. 3: Residual stress determined by conventional mechanical incremental hole drilling and strain gauge measurement and the proposed method with laser notch ablation and digital holography.

Supported by: DFG German Science Foundation
Project: Ermittlung von Eigenspannungen in beschichteten Oberflächen (OS 111/37-1).

In cooperation with: IFKB, Universität Stuttgart,
Prof. R. Gadow and IMW, Universität Stuttgart,
Prof. S. Schmauder.

References:

- [1] Pedrini, G.; Martínez-García, V.; Weidmann, P.; Wenzelburger, M.; Killinger, A.; Weber, U.; Schmauder, S.; Gadow, R.; Osten, W. "Residual stress analysis of ceramic coating by laser ablation and digital holography", *Exp. Mech.* (2016) 56: 683.
- [2] Weidmann, P.; Weber, U.; Schmauder, S.; Pedrini, G.; Osten, W. "Numerical calculation of temperature and surface topology during a laser ablation process for ceramic coatings", *Meccanica* (2016) 51: 279.

Nano-scale measurement of in-plane displacements of microscopic objects

A. K. Singh, G. Pedrini, W. Osten

Digital image correlation (DIC) digital speckle pattern interferometry (DSPI), digital holographic interferometry (DHI) and phase singularities tracking (PST) may be used to measure displacements. DIC is very robust due to its simple arrangement and is commonly used for the measurement for in-plane displacements. DSPI and DHI are interferometrical techniques allowing the measurement of in-plane and out-of-plane displacements. PST is a new tool for optical metrology that may provide displacement measurements with nanometric accuracy since a displacement of the object involves a shift of the singularities of the wavefront reflected by the object. We need phase information to find the singularities. One way to record the phase is by using digital holography. The other way is to use the intensity pattern and to process it using a Hilbert filtering in order to obtain a pseudo phase.

Figure 1 shows the setup used for the measurements of in-plane displacements of microscopic samples. The object is illuminated with coherent light emitted by a laser. The light scattered by the sample is again collected by the lens L2 which images the surface of the object on the pixelated sensor. The images recorded at different deformation states of the samples are then processed to find the in-plane displacement. A reference wave can be used when the phase of the wavefront is needed.

The test object was a rough metallic surface mounted on a calibrated piezoelectric device (Physik Instrumente P-611.1, accuracy ± 2 nm). Windows of 100×100 pixels was considered and the results obtained with the different methods are shown, together with the expected displacements (blue lines) in fig. 2. In figs. 2, a), b) the measurements obtained by digital image speckle correlation and vortices analysis, are reported. For obtaining these results the same intensity pattern were used, just the processing was different. The difference between measured and expected displacements may be used for the calculation of the accuracy of the measurements which is ± 5.6 nm for the correlation and ± 9.5 nm for the vortices tracking methods. The correlation method gives better results, the vortices method overestimate the displacement. We recorded also digital holograms for different displacements and calculated the intensity and the phase of the wavefront. The in-plane displacements

were evaluated by intensity correlation and by vortices analysis. For both evaluation methods, the displacement is underestimated and the deviation from the expected values is quite large (see fig. 2. c, d).

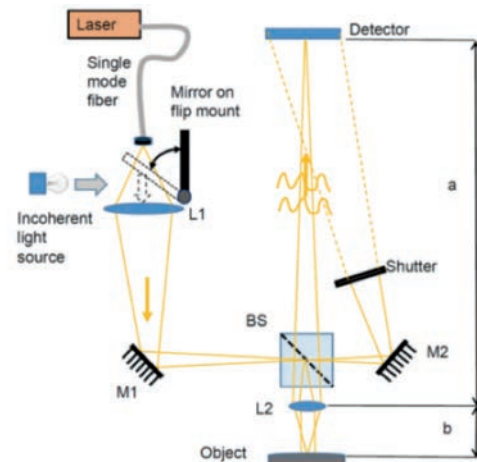


Fig. 1: Setup for the measurement of in-plane and out-of-plane (when the reference is used) displacements.

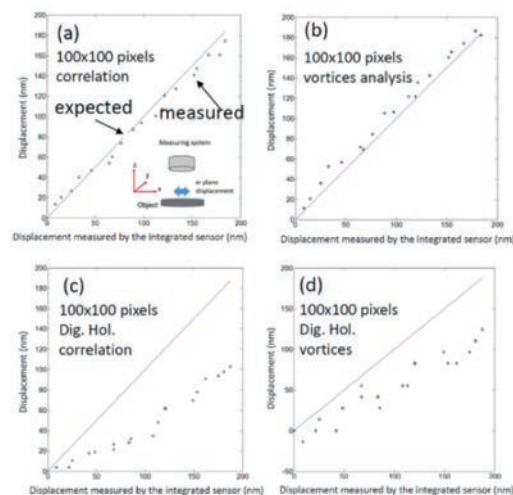


Fig. 2: Comparison of in-plane displacements measurements by different methods.

Supported by: DFG German Science Foundation Project: Remote Laboratory for Optical Micro Metrology (OS 111/39) and the Sino-German Center under grant GZ-760.

In cooperation with: Shenzhen University, China, Prof. Xiang Peng.

References:

- [1] A. Singh, G. Pedrini, X. Peng, W. Osten, "Nanoscale measurement of in-plane and out-of-plane displacements of microscopic object by sensor fusion", Opt. Eng. 0001;55(12):121722.

Combination of FEM-simulations and shearography for artwork inspection

D. Buchta, G. Pedrini, W. Osten

The preservation of artwork is an important as well as a challenging task for conservators. In recent times, the increase of museum loan services and the associated increasing number of transports makes this task even more challenging. Especially hidden defects like delaminations or woodworm tunnels in wooden panel paintings are difficult to detect. While tactile methods are rather unsuitable for the application on artworks, optical techniques provides the possibility of non-destructive testing.

Among others the so called shearography has proven its suitability for the detection of sub-surface defects [1-2]. The typical shearographic setup, shown in fig. 1, consists of an expanded laser beam, a Michelson interferometer, a camera and a loading device. Due to a slightly tilted mirror a self-reference is generated, which makes the setup very robust. The comparison of two states (before and after loading) gives information about the surface displacement induced by the loading and so about underlying damages.

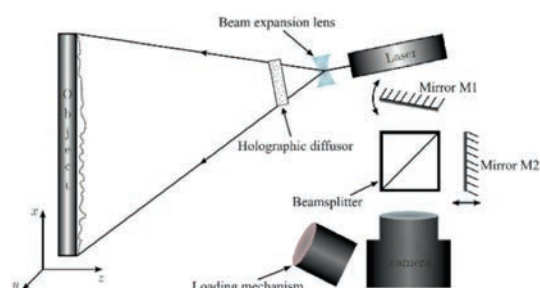


Fig. 1: Shearographic setup.

The main disadvantage of this technique is that the "indirect" measurement allows only limited conclusions about the defects. Especially, the depth cannot be determined uniquely.

To get access to this information, the deformation of the surface due to the defects under stress has to be analyzed. We do this by combining FEM-simulation with shearographic simulation. Therefore a displacement-map is generated with a standard FEM-software (COMSOL) and inserted in the shearographic simulation (matlab), which calculates sensitivity vectors and generates the phase images. In our approach we add furthermore multiplicative speckle noise to the intensity images before the phase maps are calculated to get on one hand more realistic results and on the other hand the possibility to investigate noise-reducing techniques.

Fig. 2 depicts a first comparison of measurement and simulation with different variance of the speckle noise for a wooden panel with milled notches (defects) at the backside. The panel was heated by an infrared lamp from 24°C to 26.3°C (reference state) and cooled afterwards to 25.7°C (loaded state). The good agreement especially for large speckle noise is a very promising result. In near future the simulation environment can be used to investigate different types of defects in various depth and so enlarge the information content in shearographic measurement.

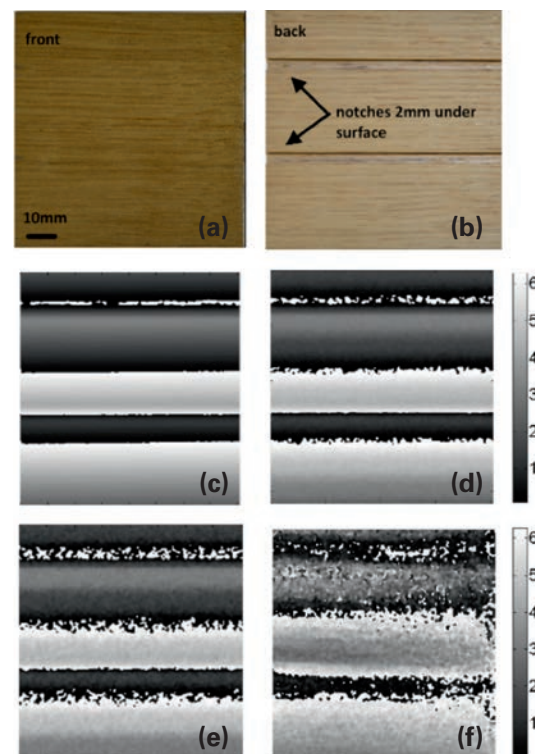


Fig. 2: Comparison of simulations for a speckle noise with variance 0 (c), 0.22 (d), 1 (e) with measurement (f) for a wooden panel with notches at the backside (a,b).

Supported by: DFG German Science Foundation
Project: Die materielle Veränderung von Kunst durch Transporte (OS 111/34-2)

In cooperation with: Staatliche Akademie der Bildenden Künste Stuttgart, Prof. Christoph Krekel

References:

- [1] Groves, R.; et al. "Shearography as part of a multi-functional sensor for the detection of signature features in moveable cultural heritage", Proc. SPIE 6618, (2007).
- [2] Buchta, D.; et al. "Artwork Inspection by Shearography with adapted loading", Experimental Mechanics, doi: 10.1007/s11340-015-0070-9 (2015).

Focus and perspective adaptive digital surgical microscope

D. Claus, C. Reichert, A. Herkommer

Conventional surgical microscopes suffer from the drawback that during the operation the surgeon has to remain in the same position for a long period of time. This causes musculoskeletal strain possibly resulting in severe headaches and chronic pains. It is our goal to provide the surgeon with a digital surgical microscope, which offers all the functionality the surgeon experiences with a conventional microscope, albeit offering the freedom of free head movement via displaying the image on a screen or digital stereoscopic displays. The digital surgical microscope is composed of two units. First, a recording unit represented by a digital recording stereo microscope, which offers accommodation and pupil shift, enabled by the application of an adaptive optomechanical system. Second, a displaying unit, which can be represented by a digital stereo displaying microscope or a 3D monitor. Head and eye tracking are applied to the displaying unit in order to obtain a signal for shifting the pupil in the recording unit. The signal relevant for the accommodation adjustment in the recording unit can be obtained from a refractometer or via eye tracking combined with scanning the topography and refocusing on the region of interest. The digital recording stereomicroscope is based on the application of focus adjustable lenses for mimicking the eye's accommodation and an x-y shifted stage for mimicking the eye's pupil movement. Furthermore, an additional optical system has been designed, which enables eye-tracking through the displaying stereomicroscope. The digital displaying stereo microscope used is a prototype developed by Carl Zeiss Meditec. The developed pupil tracking system is easily attachable to the existing digital displaying stereomicroscope. A beamsplitter plate was used to enable the combination of the eye-tracking system with the displaying system, as shown in fig. 1.

The temporal requirement imposed on the digital recording stereomicroscope is to deliver a temporal resolution better than 50 ms (20 Hz) in accordance to the human eye's latency. Therefore, fast focus adjustable lenses from Optotune AG (EL-10-30-C-VIS-LD, 60 Hz, focal length 80 mm–200 mm), and an in-house configured fast moving x-y stage with actuators from Nanotec Electronic GmbH (L2818L0604-T5X5, max. speed 140 mm/s) have been selected. The important optical parameters have been derived from a conventional stereomicroscope (Zeiss OPMI

Pico) comprising of a field of view of 30x30 mm² and an optical resolution of 50 μ m. Furthermore, special attention during the optic design was given to maintain a large NA via the introduction of the reflection prisms positioned behind the main objective, and by mounting the Optotune lens in a horizontal orientation as to minimise the effect of coma on the image quality. The final realized setup and the corresponding images obtained for different foci and different position of the pupil are shown in fig. 2.

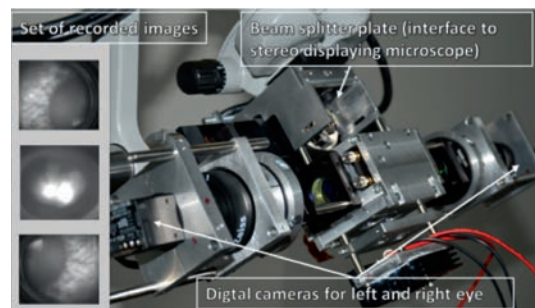


Fig. 1: Pupil-monitoring setup through digital displaying stereo-microscope.

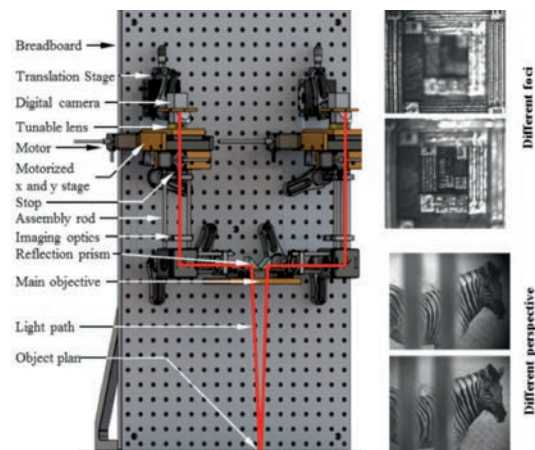


Fig. 2: Schematic setup digital recording stereomicroscope with images obtained from different foci and perspective.

Supported by: IoC215 (state of Baden-Württemberg, Carl Zeiss Meditec and the Universities of Tübingen and Stuttgart)

In cooperation with: the department of Technische Informatik at the Eberhard Karls Universität Tübingen and Carl Zeiss Vision Lab in Tübingen

References:

- [1] Claus, D.; Reichert, C.; Herkommer, A. " Focus and perspective adaptive digital surgical microscope: Opto-mechanical design and experimental implementation ", *J. Biomed. Opt.* 22(5), 056007, 2017.

Replacing conventional microscope objectives by a scattering plate: a comparative study

A. K. Singh, G. Pedrini, M. Takeda, W. Osten

Traditional lens-based microscope objectives have fixed focal length, short working distance, limited depth of focus and magnification, which often sets restrictions in applications. The correction of aberrations for microscope objectives requires a combination of spherical lenses, which increases complexity, bulkiness, and price. Aspherical elements can reduce the complex multiple-lens system and make the objectives more compact, but they demand more complex fabrication and testing procedures, which also raises the cost. Figure 1(a) and (b) show the impulse response of a conventional microscope objective and the imaging operation, respectively.

Contrary to the common belief, we regard the diffusing media itself as a useful imaging device. We exploit the lens-like behavior of a scattering layer, and develop unconventional lensless microscope objectives. The impulse response in this case is a speckle pattern as shown in Figure 1(c) which remains shift invariant in the close vicinity of the point source. This phenomenon is called memory effect, which states that each elementary point source that constitutes the object, placed in the vicinity of the reference point source, produces a shifted but similar speckle pattern to that of the point source. The images are produced from the cross-correlation of the object intensity distribution and the PSF. The images produced from the conventional microscope imaging and image reconstruction via intensity cross-correlation are shown in Figs. 1(e-h).

A result of diffuser microscope imaging of a 1951 USAF test target and a comparison with images from a conventional microscope is shown in Figure 2. It can be seen that the quality of the images, in terms of resolution and contrast, of the diffuser microscope is almost comparable to that of a conventional microscope even though the edges look less sharp.

The scattering layer microscope has following unique characteristics that are not available with traditional microscopes:

- extremely thin and light
- variable focal length and magnification,
- variable NA and field of view,

- flexible working distances,
- compatible in reflection and transmission modes,
- immune to phase disturbances and aberrations,
- easy to fabricate with scalability in device size, robust to environmental changes.

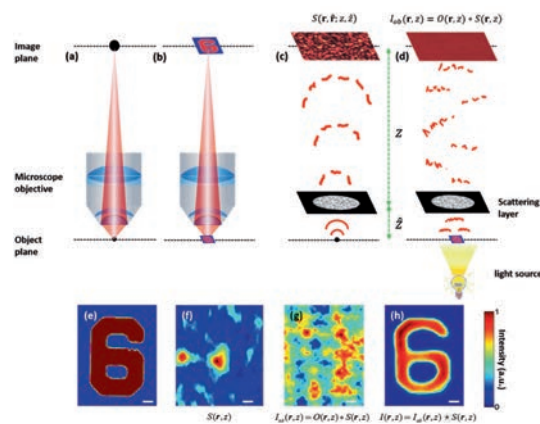


Fig. 1: Microscope imaging systems: (a) PSF of a conventional microscope objective (b) conventional microscope imaging (c) PSF of a scattering layer, which in this case is a speckle pattern, (d) microscope imaging using a scattering layer ('diffuser microscope'). The image plane is far from the diffuser, to have a larger magnification. The images are produced from the cross-correlation of the object intensity distribution and the PSF. (e) Conventional microscope image, (f) a part of the PSF of the scattering layer (speckle pattern), (g) a part of the recorded object intensity distribution and (h) the image reconstruction via intensity cross-correlation. The scale bar is $3 \mu\text{m}$ in object space.

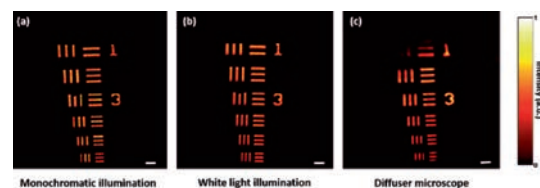


Fig. 2: Comparison of conventional and scattering layer microscope imaging: A 1951 USAF test target was used as an object. We imaged the highest resolution area of the test target, i.e. the 7th group, with smallest line thickness of $2.19 \mu\text{m}$; (a) and (b) are the images obtained with a conventional microscope for NAs 0.16 under monochromatic and white light illuminations, respectively, whereas, (c) is their diffuser microscope counterpart for the same NA. The scale bar is $21.5 \mu\text{m}$.

References:

- [1] A. Singh, D. Naik, G. Pedrini, M. Takeda, W. Osten, "Exploiting scattering media for exploring 3D objects", *Light: Science & Applications* (2017) 6, e16219; doi:10.1038/lsa.2016.219, Published online 24 February 2017.

Spectrally resolved digital holography by using a white LED

D. Claus, G. Pedrini, D. Buchta, W. Osten

Usually, coherent light sources are employed in digital holography, but short coherent light sources such as emitted by a LED can likewise be employed. The spatial coherence of the light source was increased via locating a pin-hole straight after the LED. Due to the reduced temporal coherence both interfering arms had to be well matched with sub-micrometre accuracy using a combination of a precision stage and a piezo actuator both attached a roof prism in the reference arm, as shown in fig. 1.

A series of more than 1000 interferograms have then been recorded while a shift of 100 nm between each recording position was introduced by the piezo. The piezo scanning results in a z-stack. According to the Wiener Khinchin theorem, the application of the Fourier transformation along the z-direction results in the spectral distribution, whereas the spectral components are defined by the wavenumber k ($k=1/\lambda$) and not by the wavelength. The setup as it stands shares some similarities with white light interference microscopy or optical coherence microscopy. However, the acquisition and interpretation of the data are based on lensless holography, by which lenses, which may introduce wave-aberrations as well as chromatic aberrations or result in increased manufacturing efforts and consequently cost, can be discarded. Moreover, the holograms can be refocused. The advantage of spectrally resolved holography is demonstrated for the investigation the shape of an object with a thickness larger than the product of wavelength and the difference of refractive indices between the object and surrounding medium. In this case phase jumps occur as shown in fig. 2(a), which require unwrapping routines that can introduce errors. Moreover, at very steep surfaces the density of 2π phase jumps becomes very dense so that resolved any longer. The application of the dual wavelength method (DWM) can help to overcome this issue. The difference phase map of the holographic reconstruction recorded at two different wavelengths, which

are in close proximity, can be associated with a much larger synthetic wavelength λ_{syn}

$$\frac{1}{\lambda_{syn}} = \frac{1}{\lambda_1} - \frac{1}{\lambda_2} = k_1 - k_2 = \Delta k. \quad (1)$$

Besides the aforementioned advantage, DWM enables the application of optical and electrical devices in the visible light regime although the synthetic wavelength lies in the infrared regime. However, the speckle noise is increased by a factor that equals the ratio between synthetic and mean wavelengths of the chosen wavelength pair.

The large amount of wavelength pairs available in spectrally resolved holography helps to reduce the speckle via averaging over multiple dual wavelength phase maps of different wavelength pairing. The recovery of the wavenumbers k instead of the wavelength holds the further advantage that selecting the same difference between wavenumber pairs always results in the same synthetic wavelength λ_{syn} , which is not the case in the wavelength regime, as indicated by Eq. (1). The image quality is demonstrated in fig. 2(b) and fig. 2(c), for individual and averaging over multiple dual wavelength phase maps (particularly significant for upper left corner of both image). The cross-section plot along horizontal centre of both images is shown in fig. 3.

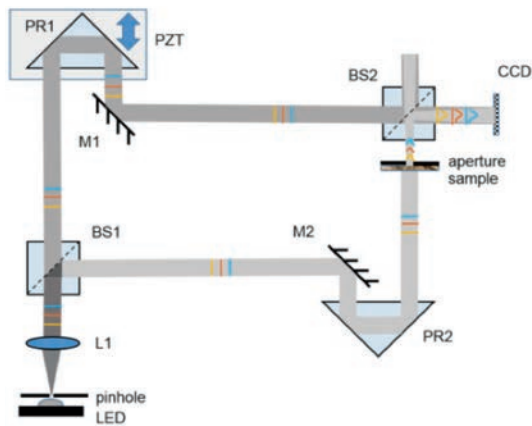


Fig. 1: Mach-Zehnder based spectrally resolved digital holographic setup.

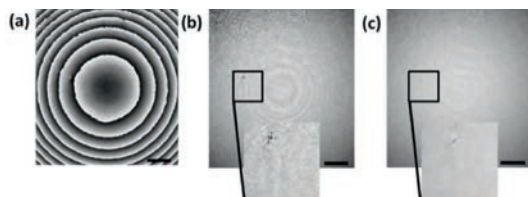


Fig. 2: Phase map of a lens in transmission mode: (a) at 447 nm, (b) at a $\lambda_{syn} = 9 \mu\text{m}$ individual, (c) $\lambda_{syn} = 9 \mu\text{m}$ averaged over 34 individual dual wavelength phase maps.

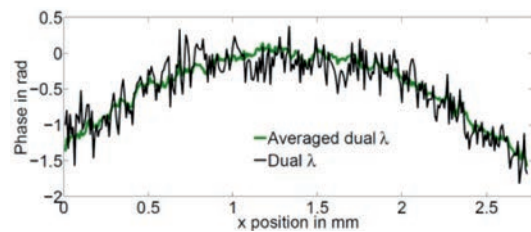


Fig. 3: Cross-section plot for individual dual wavelength and averaged dual wavelength map.

Supported by: European Commission, H2020
Project: HOLO (TWINN 687328)

References:

- [1] Claus, D.; Pedrini, G.; Buchta, D.; Osten, W "Spectrally resolved digital holography using a white light LED", SPIE Proceedings, Digital Optics Munich, Paper 10335-53, 2017.

Light field endoscopy and its parametric description

J. Liu, D. Claus, A. Herkommer, W. Osten

Imaging in minimally invasive surgery is performed via endoscopy or laparoscopy. Besides the many advantages it offers in comparison to open surgery (smaller scars, quicker recovery, and reduced risk of infections) it lacks three-dimensional vision, which makes it difficult to estimate the depth of objects and organs; useful information to navigate the instrument within the body. In fact, clinical reports demonstrate 97% of surgical accidents during laparoscopic intervention occur as a result of visual misperceptions. These errors can significantly be reduced when using 3D vision in minimally invasive surgery. We, therefore, introduce the snapshot light field imaging technique into endoscopy and build a 3D prototype, which we may thus call light field endoscope (LFE).

Our LFE works according to the following principle. A fibre based white light source is used as an illumination source. A conventional industrial endoscopy (KARL STORZ-ENDOSKOPE 86030SF) is employed. After the passage of light through the eye piece, the endoscope can be treated as infinity corrected optical system. In order to record images on the sensor, a lens is used between the endoscope and the CCD. A Schneider-Kreuznach 50 mm fix focus lens, of adjustable F-number ranging from 1.9 to 22, is employed in our setup. A microlens array (Thorlabs MLA150-5C, 10 mm x 10 mm size, 150 μm pitch size, 5.2 mm focal length) is placed at the image plane resulting in the so-called lightfield setup 1.0. A camera (SVS-Vistek eco655MVGE, 2050 x 2248 pixels, 3.45 μm pixel size), which is used to capture the light field of the specimen, is placed at the focal plane of the microlens array. The light field endoscopy setup and the light field image recorded are shown in fig. 1 and fig. 2(a), respectively.

By rearranging the pixels with respect to the location within each microlens subimage, an array of perspective images can be obtained, see fig. 2(b). At the next step, the acquired 4D light field was used to reconstruct the object at the different depth planes. According to the Fourier Slice Theorem, images

focused at different depths correspond to 2D slices at different trajectories. Therefore, the reconstruction of different depth planes from the perspective images can be accomplished via shifting and adding procedures. The results of this shifting and adding procedure are shown in fig. 3 for two objects placed at different z-positions.

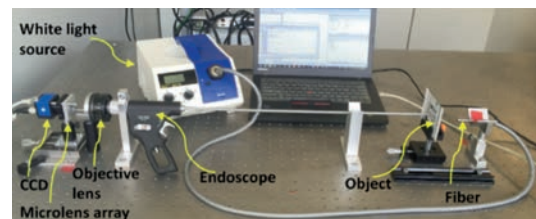


Fig. 1: Light field endoscope setup.

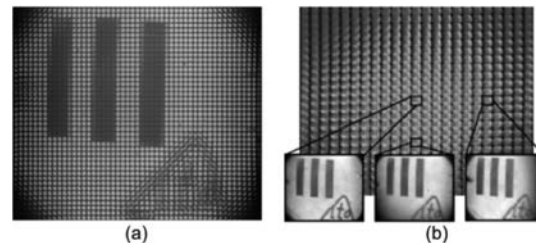


Fig. 2: (a) Recorded light field image, (b) array of reconstructed perspective images.

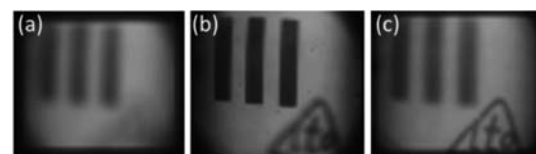


Fig. 3: Experimental results for digital refocusing (a) focused at a plane in front of endoscope's image plane, (b) focused at image plane, (c) focused at plane 10 cm behind image plane.

Supported by: Jingdan Liu acknowledges the financial support from the China Scholarship Council (CSC, No. 201506030010).

References:

- [1] Liu, J.; Claus, D.; Xu, T.; Keßner, T.; Herkommer, A.; Osten, W. "Light field endoscopy and its parametric description", *Opt. Lett.*, 42(9), 1804-1807, (2017).

Iterative phase retrieval based on variable wave-front curvature

D. Claus, G. Pedrini, W. Osten

Quantitative phase imaging enables the visualization of transparent objects with high contrast such as biological thin sections. In that manner, morphological features can be revealed intraoperatively without having to stain the sample resulting in a significant reduction of investigation time in histopathology. An environmentally stable setup is preferable to interferometrically based setup. This condition can be fulfilled via the application of phase retrieval imaging, which relies on the recording of diffraction pattern only. The key to phase retrieval imaging is the recording of the same information on multiple speckle de-correlated patterns. Various techniques have been developed based on this principle such as recording two or more intensity patterns while changing the object to sensor distance while moving an aperture across the object while illuminating the object with multiple wavelengths. The latter suffers from the problem of dispersion effects that result in different responses of the object under investigation with respect to the wavelength employed. Therefore, each of the recorded wavelength's corresponding speckle pattern may hold different information, which hinders or makes the application of the iterative phase retrieval approach impossible. Changing the object to sensor distance restricts the optical resolution, which corresponds to the diffraction pattern that is recorded furthest distant from the object (same spatial frequency content of all diffraction patterns). Here we discuss an alternative approach, whereas due to previous reasons not the distance between object and sensor, but the distance between the point source and object is changed. This has the same effect as changing the object sensor distance, albeit offering the advantage of preserving the resolution. Moreover, it is possible to employ the direct Fresnel propagation method without having to worry about the different pixel size in the reconstruction plane. Figure 1, shows the setup used to retrieve the object wavefront. The object is illuminated by a divergent wavefront originating from a point source (single mode fibre). The distance between point source and object are changed as to introduce longitudinal speckle decorrelation. The iterative reconstruction approach is based on the application of the direct Fresnel method. Due to its parabolic approximation, the Fresnel method cannot be applied in a step-wise propagation between the different diffraction planes, which are separated by a few millimeters only. In our case, the propagation is performed at each individual diffraction plane, at

which the modulus is replaced by the square root of the measured intensity. In a second step, from each diffraction plane, the wavefield is back propagated to the object plane. At the object plane, Parseval's theorem is applied, as to ensure the correct contribution of each diffraction pattern to the recovered complex amplitude. The phase retrieval approach and the results obtained are depicted in fig. 2. Furthermore, slight displacements between the individual reconstructions in the object plane could be corrected via the calculation of the amount of displacement using cross-correlation algorithm.

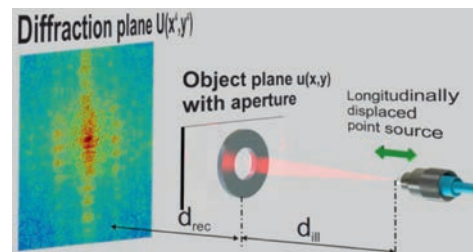


Fig. 1: Schematic setup with longitudinally displaced illumination source between consecutive recording positions.

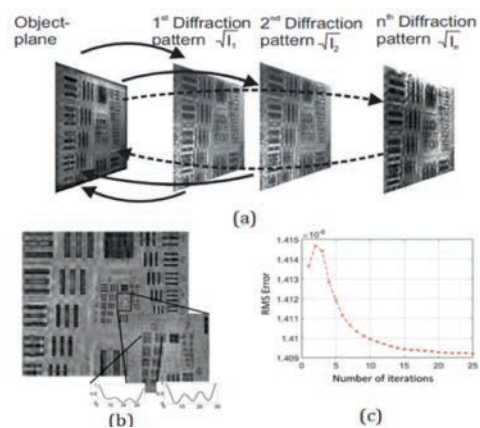


Fig. 2: (a) Phase retrieval approach, (b) modulus reconstruction, (c) RMS Error over number of iterations.

Supported by: Jointly funded project IoC105 (state of Baden-Württemberg, Aesculap AG and the Universities of Tübingen and Stuttgart under the Scope of the Industry on Campus initiative)

In cooperation with: the Institute for Materials Testing, Materials Science and Strength of Materials (IMWF) and the Institute for system dynamics (ISYS) at the University of Stuttgart, and the clinics for urology and gynaecology at the Eberhard Karls University in Tübingen.

References:

- [1] Claus, D.; Pedrini, G.; Osten, W. "Iterative phase retrieval imaging based on variable wave-front curvature ", *Appl. Opt.* 56(13), F134-F137, 2017.

Digital Holography for erosion monitoring inside the ITER Tokamak

G. Pedrini, I. Alekseenko, G. Jagannathan, G. Vayakis, W. Osten

The Tokamak reactor (see Fig. 1) is the heart of the International Thermonuclear Experimental Reactor Project (ITER Project). It fuses the hydrogen isotopes deuterium and tritium into a helium atom and a free neutron. The resulting fusion energy can be used for power generation. In nature, the fusion process takes place in stars like our sun and occurs at temperatures around 14 million Kelvin and very high pressure.

In order to obtain fusion on earth within low pressure, the temperature has to be increased significantly and thus the temperature of the plasma within the Tokamak is about 150 million Kelvin.

Because there is no material, which could withstand temperatures like these, the plasma is guided contactless by magnetic fields within the vacuum chamber. However, these fields are not fully closed, resulting in the escape of high energy particles. These particles are constantly hitting the inner wall of the reactor, which leads wear effects, affecting the overall performance of the Tokamak. Thus, there is a need for the continually measuring of the erosion at the wall, after the Tokamak was operating. An erosion monitor able to measure the changes in the surface shape with a depth resolution of 10 μm is planned. The erosion (change of shape) measurement will be done not on the whole internal surface of the Tokamak but only on two surfaces having each a size of 10x30 cm^2 .

Due to the high temperature and the radiations it will not be possible to have the measuring system inside the Tokamak, for this reason the measurements will be performed remotely where the electronic instruments

(detector, laser, controlling electronic) will be located at a distance of about 15 m from the surface to be measured.

A two (or multiple) wavelengths interferometric technique (digital holography) will be used for the erosion measurement. This technique has the ability to tackle the challenging environmental conditions within the Tokamak by a long distance measurement where a relay optic composed by mirrors, lenses and windows will be used for imaging the investigated surface on the detector.

Figure 2. (a) shows a test objects used for the first investigations. It is a rectangular metallic plate (45 x 27 mm^2) with steps having depths of 10, 20, 30, 50, 100, 150, 200 and 300 μm . The sample was located at a distance of 2.6 m and its shape was measured by multiple wavelengths digital holography. A titanium sapphire laser tunable in the range 700-820 nm was used to produce different wavelengths and digital holograms were recorded at: 757.82 nm, 758.08 nm, 758.86 nm and 759.89 nm. The phases of the wave fronts recorded at different wavelengths ($\phi_{757.82}$, $\phi_{758.08}$, $\phi_{758.86}$, and $\phi_{759.89}$) were determined by processing the digital holograms. The difference between phases recorded at different wavelengths results in phase maps containing the shape information of the object. Figures 2 (b, c, d) show the phase differences: $\phi_{758.08} - \phi_{757.82}$, $\phi_{758.86} - \phi_{757.82}$ and $\phi_{759.89} - \phi_{757.82}$, respectively. The phases are wrapped and have values in the range $(-\pi, \pi)$. When the wavelength difference between the recorded hologram is small, the phase map difference (see fig. 2. (b) does not contain phase steps but the depth information is not accurate. On the oth-

er side phase maps obtained by larger wavelengths differences contain phase steps but have better depth resolution. It is thus useful to combine different phase maps in order to obtain the shape with high resolution. Notice also that in the phase maps shown in figs. 2. (c, d) there are circular fringes due to the curvature of the wave front illuminating the sample. These fringes can be compensated by knowing curvature and direction of the illumination beam. By evaluating the phase maps it is possible to reconstruct the shape of the test object (see fig. 2.(e)). Figure 2.(f) shows the profile along a line.

With the sample located at a distance of 2.6 m from the measuring system, a depth accuracy of $\pm 5 \mu\text{m}$ was obtained. The technique seems well suited for measurements inside the Tokamak. Long distance measurements (15 m) in perturbed conditions (vibrations) are planned.

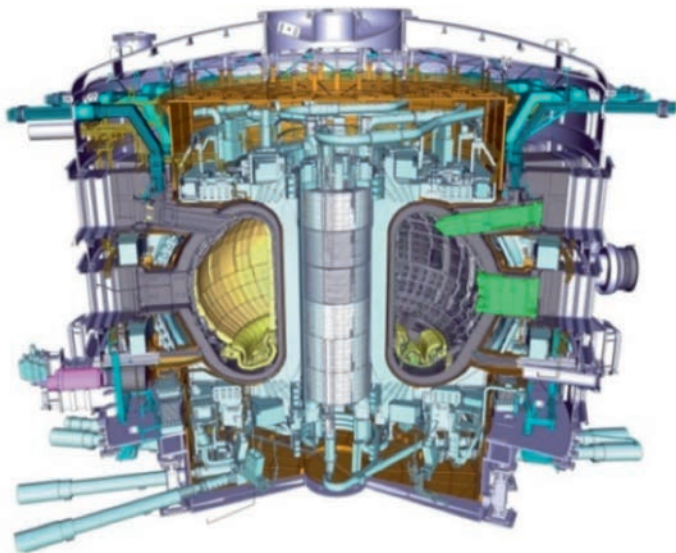


Fig. 1: Cross section of the Tokamak [1].

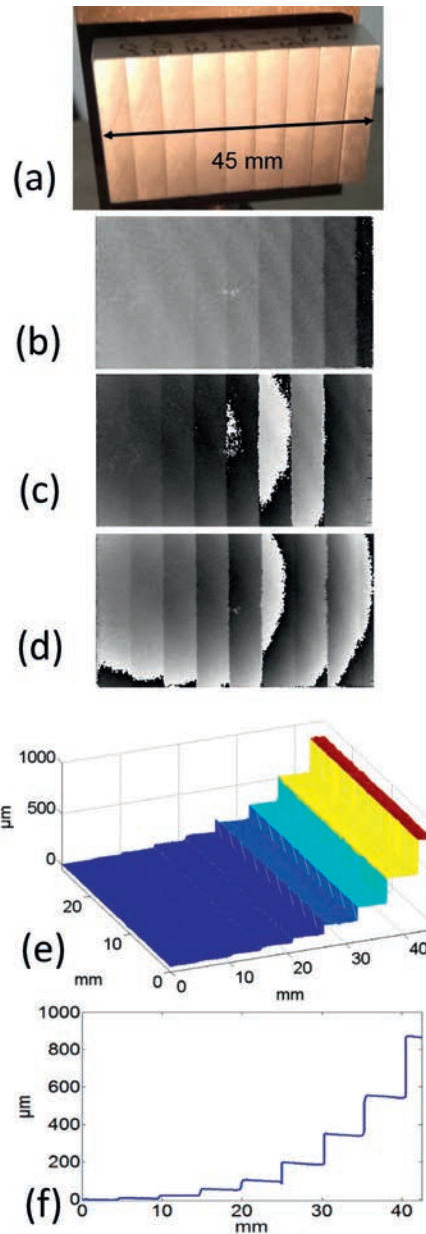


Fig. 2: Measurement of the shape of an object located at a distance of 2.6 m. (a) Photo of the object; (b-d) phase-maps; (e) measured shape; (f) profile along a line.

Supported by: International Thermonuclear Experimental Reactor (ITER).

Disclaimer:

The views and opinions expressed herein do not necessarily reflect those of the ITER Organization.

References:

- [1] iter.org/img/crop-2000-90/all/content/com/img_galleries/in-cryostat-section_rev-3_small.jpg (retrieved 17.04.2017).

Optical Design and Simulation



Design, simulation and 3D printing of complex micro-optics	88
<i>Supported by: Baden-Württemberg-Stiftung ('Opterial'), BMBF ('Printoptics') FKZ: 13N14096</i>	
Compound microlens systems for foveated imaging	89
<i>Supported by: Baden-Württemberg-Stiftung ('Opterial'), BMBF ('Printoptics')</i>	
Smartphone-microscope	90
<i>Supported by: the University of Stuttgart</i>	
Building kit for realization of optical systems	91
<i>Supported by: BMBF initiative "Open Photonics" ('BaKaRoS'), FKZ 13N14168</i>	
Design and measurements with the phase space analyzer	92
Design of large field head mounted display systems	93
<i>This work was supported by a Chinese scholarship</i>	

Design, Simulation and 3D printing of complex micro-optics

S. Thiele, S. Ristok, H. Giessen, A. Herkommer

3D printing of optics by femtosecond direct laser writing offers unique opportunities for the design of complex micro-optical systems. Since there are barely any restrictions in terms of geometry while feature sizes of <200 nm together with a sub- μm accuracy and a RMS roughness of <10 nm are achievable, an almost arbitrary distribution of refractive and diffractive power in 3D becomes possible. While this absence of restrictions allows the design of highly complex optical devices, the optimum solution is more difficult to find because of a drastically increased parameter space [1]. The aim of our work is to find methods and improve available tools in order to facilitate the search for an optimum solution.

On the size scales of our optics, diffractive effects can play a dominant role, especially if they are part of the optical function as for example in case of 3D-printed gratings, diffractive lenses or holograms. At the same time common approaches for simulation and design like the "thin element approximation" are not valid anymore if such structures are written onto curved surfaces.

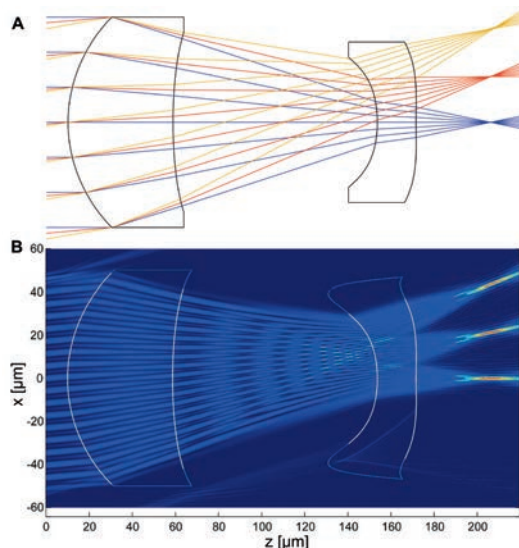


Fig. 1: (A) Raytracing plot of a telephoto doublet lens with $100\ \mu\text{m}$ aperture diameter. (B) Propagation through the same lens with the wave-propagation method.

As an ideal candidate for the wave-optical simulation the wave-propagation-method (WPM) [2] has been investigated. The algorithm uses the angular spectrum approach to propagate forward scattered scalar fields in split steps.

Figure 1 shows a comparison of the ray-optical and wave-optical model for a telephoto doublet lens in 2D. In this case, both methods are equally suited for an accurate simulation and deliver very similar results. However, as soon as surface imperfections have to be taken into account or the aperture stop gets very small, the raytracing model will be inaccurate if these features are on the size scale of only a few wavelengths. In this case, the WPM offers a computationally efficient alternative.

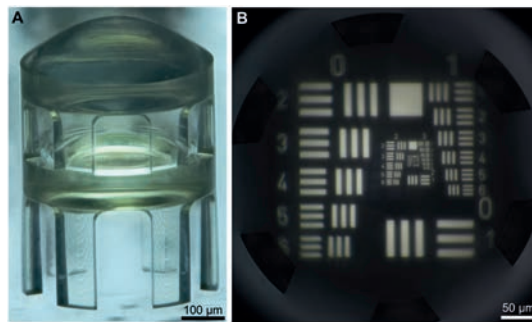


Fig. 2: (A) Micrograph of a 3D printed doublet lens with 40° field of view and diameter of $450\ \mu\text{m}$. (B) Measured imaging performance of an USAF-Target. The achieved maximum resolution in this case is $\sim 1\ \mu\text{m}$.

Since 3D direct laser writing is a very flexible process, short prototyping times can be achieved in comparison to traditional methods. This means that designs can be tested and improved with many iterations in a reasonable time frame.

Fig. 2 shows the example of an aberration corrected 3D-printed doublet lens with a field of view of 40° and an effective $f\#$ of 1.35. In Fig. 2A, a microscope image is displayed. Fig. 2B depicts an image captured by this lens. It shows distortion free imaging and a flat field.

Supported by: Baden-Württemberg-Stiftung ('Opterial'), BMBF ('Printoptics') FKZ: 13N14096

References:

- [1] Thiele, S.; Arzenbacher, K.; Gissibl, T.; Schmidt, S.; Gross, H.; Giessen, H.; Herkommer, A.M. "Design, simulation and 3D printing of complex micro-optics for imaging", Proc. IEEE OMN (2016).
- [2] Schmidt, S.; Tiess, T.; Schröter, S.; Hambach, R.; Jäger, M.; Bartelt, H.; Tünnermann, A.; Gross, H. "Wave-optical modeling beyond the thin-element-approximation", Opt Express. 24, 30188-30200 (2016).

Compound microlens systems for foveated imaging

S. Thiele, K. Arzenbacher, T. Gissibl, H. Giessen, A. Herkommer

3D printing by femtosecond direct laser writing can be applied to a variety of different substrates including CMOS imaging sensors [1]. This enables the fabrication of complex microlens systems directly on chip. We used such an approach to combine multiple lens systems with different focal lengths and to create a foveated imaging system (fig. 1) [2].

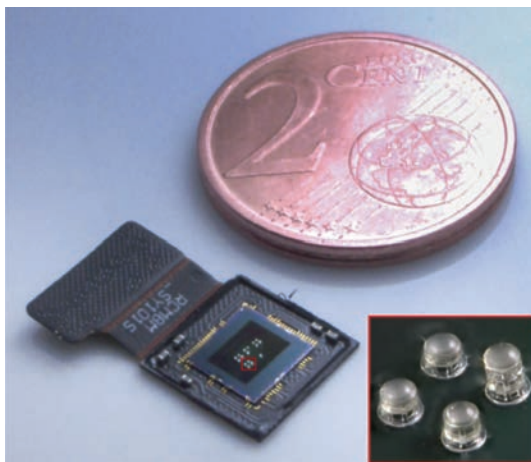


Fig. 1: CMOS-chip with groups of 3D-printed lens systems with different focal lengths.

Figure 2 shows the working principle: Images from different lenses are combined such that the object scaling stays constant which ultimately leads to an increased resolution in the center of the field of view.

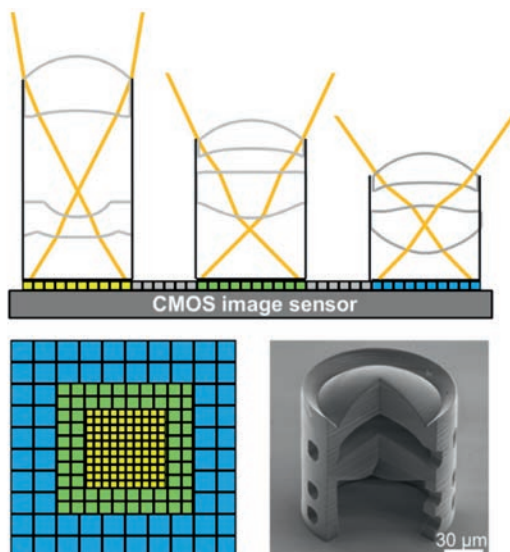


Fig. 2: Illustration of the working principle and SEM image of one lens doublet [2].

The sub images can directly be read out by the image sensor after 3D printing. Fig. 3 compares imaging results before and after image fusion for different objects. The foveated image features a considerably increased resolution in the center of the field of view.

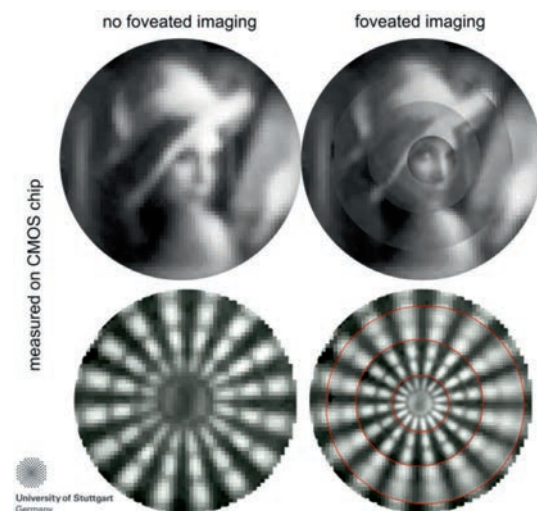


Fig. 3: Measured results from the CMOS imaging sensor [2].

The footprint of one system consisting of four doublet lenses is below $300 \times 300 \mu\text{m}^2$ while the height is $<200 \mu\text{m}$. This high degree of miniaturization can be useful for many fields of application e.g. endoscopy, optical metrology, optical sensing, or security.

Supported by: Baden-Württemberg-Stiftung ('Opterial'), BMBF ('Printoptics')

References:

- [1] Gissibl, T.; Thiele, S.; Herkommer, A. M.; Giessen, H. "Two-photon direct laser writing of ultracompact multi-lens objectives", *Nat. Phot.* 10 (2016) pp. 554–560.
- [2] Thiele, S.; Arzenbacher, K.; Gissibl, T.; Giessen, H.; Herkommer, A.M. "3D-printed eagle eye: Compound microlens system for foveated imaging", *Sci. Adv.* 3, e1602655 (2017).
- [3] Thiele, S.; Gissibl, T.; Giessen, H.; Herkommer, A.M. "Ultra-compact on-chip LED collimation optics by 3D femtosecond direct laser writing", *Opt. Lett.* 41 (2016).

Smartphone-microscope

C. Reichert, D. Claus, A. Herkommer

Widespread diseases like malaria tropica, sickle cell anemia and loiasis needs microscopic examination. With the aid of integrated complex camera modules, modern smartphones can be used for diagnostic purpose. Mobile phones are widespread in industrial, as well as in emerging and developing countries. In combination with optical systems and a diagnostic software, smartphones enable a diagnosis in remote regions. This can help to reduce the medical costs and more important save lives at poor places. The images also can be sent to skilled medical staff for an accurate diagnosis.

There are several possibilities to turn your smartphone in a microscope. The simplest way is to attach a lens (with a low focal length) in front of your smartphone camera. We use this lens as an objective. The smartphone camera (tube lens) focuses the collimated light on its sensor. The simplest and most cost-effective method is to use another smartphone camera module. This allows a full field bright-field examination of the sample. A possible optical design of the smartphone microscope with a reversed camera module is shown in fig. 1. Smartphone camera modules are made of several individual designed aspherical lenses and have only small imaging errors.

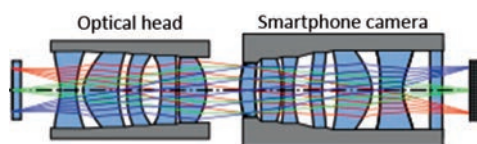


Fig. 1: Possible beam path of a smartphone microscope with a reversed camera module. As an object, we assumed a specimen behind a cover-glass (thickness 0.17 mm).

We used an iPhone 5s camera module to implement the smartphone based microscope. The complete module (see fig. 2 [A]) costs (depending transport costs and range) between 2 to 4 euro. We removed the optical module (see fig. 2 [B]) and used it as an optical head in front of the smartphone camera. Mechanical devices have been constructed for holding the optical module in front of the smartphone camera.



Fig. 2: Complete camera module of iPhone 5s [A] and different views of the removed optical module from the iPhone 5s [B].

Those devices also help to position and hold the sample at the microscope's working distance. The manufacturing of these holders has first been realized using a 3D printer. A selection of images taken from standard specimens with the smartphone microscope is shown in fig 3.

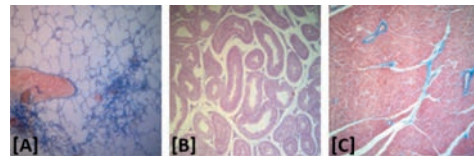


Fig. 3: Examinations with the smartphone microscope (dyed biological samples). [A] lung of a cat, [B] testicular of a mouse, [C] pancreas of a pig.

Because many biological objects are largely transparent, phase-sensitive imaging methods were investigated in combination with smartphone microscopy. Among the investigated methods are holography as well as the phase contrast microscope.

We used the schematic structure shown in fig. 4 [A] to record an in-line hologram with a smartphone. To ensure the spatial coherence from a LED we used a pinhole. The smartphone's sensor record the interference pattern. The recorded hologram and its reconstruction is shown in fig. 4 [B] and [C]. To record the original image, we used the angular spectrum implementation of Rayleigh-Sommerfeld's diffraction integral.

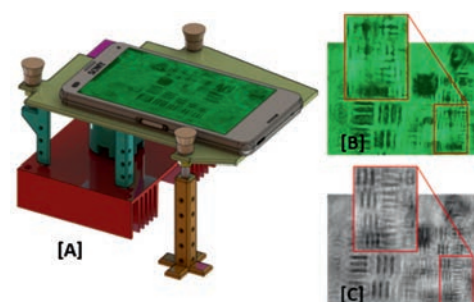


Fig. 4: [A] Structure for recording a hologram with the smartphone. [B] With smartphone recorded hologram and [C] its reconstruction.

Another method to record phase objects at an increased contrast is the phase contrast microscopy. We made a mechanical design which allows transparent objects to be imaged and subsequently displayed directly on the smartphone display with high contrast. The required phase plate was produced at the ITO.

Supported by: the University of Stuttgart

Building kit for realization of optical systems

C. Reichert, T. Haist, A. Herkommer

Photonics is found in many important areas of modern society. It is a basic competency to produce smartphones, cars and airplanes. Many technologies like data transmission with fibers networks, LASER diagnostics in medicine or energy-efficient lighting with LEDs and OLEDs would not work without modern photonic technologies. Photonics offers a significant cross-section technology to deliver innovative solutions to the markets and challenges of tomorrow.

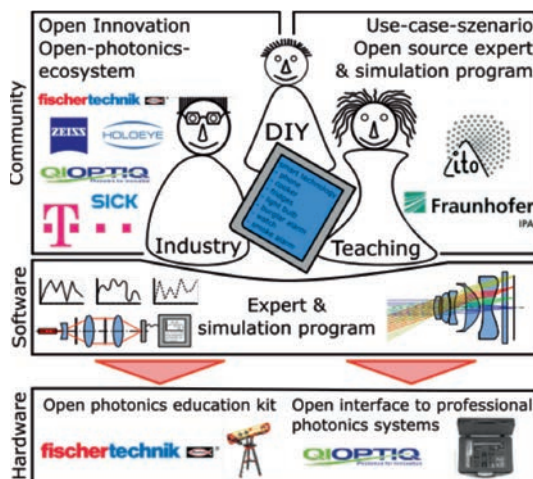


Fig. 1: Solution approaches, target groups and partners of the BMBF-project BaKaRoS.

The idea of the BMBF-Project “BaKaRoS” (Baukastensystem zur Realisierung optischer Systeme), a building kit for realization of optical systems, is to announce the topic “photonics” to a wide society. To achieve this goal, we will develop a hardware modular system combined with an open source expert and simulation program (see fig. 1). Those components help the audience (students, interested laypersons and industry users) to build simple and complex optical systems independently and at low cost. The core of the project consortium (fischer technik, T-Systems, Fraunhofer IAQ, Institut für Technische Optik) provides the necessary knowledge from all relevant fields of the project. Associated partners along the value chain (Zeiss, Qioptiq, Sick, Holoeye) address the developments and the organization of the open photonic community, but also add the view of industrial users and suppliers of optical measurement technology.

The basic system consists of existing, standardized and inexpensive building blocks with different optical functions. With those components, it should

be possible to realize many different optical setups for a wide range of applications. The basic system will be directly compatible with the leading professional optical system (microbench). This will ensure that cost-effective systems as well as high-quality superstructures can be realized. The selection and position of the components is automatically controlled by an open source expert and simulation system. To proof the problem-solving potential of the modular system different application examples from the fields of smart home, health and industry will be realized. Open innovation approaches for the long-term beneficial cooperation between science, business and creative citizens under the vision “open-photonics-ecosystem” will be analyzed and implemented. On the system’s web-based platform users can contribute and discuss complete solutions as well as subsystems. Thanks to the open-source implementation, dedicated users can continue to expand the hardware components as well as the software for operation (e.g. imaging processing). The implemented expert system uses a consistent modular design. Ultimately three main areas are essential: Kernel (ray tracing as well as optimization), Photonic programming language and User Interface (see fig. 2).

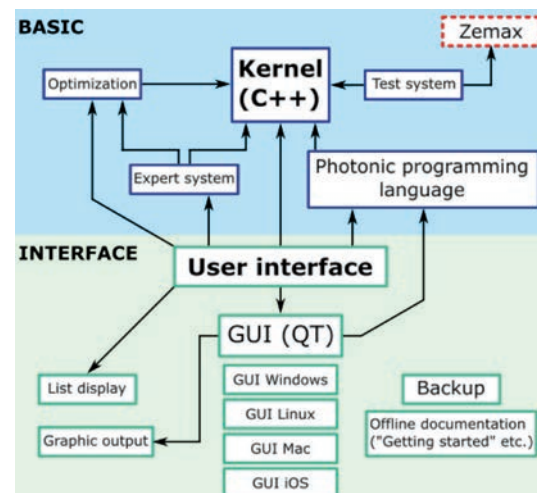


Fig. 2: Overview of the software system.

The implementation for the basic functionality takes place in C++ to achieve the highest possible target group of ambitious hobbyists. The interface can be from Windows, Mac, OSX and Linux.

Supported by: BMBF initiative “Open Photonics” (“BaKaRoS”). FKZ 13N14168.

Design and measurements with the phase space analyzer

D. Rausch, A. Herkommer

In illumination design usually a large number of rays must be traced to get accurate results. This is necessary to get information about the integral radiometric quantities. The phase space concept [1] is another way on looking at the mapping of radiance patches from the source to the target in a phase space diagram, as illustrated in fig. 1.

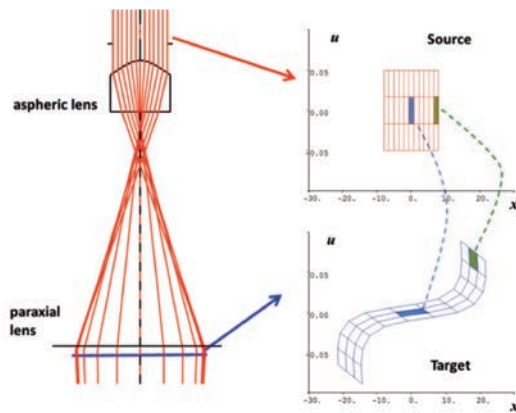


Fig. 1: Phase space mapping of a Gauss to Top-Hat-Beam shaper, illustrating the angular (u) and spatial (x) re-distribution of radiance.

How to observe this mapping? Experimentally, the phase space analyzer [2] provides an easy way to observe a one dimensional radiation field directly in position and angle. With the help of slit apertures and cylindrical lenses the experimental setup can be realized in the lab. We used the setup to analyze different optical systems. Figure 2 illustrates the measured phase space distribution of a hyperchromatic lens. Spherical and axial chromatic aberrations are nicely visible in phase space and agree well with Matlab simulations. Quantitatively the angles between the colours are measured to get the axial chromatic aberrations [3].

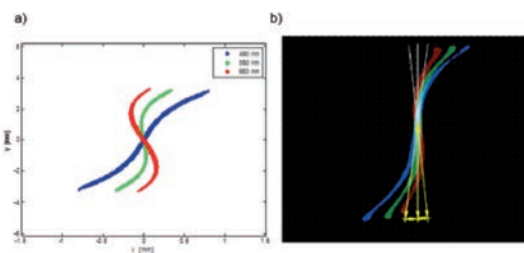


Fig. 2: Matlab-Simulation of a hyperchromatic system after the phase space analyzer. b) Detector image with the tangents to measure the difference in angle.

We also used the experimental setup to get the phase space diagram for a total internal reflector (TIR) in [4].

Instead of only analyzing the radiance distribution an optimization can be performed. In the design software ZEMAX we can attach a virtual phase space analyzer behind the optical system. Then we define a number of reference rays at the input and observe and control their position in spatial and angular direction at the phase space analyzer exit. The radiance patch attached to each ray will then be mapped according to the reference ray on the target. For example demanding an equidistant separation between the reference rays at target and choosing a Gaussian distribution at input, as illustrated in fig. 3, the resulting optical system will resemble a Gauss to Top-Hat beam shaper. In addition, the optimization does not only allow to control the spatial shape, but also the angular behavior (e.g. tolerance on laser tilt), since the complete phase space volume is optimized.

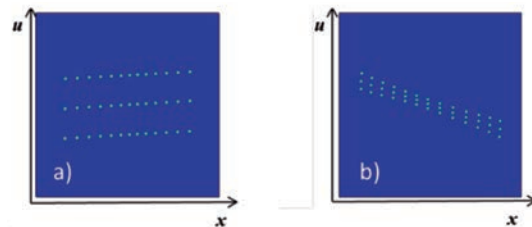


Fig. 3: a) The input reference ray distribution chosen to be Gaussian. b) The output reference ray in the phase space diagram after optimization. The points are now equidistant distributed and also different angles lead to same positions, thus the Top-Hat shaper will be insensitive to tilt.

References:

- [1] Rausch, D.; Herkommer, A. M. "Phase space approach to the use of integrator rods and optical arrays in illumination systems", AOT Vol.1, 2012.
- [2] Weber, H. "Wave optical analysis of the phase space analyzer", Journal of Modern Optics, Vol.39, pp.543-559, 1992.
- [3] Jung, C. "Vermessung von chromatischen Aberrationen mit Hilfe des Phasenraumanalysators", Bachelorthesis, 2017.
- [4] Hokenmaier, L. "Phasenraumanalyse von speziellen Beleuchtungsoptiken", Bachelorthesis, 2017.

Design of large field head mounted display systems

B. Chen, A. Herkommer

Head mounted displays (HMD), as one type of wearable device, are nowadays widely employed in aviation, video, 3D gaming, and training. From the concept point of view, HMDs can be categorized into two types: Virtual Reality and Augmented Reality. The HMDs projecting only computer-generated images are called Virtual Reality. The augmented type HMDs, or see-throughs, display both virtual image and real-world views. We present novel optical design concepts for folded HMD geometries, all based on freeform surfaces.

Generally freeform surfaces offer more capacity to correct particularly off-axis aberrations. Therefore they are widely employed in decentered and tilted systems [1, 2]. Additionally, today's highly developed single diamond turning technology allows for manufacturing complex freeform surfaces for imaging applications.

The total internal reflection (TIR) prism type geometry described in [3], and illustrated in fig. 1, represents a basic design type for HMD optics, which is widely developed by later designers.

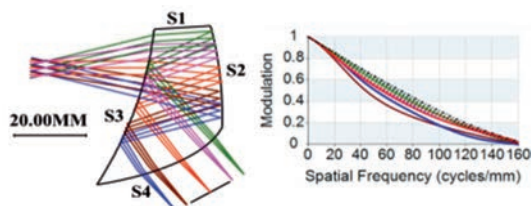


Fig. 1: Re-optimized reference type geometry for a HMD optics and corresponding MTF

This concept is employed as a reference. In contrast, our investigation [4] also considers catadioptric HMDs and prisms with different reflection folding geometry. These two types of HMDs are seldom investigated and may have mechanical disadvantages; however, the optical performances of these two alternate types are rather fine, since they offer better performance and larger field of view as compared to the reference.

The designed optical systems and the corresponding MTF are shown in fig. 1-3. In fig. 1, a re-optimized reference prism geometry, with one TIR surface, similar to the patent lens is presented. In fig. 2 we illustrate a

catadioptric system with one lens and two mirrors. An alternate prism-geometry without TIR surface, but with different folding geometry is depicted in fig. 3.

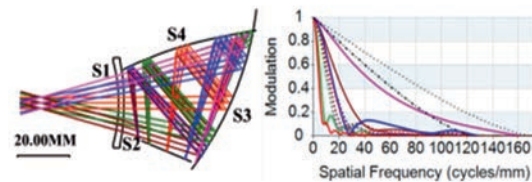


Fig. 2: Catadioptric setup, employing one lens and two mirror surfaces

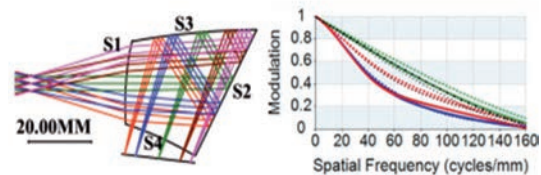


Fig. 3: Alternate prism-geometry, without total internal reflection surface.

The performances of our designs are all better than the original patent lens. Moreover, the performances of the two prisms in fig. 1 and fig. 3 are excellent. All fields are diffraction limited or close to being diffraction limited. Compared with these two prisms, the performance of the catadioptric type is worse and the size is relative larger. However, the weight might be attractive, as only a thin lens and two mirrors are applied. Note that for all design we only use two anamorphic surfaces and the highest order of the aspherical terms is 6, which is beneficial for the manufacturing complexity.

This work was supported by a Chinese scholarship.

References:

- [1] Chen, B.; Herkommer, A. M. "High order surface aberration contributions from phase space analysis of differential rays", *Optics express* 24.6 (2016) 5934-5945.
- [2] Chen, B.; Herkommer, A. M. "Generalized Aldis theorem for calculating aberration contributions in freeform systems", *Optics Express* 24.23 (2016): 26999-27008.
- [3] K. Takahashi, "Head or face mounted image display apparatus", U.S. Patent No. 5, 701, 202. 23 Dec. 1997.
- [4] Chen, B.; Herkommer, A. M. "Alternate optical designs for head-mounted displays with a wide field of view", *Applied Optics* 56.4 (2017) 901-906.

Invited lectures on international conferences

2015

A. Herkommer (Plenary Talk)

Application of phase space methods in geometrical optical design and system analysis

International Conference on Optical Instrument and Technology (OIT 2015), 19.5.2015, Beijing, China

A. Herkommer

Visualizing Surface Aberration Contributions in Freeform Systems

Freeform Optics. Optical Society of America, 10.6.2015, Arlington, Virginia, United States

W. Osten, et al

Unconventional Implementations and Applications of Digital Holography

K.-H. Lohmann Symposium, Erlangen 2015

W. Osten

Prospects and Challenges for the Optical Inspection of Micro- and Nano-Structures

Congress Physics Society of the Philippines, Vigan, Philippines, June 2015

W. Osten

Bildgebende optische 3D-Messtechnik: Stand der Technik und zukünftiges Entwicklungspotential

58. Bildverarbeitungsforum, Oberkochen, Juli 2015

W. Osten

Different approaches to overcome existing limits in optical micro and Nano Metrology

Woman in Optics Congress, Marburg, July 2015

G. Pedrini

Phase retrieval methods for imaging and optical metrology

The 12th International Conference on Correlation Optics, "Correlation Optics'15", 14-18 September 2015, Chernivtsi, Ukraine

W. Osten

What Optical Metrology can do for the Inspection of Micro and Nano Components

International Symposium on 3D Imaging, Metrology, and Data Security in Shenzhen, China, September 2015

G. Pedrini

Phase retrieval methods for imaging and optical metrology

International Symposium on 3D Imaging, Metrology, and Data Security, September 26th - 29th, 2015, Shenzhen, China

W. Osten

Inverse Problems in Optical Metrology: Exemplary Solving Strategies

ISOT 2015, Neuchatel, October 2015

Invited lectures on international conferences

2016

A. Herkommer

Visualizing Illumination Performance by Phase Space Methods

10th International Conference on Optics-photonics Design and Fabrication, ODF '16, Weingarten, Germany, 1.3.2016

W. Osten

Optische Messtechnik im Spannungsfeld zwischen Wunsch und Wirklichkeit

Zeiss-Optik-Kolloquium, Jena, March 2016

W. Osten

Different Approaches for Resolution Enhancement in Optical Nano Metrology

E-MRS 2016, Lille, France, May 2016

W. Osten

Optical Metrology – Tutorial

euspen 16th International Conference and Exhibition, Nottingham, GB, May 2016

W. Osten

How Optics has influenced Experimental Mechanics?

ICEM 17, Rhodes, Greece, July 2016

W. Osten

Advanced Optical Metrology between the Poles of Desire and Reality

8th International Conference on Information Optics and Photonics CIOP 2016, Shanghai, China, July 2016

A. Herkommer

Optical design tools for computational imaging systems

Computational Optical Sensing and Imaging (COSI), 27.7.2016, Heidelberg, Germany

T. Haist, M. Hasler, W. Osten

Application of Spatial Light Modulators in Holography and Beyond

OSA: Digital Holography & 3-D Imaging (DH), July 2016, Heidelberg, Germany

W. Osten, et al

Different Approaches for Resolution Enhancement in Optical Nano Metrology

SPIE Annual Meeting 2016, San Diego, USA, August 2016

S. Thiele, K. Arzenbacher, T. Gissibl, H. Giessen, A. Herkommer

Design rules for 3D printed optical systems in the sub-millimeter-range

EOSAM 2016, TOM3 – "Optical System Design and Manufacturing", Berlin, Germany, 27. September 2016

K. Frenner, L. Fu, W. Osten

Discretization of rough surfaces with surface integral equations: A step towards rigorous speckle simulation on large areas

EOSAM 2016, Frontiers in Optical Metrology, Berlin Adlershof, Germany, 26 - 30 September 2016

W. Osten

Optical Metrology in the Conflict between Desire and Reality

SPIE Annual Meeting 2016, San Diego, USA, September 2016

W. Osten

Optical Metrology in the Conflict between Desire and Reality: Challenges and Solving Strategies

icOPEN 2016, Chengdu, China, September 2016

S. Thiele

Direktes Laserschreiben von mikrooptischen Systemen in 3D – in einem Schritt vom Digitalmodell zum Prototypen

6. Wetzlarer Herbsttagung, Wetzlar, Germany, 28. September 2016

W. Osten, et al

Spatially Tunable Polarization Devices for Optical Imaging and Metrology employing Photoreversible Polarization Elements.

IWPPI 2016, Nasu, Japan, October 2016

Invited lectures on international conferences

2017

W. Osten

Exploiting the whole information content of the light field: Approaches and Examples

10th Anniversary Conference of CORE, Utsunomiya, Japan, October 2016

W. Osten

Optical Metrology between the Poles of Desire and Reality

International Conference on Microscale Morphology of Component Surfaces (MICOS), Kaiserslautern, October 2016

W. Osten

Optische Messtechnik – eine kritische Bestandsaufnahme im Licht aktueller Herausforderungen

OPTECNET-Congress 2017, Mainz, Germany, March 2017

W. Osten

Exploiting the whole Information Content of the Light Field: Approaches and Examples

icOPEN 2017, Singapore, April 2017

W. Osten

Optical Metrology – Tutorial

euspem 17th International Conference and Exhibition, Hannover, May 2017

W. Osten

Exploiting the whole Information Content of the Light Field: Approaches & Limitations

Applied Optics and Photonics China – AOPC 2017, Beijing, China, June 2017

W. Osten

Exploiting the whole Information Content of the Light Field: The Role of Polarization and of the Angular Spectrum

Congress Physics Society of the Philippines, Cebu, Philippines, June 2017

T. Haist

Using spatial light modulators

SLM-Tutorial at the New SPIE Digital Optical Technologies conference, Munich, Germany, June 2017

W. Osten

Exploiting the whole information content of the Light Field: The role of Coherence and Time of Flight

9th International Conference on Information Optics and Photonics – CIOP 2017, Harbin, China, July 2015

Editorial work

Lehmann, P., Osten, W.; Albertazzi, A. (Eds.):

Optical Measurement Systems for Industrial Inspection IX

Proc. SPIE Vol. 9525, Bellingham 2015

Gorecki, C.; Asundi, A.; Osten, W. (Eds.):

Optical Micro- and Nanometrology in Microsystems Technology VI

Proc. SPIE Vol. 9890, Bellingham 2016

Mendoza, F.; Georges, M.; Lehmann, P.; Osten, W.; Albertazzi A. (Eds.):

Special Section on Speckle Based Metrology

Optical Engineering. Vol. 55 (2016) 12, 121701-1-2

Osten, W.; Seewig, J.:

Optical surface metrology in the context of enhanced resolution and precision

Special Issue of the IOP Journal "Surface Topography: Metrology and Properties" 2016, http://iopscience.iop.org/2051-672X/focus/Optical_surface_metrology

Tsang, P.W.M.; Poon, T.-C.; Osten, W.:

Digital Holography for Industrial Applications

Special Issue of the IEEE Transaction for Industrial Informatics 2016

Banerjee, P.; Osten, W.; Picart, P.; Cao, Liangcai, Nehmetalla, G. (Eds.):

Digital Holography and 3D Imaging: Joint feature issue in Applied Optics and Journal of the Optical Society of America B

Applied Optics, Vol. 56 (May 2017), Doc. ID 292363

Lehmann, P.; Osten, W.; Albertazzi, A. (Eds.):

Optical Measurement Systems for Industrial Inspection X

Proc. SPIE Vol. 10329, Bellingham 2017

Awards

G. Baer:

Winner of the „Prize for special scientific achievements“ of the „Vereinigung von Freunden der Universität Stuttgart“ for his dissertation "Ein Beitrag zur Kalibrierung von Nicht-Null-Interferometern zur Vermessung von Asphären und Freiformflächen", 2017

M. L. Gödecke, S. Peterhänsel, K. Frenner, W. Osten:

Winner of the 2016 Karel Urbanek Best Student Paper Award at the SPIE Advanced Lithography Symposium in San Jose

M. L. Gödecke, S. Peterhänsel, K. Frenner, W. Osten:

Winner of the 2016 Best Student Paper Award at the SPIE Photonics Europe Symposium in Brussels

W. Osten:

Senior Member of IEEE – The Institute of Electrical and Electronic Engineers, 2016

W. Osten:

Fellow of EOS – The European Optical Society EOS, 2016

W. Osten:

The 2016 Algerian Paper of the Year Award, 2016

W. Osten:

Outstanding Editor Award of the Nature Journal "Light: Science & Applications" in the Year 2016

W. Osten:

Bestowal of the academic degree of an honorary doctor Dr.-Ing. E.h. of the Technische Universität Ilmenau, Germany, 2017

S. Thiele, A. Herkommer:

Winner of the first price "Ideenwettbewerb 3D-Druck der Baden-Württemberg Stiftung" at the „Forschungstag 2017“

W. Osten: Board Member

W. Osten

Elected Member of the Board of Directors of the SPIE for 2015-2017

W. Osten

Member of the Advisory Board of the Dept. "Mechanical Engineering" of the Worcester Polytechnic Institute, Worcester, USA

W. Osten

Member of the Advisory Board of the "Centre for Optical and Laser Engineering" in the School of Mechanical and Aerospace Engineering at the Nanyang Technological University, Singapore

W. Osten

Member of EAC – The European Advisory Committee of SPIE

W. Osten

Member of the Supervisory Board of the Hahn-Schickard-Gesellschaft, Baden-Württemberg

W. Osten

Member of the Advisory Board of the Kiepenheuer Institute for Solar Physics, Freiburg

W. Osten

Head of the Advisory Board of the Centre for Sensor Systems ZESS, Siegen

W. Osten

Member of the Scientific Advisory Board of the Res. Community for Precision Mechanics, Optics and Medical Engineering FOM, Berlin

W. Osten

Member of the Advisory Board of The Hannover Center for Optical Technologies HOT, Hannover

W. Osten

Member of the Steering Comm. of the Congress "Laser – World of Photonics" in Munich, biennial international congress

W. Osten

Member of the VDI/VDE – GMA Advisory Board FB 8 "Optische Technologien"

W. Osten

Member of the International Program Committees of numerous International Scientific Conferences

Membership of Editorial Boards

W. Osten

Co-Editor of the Journal
"Applied Physics B: Lasers and Optics"

W. Osten

Member of the Editorial board of the Nature
Journal "Light: Science & Applications"

W. Osten

Member of the Editorial board of
"Chinese Optics Letters"

W. Osten

Member of the Editorial board of the Journal
"Strain"

W. Osten

Member of the Editorial board of the Journal
"Optics and Lasers in Engineering"

W. Osten

European Editor of the Journal
"Holography and Speckle"

W. Osten

Member of the Editorial board of the Journal
"Opto-Mechatronics"

W. Osten

Member of the Editorial board of the Journal
"Optica Applicata"

W. Osten

Member of the Editorial board/Topical Editor
of the Journal "3D Research"

W. Osten

Associate Editor of the Journal "IEEE Trans-
actions on Industrial Informatics"

G. Pedrini

Topical Editor of the Journal "Applied Optics"

Reviewed papers

2015

Albero, J.; Perrin, S.; Bargiel, S.; Passilly, N.; Baranski, M.; Gauthier-Manuel, L.; Bernard, F.; Lullin, J.; Froehly, L.; Krauter, J.; Osten, W.; Gorecki, C.

Dense arrays of millimeter-sized glass lenses fabricated at wafer-level

Optics Express 23 (2015) 9 pp. 11702-11712

Azzem, S. M.; Bouamama, L.; Simoens, S.; Osten, W.

Two beams two orthogonal views particle detection

Journal of optics 17 (2015) 4 Nr. 045301

Buchta, D.; Hein, N.; Pedrini, G.; Krekel, C.; Osten, W.

Artwork Inspection by Shearography with Adapted Loading

Experimental Mechanics 55 (2015) 9 pp. 1691-1704

Faridian, A.; Ferreras Paz, V.; Frenner, K.; Pedrini, G.; Den Boef, A.; Osten, W.

Phase-sensitive structured illumination to detect nanosized asymmetries in silicon trenches

Journal of Micro-Nanolithography
MEMS and MOEMS 14 (2015) 2 Nr. 021104

Gilbergs, H.; Fang, H.; Frenner, K.; Osten, W.

Adaptive state observer and PD control for dynamic perturbations in optical systems

Opt. Express 23 (2015) 4 pp. 4002-4011

Haist, T.; Gronle, M.; Bui, D. A.; Osten, W.

Holographic multipoint generation for sensing positions

TM-Technisches Messen 82 (2015) 5
Special Issue: SI pp. 273-279

Haist, T.; Osten, W.

Holography using pixelated spatial light modulators-Part 1: theory and basic considerations

Micro-Nanolithography
MEMS and MOEMS 14 (2015) 4 Nr. 041310

Haist, T.; Osten, W.

Holography using pixelated spatial light modulators-Part 2: applications

Micro-Nanolithography
MEMS and MOEMS 14 (2015) 4 Nr. 041311

Haist, T.; Peter, A.; Osten, W.

Holographic projection with field-dependent aberration correction

Opt. Express 23 (2015) 5 pp. 5590-5595

Hasler, M.; Stahl, J.; Haist, T.; Osten, W.

Object field expansion in spatial light modulator-based phase contrast microscopy

Optical Engineering 54 (2015) 4 Nr. 043107

Kranz, O.; Geckeler, R.; Just, A.; Krause, M.; Osten, W.

From plane to spatial angles: PTB's spatial angle autocollimator calibrator

Advanced Optical Technologies 4 (2015) 5-6 pp. 397-411

Osten, W. (Ed.)

Optical Inspection of Microsystems

Chinese Edition, China Machine Press 2015

Peterhänsel, S.; Gödecke, M. L.; Ferreras Paz, V.; Frenner, K.; Osten, W.

Detection of overlay error in double patterning gratings using phase-structured illumination

Optics Express 23 (2015) 19 pp. 24246-24256

Peterhänsel, S.; Laamanen, H.; Lehtolahti, J.; Kuittinen, M.; Osten, W.; Tervo, J.

Human color vision provides nanoscale accuracy in thin-film thickness characterization

Optica 2 (2015) 7 pp. 627-630

Reinhardt, C.; Ferreras-Paz, V.; Zheng, L.; Kurselis, K.; Birr, T.; Zywitz, U.; Chichkov, B.; Frenner, K.; Osten, W.

Design and fabrication of near-to-far-field-transformers by sub-100 nm two photon polymerization

In: K. Köning, A. Ostendorf (Eds.): Optically Induced Nanostructures, de Gruyter, Berlin 2015

Reviewed Papers

2016

Suhr, H.; Herkommer, A.

In situ microscopy using adjustment-free optics

Journal of biomedical optics 20 (2015) 11 Nr. 116007

Zheng, J.; Pedrini, G.; Gao, P.; Yao, B.; Osten, W.

Autofocusing and resolution enhancement in digital holographic microscopy by using speckle-illumination

Journal of Optics 17 (2015) 8 Nr. 085301

Albero, J.; Perrin, S.; Passilly, N.; Krauter, J.; Gauthier-Manuel, L.; Froehly, L.; Lullin, J.; Bargiel, S.; Osten, W.; Gorecki, C.

Wafer-level fabrication of multi-element glass lenses: lens doublet with improved optical performances

Optics Letters 41 (2016) 1 pp. 96-99

Blattmann, M.; Kretschmer, S.; Thiele, S.; Ataman, C.; Zappe, H.; Herkommer, A.; Seifert, A.

Bimodal endoscopic probe combining white-light microscopy and optical coherence tomography

Applied Optics 55 (2016) 15 pp. 4261-4269

Chen, B.; Herkommer, A. M.

High order surface aberration contributions from phase space analysis of differential rays

Opt. Express 24 (2016) 6 pp. 5934-5945

Chen, B.; Herkommer, A. M.

Generalized Aldis theorem for calculating aberration contributions in freeform systems

Optical Express 24 (2016) 23 pp. 26999-27008

Eckerle, M.; Dietrich, T.; Schaal, F.; Pruss, C.; Osten, W.; Abdou Ahmed, M.; Graf, T.

Novel thin-disk oscillator concept for the generation of radially polarized femtosecond laser pulses

Optics Letters 41 (2016) 7 pp. 1680-1683

Fortmeier, I.; Stavridis, M.; Wiegmann, A.; Schulz, M.; Osten, W.; Elster, C.

Evaluation of absolute form measurements using a tilted-wave interferometer

Optics Express 24 (2016) 4 pp. 3393-3404

Fu, L.; Berrier, A.; Li, H.; Schau, P.; Frenner, K.; Dressel, M.; Osten, W.

Depolarization of a randomly distributed plasmonic meander metasurface characterized by Mueller matrix spectroscopic ellipsometry

Optical Express 24 (2016) 24 pp. 28056-28064

Fuhl, W.; Santini, T.; Reichert, C.; Claus, D.; Herkommer, A. M.; Bahmani, H.; Rifai, K.; Wahl, S.; Kasneci, E.

Non-intrusive practitioner pupil detection for unmodified microscope oculars

Computers in Biology and Medicine 79 (2016) 2 pp. 36-44

Giessen, H.; Gissibl, T.; Thiele, S.; Herkommer, A. M.

Das kleinste Endoskop der Welt per 3D-Druck

Physik in unserer Zeit 47 (2016) 5 pp. 214-215

Gissibl, T.; Thiele, S.; Herkommer, A.M.; Giessen, H.

Two-photon direct laser writing of ultracompact multi-lens objectives

Nature Photonics 10 (2016) pp. 554-560

Gissibl, T.; Thiele, S.; Herkommer, A.M.; Giessen, H.

Sub-micrometre accurate free-form optics by three-dimensional printing on single-mode fibres

Nature Communications 7:11763 doi: 10.1038/ncomms11763 (2016)

Gronle, M.; Osten, W.

Multi-scale referencing and coordinate unification of optical sensors in multi-axis machines

Advanced Optical Technologies 5 (2016) 5-6 pp. 389-403

Gronle, M.; Osten, W.

View and sensor planning for multi-sensor surface inspection

Surface Topography: Metrology and Properties 4 (2016) 2 Nr.: 024009

Hahn, R. .; Krauter, J.; Koerner, K.; Gronle, M.; Osten, W.

Single-shot low coherence pointwise measuring interferometer with potential for in-line inspection

Measurement Science and Technology 28 (2016) 2 Nr.: 025009

Huang, Y.; Ma, J.; Yuan, C.J.; Pruss, C. ; Sun, W.; Liu, M. ; Zhu, R.; Gao, Z.; Osten, W.

Absolute test for cylindrical surfaces using the conjugate differential method

Optical Engineering 55 (2016) 11 Nr. 114104

Khodadad, D.; Singh, A. K.; Pedrini, G.; Sjö Dahl, M.

Full-field 3D deformation measurement: comparison between speckle phase and displacement evaluation

Applied Optics 55 (2016) 32 pp. 7735-7743

Lingel, C.; Haist, T.; Osten, W.

Spatial-light-modulator-based adaptive optical system for the use of multiple phase retrieval methods

Applied Optics 55 (2016) 36 pp. 10329-10334

Mahajan, S.; Trivedi, V.; Renganathan, A. K.; Chhaniwal, V.; Javidi, B.; Pedrini, G.; Osten, W.; Anand, A.

Wide-Field Lensless 3D Imaging and Visualization of Microobjects

Journal of Display Technology 12 (2016) 11 pp. 1283-1289

Mendoza Santoyo, F.; Georges, M.; Lehmann, P.; Osten, W.; Albertazzi G. Armando, Jr.

Speckle Metrology

Optical Engineering 55 (2016) 12 Nr. 121701

Pedrini, G.; Martínez-García, V.; Weidmann, P.; Wenzelburger, M.; Killinger, A.; Weber, U.; Schmauder, S.; Gadow, R.; Osten, W.

Residual Stress Analysis of Ceramic Coating by Laser Ablation and Digital Holography

Experimental Mechanics 56 (2016) 5 pp. 683-701

Peterhänsel, S.; Gödecke, M. L.; Frenner, K.; Osten, W.

Phase-structured illumination as a tool to detect nanometer asymmetries

Journal of Micro/Nanolithography, MEMS, and MOEMS 15 (2016) 4 Nr. 044005

Schaal, F.; Rutloh, M.; Weidenfeld, S.; Osten, W.

Spatially tunable Polarization Devices

In: Zappe, H.; Duppe C. (Eds.): Tunable Micro Optics. Cambridge Univ. Press, Cambridge 2016, pp. 197-218

Reviewed Papers

2017 (up to June 2017)

Singh, A. K.; Pedrini, G.; Peng, X.; Osten, W.

Nanoscale measurement of in-plane and out-of-plane displacements of microscopic object by sensor fusion

Optical Engineering 55 (2016) 12 Nr. 121722

Singh, A. K.; Naik, D. N.; Pedrini, G.; Takeda, M.; Osten, W.

Exploiting scattering media for exploring 3D objects

Light: Science & Applications 6 (2017) e16219

Takeda, M.; Singh, A. K.; Naik, D. N.; Pedrini, G.; Osten, W.

Holographic Correloscopy – Unconventional Holographic Techniques For Imaging a Three-Dimensional Object through an Opaque Diffuser or Via a Scattering Wall: A Review

IEEE Transactions on Industrial Informatics 12 (2016) 4 pp. 1631-1640

Talpur, T.; Herkommer, A.M.

Review of freeform TIR collimator design methods

Advanced Optical Technology 5 (2016) 2 pp.137–146

Thiele, S.; Gissibl, T.; Giessen, H.; Herkommer, A. M.

Ultra-compact on-chip LED collimation optics by 3D femtosecond direct laser writing

Optics Letters 41 (2016) 13 pp. 3029-3032

Tsang, P.W.M.; Osten, W.

Digital Holography for Industrial Applications

IEEE Transactions on Industrial Informatics 12 (2016) 4 pp. 1560-1563

Weidmann, P.; Weber, U.; Schmauder, S.; Pedrini, G.; Osten, W.

Numerical calculation of temperature and surface topology during a laser ablation process for ceramic coatings

Meccanica 51 (2016) 2 pp. 279-289

Banerjee, PP.; Osten, W.; Picart, P.; Cao, LC. ; Nehmetallah, G.

Digital Holography and 3D Imaging: introduction to the joint feature issue in Applied Optics and Journal of the Optical Society of America B

Applied Optics 56 (2017) 13 pp. DH1-DH4

Banerjee, PP.; Osten, W.; Picart, P.; Cao, LC. ; Nehmetallah, G.

Digital Holography and 3D Imaging: introduction to the joint feature issue in Applied Optics and Journal of the Optical Society of America B

Journal of the Optical Society of America B - Optical Physics 34 (2017) 5 pp. DH1-DH4

Bilski, B.; Frenner, K.; Osten, W.

Effective CD: a contribution toward the consideration of line edge roughness in the scatterometric critical dimension metrology

J. Micro/Nanolith. MEMS MOEMS 16 (2017) 2 Nr. 024002

Bielke, A.; Pruss, C.; Osten, W.

Design of a variable diffractive zoom lens for interferometric purposes

Optical Engineering 56 (2017) 1 Nr. 014104

Boettcher, T.; Gronle, M.; Osten, W.

Multi-layer topography measurement using a new hybrid single-shot technique: Chromatic Confocal Coherence Tomography (CCCT)

Optics Express 25 (2017) 9 pp. 10204-10213

Claus, D.; Pedrini, G.; Osten, W.

Iterative phase retrieval based on variable wavefront curvature

Applied Optics 56 (2017) (2017) 13 pp. F134-F137

Eckerle, M.; Beirow, F.; Dietrich, T.; Schaal, F.; Pruss, C.; Osten, W.; Aubry, N.; Perrier, M.; Didierjean, J.; Délen, X.; Balembois, F.; Georges, P.; Abdou Ahmed, M.; Graf, T.

High-power single-stage single-crystal Yb:YAG fiber amplifier for radially polarized ultrashort laser pulses

Applied Physics B (2017) 123:139

Hahn, R.; Krauter, J.; Koerner, K.; Gronle, M.; Osten, W.

Single-shot low coherence pointwise measuring interferometer with potential for in-line inspection

Measurement Science and Technology 28 (2017) 2 Nr. 025009

Liu, J.; Claus, D.; Xu, T.; Kessner, T.; Herkommer, A.; Osten, W.

Light field endoscopy and its parametric description

Optics Letters 42 (2017) 9 pp. 1804-1807

Narayanamurthy, C.S.; Pedrini, G.; Osten, W.

Digital holographic photoelasticity

Applied Optics 56 (2017) 13 pp. F213 - F217

Pruss, C.; Baer, G.; Schindler, J.; Osten, W.

Measuring aspheres quickly: tilted wave interferometry

Optical Engineering 56 (2017) 11 pp. 111713

Rausch, D.; Rommel, M.; Herkommer, A.

Illumination design for extended sources based on phase space mapping

Optical Engineering 56 (2017) 6 pp. 065103

Singh, A.K.; Naik, D.N.; Pedrini, G.; Takeda, M.; Osten, W.

Exploiting scattering media for exploring 3D objects

Light Science & Applications 6 (2017) Nr. e16219

Thiele, S.; Arzenbacher, K.; Gissibl, T.; Giessen, H.; Herkommer, A.M.

3D-printed eagle eye: Compound microlens system for foveated imaging

Science Advances 3 (2017) e1602655

Yang, H.; Haist, T.; Gronle, M.; Osten, W.

Simulation of microscopic metal surfaces based on measured microgeometry

Simulation mikroskopischer Metalloberflächen unter Verwendung von gemessenen Mikrogeometrien

tm - Technisches Messen (2017) ISSN (Online) 2196-7113, ISSN (Print) 0171-8096

Conference proceedings and journals

2015

Bielke, A.; Baer, G.; Pruss, C.; Osten, W.

Model-based calibration of an interferometric setup with a diffractive zoom-lens

Proc. SPIE. 9618 (2015) pp. 961807
International Conference on Optical Instruments and Technology: Optical Systems and Modern Optoelectronic Instruments

Blattmann, M.; Kretschmer, S.; Thiele, S.; Zappe, H.; Herkommer, A.; Seifert, A.

MEMS endomicroscope for simultaneous bright-field microscopy and optical coherence tomography

Solid-State Sensors, Actuators and Microsystems (TRANSDUCERS) Transducers-2015 18th International Conference on. IEEE, Anchorage, AK (2015) pp. 216-219

Buchta, D.; Hein, N.; Pedrini, G.; Krekel, C.; Osten, W.

Combination of topology and structural information for damages and deterioration analysis of artworks

Proc. SPIE. 9527 (2015) pp. 95270Q
Optics for Arts, Architecture, and Archaeology V

Claus, D.; Schumacher, P. M.; Labitzke, T.; Mlikota, M.; Weber, U.; Schmauder, S.; Schierbaum, N.; Schäffer, T. E.; Wittmüß, P.; Teutsch, T.; Tarin, C.; Hoffmann, S.; Taran, F. A.; Brucker, S.; Mischinger, J.; Stenzel, A.; Osten, W.

Intraoperative model based identification of tissue properties using a multimodal and multiscale elastographic measurement approach

Proc. SPIE. 9540 (2015) pp. 95400M
Novel Biophotonics Techniques and Applications III

Claus, D.; Schumacher, P. M.; Wilke, M.; Mlikota, M.; Weber, U.; Schmauder, S.; Schierbaum, N.; Schäffer, T. E.; Wittmüß, P.; Teutsch, T.; Tarin, C.; Hoffmann, S.; Brucker, S.; Mischinger, J.; Schwentner, C.; Stenzel, A.; Osten, W.

Intraoperative model based identification of tissue properties based on multimodal and multiscale measurements

Proc. SPIE. 9328 (2015) pp. 932805
Imaging, Manipulation, and Analysis of Biomolecules, Cells, and Tissues XIII

Fu, L.; Schau, P.; Frenner, K.; Osten, W.

A cascaded plasmonic superlens for near field imaging with magnification

Proc. SPIE. 9526 (2015) pp. 95260Z
Modeling Aspects in Optical Metrology V

Gao, P.; Zheng, J.; Yao, B.; Pedrini, G.; Osten, W.

Autofocusing and resolution enhancement in speckle-illuminated digital holographic microscopy

Proc. OSA Conference (2015) "Digital Holography and Three-Dimensional Imaging", Shanghai, China, 24–28 May 2015, paper DT3A.2

Gronle, M.; Osten, W.

Inspektion technischer Objekte mit einem flexiblen, automatisierten Multisensorsystem

VDI-Tagung "Multisensorik in der Fertigungsmesstechnik", Nürtingen, 2015

Haist, T.; Gronle, M.; Bui, D. A.; Jiang, B.; Pruss, C.; Schaal, F.; Osten, W.

Towards one trillion positions

Proc. SPIE. 9530 (2015) pp. 953004
Automated Visual Inspection and Machine Vision

Haist, T.; Gronle, M.; Bui, D. A.; Osten, W.

Holographic multipoint generation for sensing positions

TM-Technisches Messen 82 (2015) 5 pp. 273-279

Krauter, J.; Boettcher, T.; Körner, K.; Gronle, M.; Osten, W.; Passilly, N.; Froehly, L.; Perrin, S.; Gorecki, C.

Performance analysis of a full-field and full-range swept-source OCT system

Proc. SPIE. 9576 (2015) pp. 957609
Applied Advanced Optical Metrology Solutions

Krauter, J.; Boettcher, T.; Körner, K.; Gronle, M.; Osten, W.; Passilly, N.; Froehly, L.; Perrin, S.; Gorecki, C.

Full-field swept-source optical coherence tomography with phase-shifting techniques for skin cancer detection

Proc. SPIE. 9529 (2015) pp. 952913
Optical Methods for Inspection, Characterization, and Imaging of Biomaterials II

Lingel, C.; Haist, T.; Osten, W.

Holographic Multipoint Raman Microscopy

Proc. DGaO 116. Tagung (2015) P 33

Osten, W.; Pedrini, G.; Weidmann, P.; Gadow, R.

A flexible method for residual stress measurement of spray coated layers by laser made hole drilling and SLM based beam steering

Proc. SPIE. 9660 (2015) pp. 96600H
SPECKLE 2015: VI International Conference on Speckle Metrology

Pruss, C.; Bielke, A.; Baer, G.; Schindler, J.; Osten, W.

Calibration of interferometric non-null test setups

Proc. DGaO 116. Tagung (2015) P 13

Schindler, J.; Baer, G.; Pruss, C.; Osten, W.

Wave front calibration in 3D space

EOSMTOC 2015, Munich (2015)

Schindler, J.; Schau, P.; Brodhag, N.; Frenner, K.; Osten, W.

Retrieving the axial position of fluorescent light emitting spots by shearing interferometry

Journal of Biomedical Optics 21 (2016) 12 Nr.: 125009

Schumacher, P. M.; Claus, D.; Mlikota, M.; Schierbaum, N.; Osten, W.

Determination of mechanical properties of soft tissue by rolling indentation, digital image correlation and finite element modelling

Proc. DGaO 116. Tagung (2015) B 25

Singh, A.K.; Naik, D.N.; Pedrini, G.; Takeda, M.; Osten, W.

Real-time imaging through thin scattering layer and looking around the opaque surface

Proc. OSA Conference (2015) "Digital Holography and Three-Dimensional Imaging", Shanghai, China, 24–28 May 2015, paper DTh3A.5

Talpur, T.; Herkommer, A.

TIR collimator designs based on point source and extended source methods

Proc. SPIE 9629, Optical Systems Design (2015): Illumination Optics IV, 962906

Yang, H.; Haist, T.; Gronle, M.; Osten, W.

Realistic simulation of camera images of local surface defects in the context of multi-sensor inspection systems

Proc. SPIE. 9525 (2015) pp. 952522
Optical Measurement Systems for Industrial Inspection IX

Zepp, A.; Gladysz, S.; Barros, R.; Osten, W.; Stein, K.

Analogue holographic wavefront sensor: a performance analysis

Proc. SPIE. 9614 (2015) pp. 96140G
Laser Communication and Propagation through the Atmosphere and Oceans IV

Conference proceedings and journals

2016

Achimova, E.; Abaskin, V.; Claus, D.; Pedrini, G.; Prisacar, A.; Triduh, G.

Multimodal characterisation of a novel one-step process generated diffractive element

Imaging and Applied Optics 2016, OSA Technical Digest (online) (Optical Society of America, 2016), Heidelberg, Germany, 25–28 July 2016, paper JW4A.30

Bielke, A.; Baer, G.; Pruss, C.; Osten, W.

Model-based calibration of an adaptive interferometric setup

Proc. DGaO 117. Tagung (2016) P29

Boettcher, T.; Hofer, T.; Gronle, M.; Osten, W.

Chromatic Confocal Coherence Tomography (CCCT) for multi-layer measurement

Proc. EOSAM 2016, 2016

Claus, D.; Thiem, J.; Hennenlotter, J.; Pedrini, G.; Stenzl, A.; Osten, W.

Iterative phase retrieval imaging based on variable wavefront curvature for biomedical imaging

Imaging and Applied Optics 2016, (Optical Society of America, 2016), Heidelberg, Germany, 25–28 July 2016, paper JW4A.25

Claus, D.; Thiem, J.; Pedrini, G.; Osten, W.

Iterative phase retrieval imaging based on alternating wavefront curvature

Proc. DGaO 117. Tagung (2016) P31

Fu, L.; Frenner, K.; Li, H.; Osten, W.

A silicon superlens with a simple design working at visible wavelengths

Proc. SPIE. 9890 (2016) pp. 98900I
Optical Micro- and Nanometrology VI

Gödecke, M. L.; Peterhänsel, S.; Frenner, K.; Osten, W.

Measurement of asymmetric side wall angles by coherent scanning Fourier scatterometry

Proc. SPIE. 9778 (2016) pp. 97780G
Metrology, Inspection, and Process Control for Microlithography XXX

Gödecke, M. L.; Peterhänsel, S.; Frenner, K.; Osten, W.

Robust determination of asymmetric side wall angles by means of coherent scanning Fourier scatterometry

Proc. SPIE. 9890 (2016) pp. 98900M
Optical Micro- and Nanometrology VI

Hasler, M.; Haist, T.; Osten, W.

Adjustment and Application of Spatial Light Modulators for Holography

Proc. OSA Conference (2016) "Digital Holography and Three-Dimensional Imaging", Heidelberg, Germany, 25–28 July 2016, paper DW1D.1

Hahn, R.; Körner, K.; Krauter, J.; Gronle, M.; Osten, W.

Single-shot low coherence point interferometer with potential for inline-inspection

Proc. EOSAM 2016, 2016

Keck, A.; Sawodny, O.; Gronle, M.; Haist, T.; Osten, W.

Active Compensation of Dynamic Errors in a Coordinate-Measuring Machine

IFAC-PapersOnLine 49 (2016) 21 pp. 636–641

Osten, W.

Optical metrology in the conflict between desire and reality

Proc. SPIE. 9960 (2016) pp. 99600P
Interferometry XVIII

Osten, W.; Pruss, C.; Schaal, F.; Stumpe, J.

Spatially Tunable Polarization Devices for Optical Imaging and Metrology employing photoreversible polarization elements

Proc. of the International Workshop on Photonics Polymer for Innovation "IWPPPI" in Tochigi, Japan (2016)

Passilly, N.; Perrin, S.; Albero, J.; Krauter, J.; Gaiffe, O.; Gauthier-Manuel, L.; Froehly, L.; Lullin, J.; Bargiel, S.; Osten, W.; Gorecki, C.

Wafer-level fabrication of arrays of glass lens doublets

Proc. SPIE. 9888 (2016) pp. 98880T
Micro-Optics

Passilly, N.; Perrin, S.; Lullin, J.; Albero, J.; Bargiel, S.; Froehly, L.; Gorecki, C.; Krauter, J.; Osten, W.; Wang, W.-S.; Wiemer, M.

Array-type miniature interferometer as the core optical microsystem of an optical coherence tomography device for tissue inspection

Proc. SPIE. 9890 (2016) pp. 98900C
Optical Micro- and Nanometrology V

Pedrini, G.; Claus, D.; Osten, W.

Digital holography using wavefront scanning

Imaging and Applied Optics 2016, OSA Technical Digest (online) (Optical Society of America, 2016), Heidelberg, Germany, 25–28 July 2016, paper DW5E.3

Pedrini, G.; Martínez-García, V.; Weidmann, P.; Singh, A.; Osten, W.

Optical Methods for the Analysis of Residual Stresses and Measurement of Displacements in the Nanometric Range

2016 IEEE 14th International Conference on Industrial Informatics (INDIN) 978-1-5090-2870-2/16 pp. 570-575

Rausch, D.; Herkommer, A.

Design and applications of a phase space analyzer

Proc. SPIE 9889 (2016) pp. 98890N
Optical Modelling and Design IV

Röder, M.; Hera, D.; Thiele, S.; Pruss, C.; Osten, W.; Zimmermann, A.

3D Laser direct-writing based master fabrication for injection compression molding of diffractive-refractive lenses

EOSAM 2016, Berlin, Germany

Schindler, J.; Brodhag, N.; Schau, P.; Frenner, K.; Osten, W.

Shearing interferometry and structured illumination for the depth-resolved detection of fluorescent light

Proc. DGAO 117. Tagung (2016) P30

Schindler, J.; Elmaklizi, A.; Voit, F.; Hohmann, A.; Schau, P.; Brodhag, N.; Krauter, P.; Frenner, K.; Kienle, A.; Osten, W.

Resolving the depth of fluorescent light by structured illumination and shearing interferometry

Proc. SPIE. 9718 (2016) pp. 97182H
Quantitative Phase Imaging II

Siller, A.; Pruss, C.; Hopp, D.; Osten, W.

Neuer Sensor zur exakten Bestimmung von Drehwinkeln

MTZ Motortechnische Zeitschrift 77(4) (2016) pp. 60-63

Thiele, S.; Arzenbacher, K.; Gissibl, T.; Schmidt, S.; Gross, H.; Giessen, H.; Herkommer, A. M.

Design, simulation and 3D printing of complex micro-optics for imaging

International Conference on Optical MEMS and Nanophotonics (OMN) (2016) pp. 1-2

Yang, H.; Haist, T.; Gronle, M.; Osten, W.

Realistic simulation of camera images of micro-scale defects for automated defect inspection

Forum Bildverarbeitung2016 - KIT Scientific Publishing (2016) pp.63

Zhou, M.; Singh, A. K.; Pedrini, G.; Osten, W.; Yao, B.

Speckle-correlation Microscopic Imaging through Scattering Medium

Imaging and Applied Optics 2016, OSA Technical Digest (online) (Optical Society of America, 2016), Heidelberg, Germany, 25–28 July 2016, paper DT1E.2

Conference proceedings and journals

2017

Bielke, A.; Pruss, C.; Osten, W.

Streulichtreduzierung bei einem variablen Interferometer-Objektiv mit zwei diffraktiven Elementen

Proc. DGaO 118. Tagung (2015) B 29

Bilski, B.; Frenner, K.; Osten, W.

Effective-CD: a contribution toward the consideration of line edge roughness in the scatterometric critical dimension metrology

J. Micro/Nanolith. MEMS MOEMS 16 (2017) 2, Nr. 024002

Boettcher, T.; Gronle, M.; Osten, W.

Single-shot multilayer measurement by chromatic confocal coherence tomography

Proc. of SPIE (2017) Vol. 10329-18

Buchta, D.; Claus, D.; Pedrini, G.; Osten, W.

Depth-resolved Hyperspectral Digital Holography

Digital Holography and Three-Dimensional Imaging, OSA Technical Digest (online) Optical Society of America (2017) paper W4A.3.

Buchta, D.; Heinemann, C.; Pedrini, G.; Krekel, C.; Osten, W. (invited paper)

Lock-in-shearography for the detection of transport-induced damages on artwork

Proc. of SPIE (2017) Vol. 10331-15

Chen, B.; Herkommer, A.

Comparison of different designs of head mounted displays with large field of view

Proc. of SPIE (2017) Vol. 10335-5

Claus, D.; Böttcher, T.; Osten, W.

Hybrid optical design for a wide field chromatic confocal scanning interferometer

Proc. DGaO 118. Tagung (2015) B 35

Claus, D.; Mlikota, M.; Geibel, J.; Reichenbach, T.; Pedrini, G.; Mischinger, J.; Schmauder, S.; Osten, W.

Large-field-of-view optical elastography using digital image correlation for biological soft tissue investigation

J. Med. Imag. 4 (2017) 1 Nr. 014505

Gödecke, M. L.; Peterhänsel, S.; Buchta, D.; Frenner, K.; Osten, W.

Detection of grating asymmetries by phase-structured illumination

Proc. of SPIE (2017) Vol. 104490C

Krauter, J.; Boettcher, T.; Gronle, M.; Osten, W.

Low-coherence Interferometry for Industrial Applications

Proc. of AMA, 2017

Krauter, J.; Gronle, M.; Osten, W.

Optical inspection of hidden MEMS structures

Proc. of SPIE (2017) Vol. 10329-39

Li, H.; Fu, L.; Frenner, K.; Osten, W.

Nanofabrication results of a novel cascaded plasmonic superlens: lessons learned

Proc. of SPIE (2017) Vol. 10330-36

Pruss, C.; Mateo, C.-M.; Schwanke, O.; Fu, L.; Dietrich, T.; Rumpel, M.; Ahmed, M. A.; Graf, T.; Osten, W.

Sub-lambda Polarisationsformer für Hochleistungslaser

Proc. DGaO 118. Tagung (2015) P 11

Schindler, J.; Pruss, C.; Osten, W.

Increasing the accuracy of tilted-wave-interferometry by elimination of systematic errors

Proc. of SPIE (2017) Vol. 10329-3

Yang, H.; Haist, T.; Gronle, M.; Osten, W.

Simulated BRDF based on measured surface topography of metal

Proc. of SPIE (2017) Vol. 10334-4

Patents

Patent Applications

Körner, Klaus; Boettcher, Tobias; Lyda, Wolfram; Gronle, Marc; Osten, Wolfgang

Vorrichtung und Verfahren zur multi- oder hyperspektralen Bildgebung und / oder zur Distanz- und / oder 2-D oder 3-D Profilmessung eines Objekts mittels Spektrometrie
DE 102014002514 A1Date of publication: 27.08.2015

Verfahren und Vorrichtung zum Erzeugen von multi- oder hyperspektralem Licht, zur hyperspektralen Bildgebung und/oder zur Distanz- und/oder 2-D oder 3-D Profilmessung eines Objekts mittels Spektrometrie
EP 3108216 A2Date of publication: 28.12.2016
WO 2015124288 A3Date of publication: 22.10.2015
WO 2015124288 A2Date of publication: 27.08.2015

Osten, Wolfgang; Pedrini, Giancarlo; Körner, Klaus; Gadow, Rainer

Optisches Verfahren und Anordnung zur Eigenspannungsmessung, insbesondere an beschichteten Objekten
WO 2016184578 A1Date of publication: 24.11.2016
DE 102015006697 A1Date of publication: 24.11.2016

Körner, Klaus; Röseler, Arnulf; Claus, Daniel; Osten, Wolfgang

Vorrichtung und Verfahren zur spektroskopischen Ellipsometrie, insbesondere zur spektroskopischen Infrarot-Ellipsometrie
EP 3026422 A1Date of publication: 01.06.2016
US 20160146722 A1Date of publication: 26.05.2016

Körner, Klaus; Claus, Daniel; Herkommer, Alois; Osten, Wolfgang

Messsonde, Vorrichtung und Verfahren zur markierungsfreien abgeschwächten Reflexions-Infrarotspektroskopie
EP 3026426 A1Date of publication: 01.06.2016

Measuring probe, an apparatus and a method for label free attenuated reflection infrared spectroscopy
US 20160143539 A1Date of publication: 26.05.2016

Körner, Klaus; Claus, Daniel; Pruss, Christof; Herkommer, Alois; Osten, Wolfgang

Verfahren und Anordnung zur optischen Absorptionsmessung
EP 2997883 A1Date of publication: 23.03.2016

Method and Apparatus for Optical Absorption Measurements
US 20160076997 A1Date of publication: 17.03.2016

Baer, Goran; Pruss, Christof; Osten, Wolfgang

Verfahren zur Kalibrierung eines Messgerätes
WO 2015173346 A3Date of publication: 03.03.2016
WO 2015173346 A2Date of publication: 19.11.2015
DE 102014209040 A1Date of publication: 19.11.2015
Assignee: Carl Mahr Holding GmbH

Körner, Klaus; Herkommer, Alois; Osten, Wolfgang

Verfahren und Anordnung, insbesondere auch zur bildgebenden Fourier- Transformations-Spektroskopie im mobilen Einsatz
EP 2912420 A1Date of publication: 02.09.2015

Körner, Klaus; Osten, Wolfgang

Robust One-Shot Interferometer and OCT Method for Material Measurement and Tumor Cell Recognition
US 20150077760 A1Date of publication: 19.03.2015

Körner, Klaus; Osten, Wolfgang

Verfahren und Anordnung zur robusten One-shot-Interferometrie, insbesondere auch zur optischen Kohärenz-Tomografie nach dem Spatial-domain-Ansatz (SD-OCT)
DE 102013016752 A1Date of publication: 05.03.2015

Körner, Klaus; Osten, Wolfgang

Robustes One-Shot-Interferometer und OCT- Verfahren, insbesondere zur Materialmessung und auch Tumorzellen-Erkennung
EP 2843360 A1Date of publication: 04.03.2015

Granted Patents

Körner, Klaus; Röseler, Arnulf; Claus, Daniel; Osten, Wolfgang

Apparatus and a method for spectroscopic ellipsometry, in particular infrared spectroscopic ellipsometry

US 9383306 B2Date of publication: 05.07.2016

Grimm, Friedrich; Herkommer, Alois

Röhrenkollektor mit einem Konzentratelement und einem Empfängerelement

DE 102014006126 B3.....Date of publication: 11.06.2015
Assignee: Grimm, Friedrich; Herkommer, Alois

Körner, Klaus; Herkommer, Alois; Osten, Wolfgang

Verfahren und Anordnung, insbesondere auch zur bildgebenden Fourier- Transformations-Spektroskopie im mobilen Einsatz

EP 2912420 B1.....Date of publication: 11.05.2016

Körner, Klaus; Pedrini, Giancarlo; Pruss, Christof; Osten, Wolfgang

Method and arrangement for short coherence holography

US 9175954 B2.....Date of publication: 03.11.2015
GB 2505106 B.....Date of publication: 30.09.2015

Körner, Klaus; Boettcher, Tobias; Lyda, Wolfram; Gronle, Marc; Osten, Wolfgang,

Vorrichtung und Verfahren zur multi- oder hyperspektralen Bildgebung und / oder zur Distanz- und / oder 2-D oder 3-D Profilmessung eines Objekts mittels Spektrometrie

DE 102014002514 B4.....Date of publication: 29.10.2015

Frenner, Karsten; Osten, Wolfgang; Pruss, Christof; Schweizer, Heinz

Nahfeldlinse zur Fokussierung eines elektromagnetischen Nahfeldes

DE 102011006106 B4.....Date of publication: 15.10.2015

Hopp, David; Pruss, Christof; Osten, Wolfgang

Device and method for optically compensating for the measuring track decentralization in rotation angle sensors

KR 101545134 B1Date of publication: 20.08.2015
US 9068862 B2Date of publication: 30.06.2015
CN 102483336 BDate of publication: 17.06.2015

Körner, Klaus; Berger, Reinhard; Osten, Wolfgang

Method and arrangement for robust interferometry for detecting a feature of an object

US 8934104 B2.....Date of publication: 13.01.2015

Doctoral thesis, Master & Bachelor thesis and Student research thesis

Doctoral thesis 2015–2016

Erdogan, Veysel

Ein systematischer Zugang für die Beschreibung von Inspektionsaufgaben am Beispiel der Oberflächeninspektion in der Automobilindustrie

10/2015

Warber, Michael

Zum Einsatz von Lichtmodulatoren für die computer-basierte Mikroskopie

12/2015

Geiger, Florian

Ein bildgebendes Quantenkaskadenlaser-Spektrometer zur intraoperativen Gewebedifferenzierung in der chirurgischen Onkologie

11/2015

Bilski, Bartosz

Line Edge Roughness in Optical Critical Dimension Metrology

01/2016

Mauch, Florian

Modellbasierte Charakterisierung optischer Messsysteme mittels GPU beschleunigter Optiksimulation

08/2016

Fortmeier, Ines

Zur Optimierung von Auswerteverfahren für Tilted-Wave Interferometer

04/2016

Kranz, Oliver

Modellierung und experimentelle Erprobung eines Raumwinkel-Kalibriersystems für zweiachsige Autokollimatoren

oral examination: 09/2016

Pehnelt, Sebastian

Optische Erfassung und Bewertung von Kennwerten zur Beurteilung der Mikrotopographie von Zylinderlaufbahnen

oral examination: 11/2016

Baer, Goran

Ein Beitrag zur Kalibrierung von Nicht-Null Interferometern zur Vermessung von Asphären und Freiformflächen

oral examination: 12/2016

Master thesis 2015–2016

Grumbrecht, Mario Till

Optimierte Messdatenvorbereitung
für Tilted Wave Interferometer
02/2015

Jiang, Bofan

Realisierung und Kalibrierung eines hybriden
telezentrischen Objektivs
02/2015

Abele, Andreas

Rechnerische Verbesserung der
Ortsauflösung von Phasenbildern
03/2015

Schiele, Frank

Automatisierung eines Inspektions-
mikroskops auf Basis der Open Source
Software itom zur Kontrolle diffraktiver
Mikrostrukturen
08/2015

Jin, Siqi

Sicherheitskonzepte für
Laserscheinwerfer
10/2015

Reichert, Carsten

Entwicklung neuer optischer Konzepte
für Smartphone-Vorsatzoptiken
12/2015

Arzenbacher, Kathrin

Design und generative Fertigung von
Mikro-Abbildungsoptiken für
medizintechnische Anwendungen
02/2016

Edenharder, Stefan

Holographic Raman imaging of
specific gaseous molecules
03/2016

Thiem, Jonas Maximilian

Phasenrekonstruktion mittels gekrümmter
Beleuchtung angewandt auf medizinische
Bildgebung
03/2016

Karadali, Terpsithea

Synthese und Modifikation sauerstoff-
haltiger Elektrodenmaterialien für Lithium-
Ionen Zellen durch elektromagnetische
Strahlung
04/2016

Hahn, Robin

Konzept, Design und Validierung
eines Weißlichtinterferometers mit
einem 3-fach Referenzspiegel
06/2016

Braun, Christina

Entfernung spekularer Reflexe in digitalen
Bildern mithilfe von Polarisationsinformation
6/2016

Krist, Florian

Entwicklung und Auslegung eines Optik-
Konzepts für den Laser Metal Fusion
Prozess zur Erhöhung der Produktivität
06/2016

Ni, Chenghan

Aufbau und Erprobung der Lock-in Shearo-
grafie für den Einsatz an Kunstwerken
06/2016

Hofer, Tobias

Chromatisch Konfokale Messverfahren
mit diffraktivem optischen Element an
Mehrschichtsystemen
10/2016

Bachelor thesis 2015–2016

Kübler, Johannes

Entwicklung eines Spektrometers für die Fluoreszenz-Lebensdauer-Messung in der Ophthalmoskopie basierend auf einer digitalen Mikrospiegel-Einheit

10/2016

Hasenohr, Thomas

Detektion und Erfassung von Objekten in niedrigen Erdborbit

10/2016

Schwanke, Oliver

Realisierung eines Stepped Masked Interference Lithography Exposure (SMILE) Aufbau

11/2016

Faulhaber, Andreas

Design und Aufbau eines Low-Cost-Pulsoxymeter Bausatzes für Entwicklung und Lehre

12/201

Hecker, Sebastian

Weiterentwicklung eines Moduls zur Bearbeitung transparenter Materialien mit ultrakurzen Laserpulsen

12/2016

Erlenwein, Caroline Jasmin

Simulation von Lichtstreuung in biologischem Gewebe und Gewebephantomen

02/2015

Grupp, Barbara

Optische Simulation: Anwendung der Lichtfeldkamera für die dreidimensionale endoskopische Bildgebung

02/2015

Barth, Julian

Kalibrierung eines Streifenprojektionssystems zur Bestimmung der Morphologie von Organen

03/2015

Koschig, Maximilian

Messverfahren zur Verbesserung des postoperativen visuellen Ergebnisses während Katarakt-Operationen und Validierung der intraoperativen Biometrie mittels Raytracing

03/2015

Reichenbach (Labitzke), Thomas

Elastografie: Phantomherstellung und Messung

07/2015

Rubers, Julius

Realisierung einer individuellen Mikroskopbeleuchtung mittels DLP Technologie

07/2015

Freyburger, Moritz

Automatisierte Justage planer Substratoberflächen für die Laserdirektbelichtung

08/2015

Erb, Jennifer

Entwicklung und Erprobung eines Optiksyst-
ems zur Abbildung unterschiedlich entfern-
ter Objekte auf einem Sensor
08/2015

Fleig, Felix

Machbarkeitsstudie einer LED-Dentalleuchte
09/2015

Lesmeister, Jakob

Auslegung und Optiksimation der
Bildentstehung in einer Lichtfeldkamera
09/2015

Sanftmann, Beate

Bewertung von additiven Fertigungs-
verfahren für Optikkomponenten
09/2015

Salzmann, Kai

Computergestützte Bildgebung
für 3D-Messdruck
09/2015

Hermanutz, Lena Sophie

Experimentelle Untersuchung eines neuen
Verfahrens zur Blickrichtungsdetektion
10/2015

Hutter, Marco

Optikdesign und Algorithmenentwicklung
für eine 3D-gedruckte ultraflache
Facettenaugenkamera
10/2015

Knab, Aline

Weiterentwicklung eines tragbaren
hyperspektralen Abbildungssystems
11/2015

Petersen, Barbara

Design und Realisierung einer Technik zur
Untersuchung elektrisch durchstimmbarer
Linsen
11/2015

Keßner, Thorben

Experimenteller Aufbau einer
endoskopischen Lightfield-Kamera
11/2015

Serbes, Hüseyin

Aufbau und Anwendung eines mobilen
Shearografie-Sensors zur Diskriminierung
unterschiedlicher Gewebetypen
12/2015

Kaufmann, Sven

Digital holografische Tomografie zur
Untersuchung biologischer Proben
02/2016

Rüdinger, Andrea

Low Cost Shack-Hartmann Sensorik mittels
holographischer Mehrpunktgenerierung
02/2016

Geibel, Jonathan

Chromatische Beleuchtungs- und Indenter-
geometrieangepassung für die Erkennung von
Gewebeverhärtungen mittels Elastographie
04/2016

Zähler, Matthias Paul Walter

Entwicklung und Aufbau von Modellsyste-
men zur realistischen Nachbildung des men-
schlichen Auges und des Sehvermögens
04/2016

Okuka, Ana-Maria

Untersuchung zur Eignung eines neuartigen
Mikrolinsenarrays für Lichtfeld-Anwendungen
04/2016

Scholz, Claudia

Vergleich zwischen digital holographischer
Mikroskopie und des Phase Retrieval Ver-
fahrens für die Visualisierung von Zellen
06/2016

Student research thesis 2015–2016

Bui, Duc Anh

Subpixelgenaue Positionsbestimmung mittels holografischer Mehrpunktgenerierung
02/2015

Hoppe, Martin

Aufbau und Inbetriebnahme einer Steuerung für ein Aerial-Image Mikroskop mit konfokaler Diskriminierung zur Messung von Sub-Lambda Strukturen
06/2015

Luft, Andreas

Optische Simulation: Analyse einer hoch-effizienten und neuartigen Solarleuchte
06/2015

Joas, Sebastian

Development and Implementation of a Quantitative Phase Imaging System for Cell Imaging
07/2015

Brodhag, Nicole

Charakterisierung eines Aufbaus zur tiefenaufgelösten Fluoreszenzdetektion in streuenden Medien
10/2015

Appel, Kristin

Vermessung von plasmonischen Linsen mit Hilfe eines Laser- Scanning-Mikroskops mit konfokaler Diskriminierung
11/2015

Wagner, Patrick

Schnelle Erfassung von Multispot-Bildern mit anpassbarer ROI
12/2015

Haas, Daniel

Konstruktion und Test eines Aufbaus zur digitalen Holografie im tiefen UV-Bereich
04/2016

Werz, Marco

Konstruktion und Prüfung eines optischen Sensors mittels vergleichender NIR-Spektroskopie
04/2016

Guo, Chenchen

Investigation of the optical performance of the monochromatic design types of a patent database
05/2016

Yan, Hao

Analysis of color-corrected optical design types
05/2016

Heske, Joachim Matthias

Simulationsstudie zur evaneszenten Nano-Ellipsometrie in der Otto-Anordnung
06/2016

Capitaine, Fabian

Untersuchung Dezentrierungsfehler in typischen Experimentalsystemen basierend auf Cage-Systemen
06/2016

Haub, Michael

Implementierung und Erprobung eines Defekterkennungssystems mit Hilfe eines automatisierten Inspektionsmikroskops für die Herstellung von diffraktiven Mikrostrukturen
07/2016

Lindenmann, Julia

Simulationsstudie zur Shearing-Interferometrie für die medizinische Diagnostik

07/2016

Kraus, Niclas

Auslegung, Simulation und Konstruktion von optischen Demonstrationsversuchen

07/2016

Ritter, Jonas

Coherence and polarization speckle by using a rotating rough-surfaced retardation plate

08/2016

Dukart, Stefan

Robuste Signalauswertung für einen Wellenfrontsensor mit holografischer Mehrpunktprojektion

08/2016

Schäfer, Max Bert

Entwicklung eines Goniometers zur Vermessung endoskopischer Beleuchtungssysteme

08/2016

Erlenwein, Caroline

Fusion optischer und inertialer Bewegungserfassung für die Neuroforschung

09/2016

Vasilev, Boris

Aufbau einer computergesteuerten einstellbaren Winkelverkipfung für die laterale Shearing Interferometrie

10/2016

Gao, Kaiyuan

Analyse von patentierten optischen Systemen hinsichtlich der Lage im FOV-NA-Diagramm

11/2016

Quasthoff, Michael

Machbarkeitsstudie zur Verwendung und dem Bau von optischen Technologien im eigenen Zuhause

11/2016

Körner, Frank

Charakterisierung eines mikroskopischen Streifenprojektionssystems auf Basis des Fairen Datenblatts

12/2016

Stuttgart Scientific Symposium 2015 "Light for the future"

*dedicated to the 30th Stuttgart Optics Colloquium
and the International Year of Light 2015*

am 25. Februar 2015, Teilnehmer: ca. 250



Opening Prof. Dr. Wolfgang Osten
Institute for Applied Optics (ITO) of the University of Stuttgart

Welcome address Prof. Dr. Wolfram Ressel
Rector of the University of Stuttgart

Welcome address Ministerialdirigent Günther Leßnerkraus
*Abteilungsleiter Industrie, Innovation und wirtschaftsnahe Forschung im
Ministerium für Finanzen und Wirtschaft Baden-Württemberg*

"High-performance research infrastructures as basis for economic success in lasers and photonics" Prof. Dr. Andreas Ostendorf
President Wissenschaftliche Gesellschaft für Lasertechnik WLT e.V.

"Light in SCoPE: Optics research at the University of Stuttgart" Prof. Dr. Wolfgang Osten
Institute for Applied Optics (ITO) of the University of Stuttgart

"2015 International Year of Light under UNESCO auspices – celebrating the importance of light and light-based technologies in shaping the society" Dr. Jean-Paul Ngome Abiaga
International Basic Sciences Programme (IBSP) of UNESCO

Welcome address "Germany – a country with a bright tradition in optics" Dr. Frank Höller
President Deutsche Gesellschaft für Angewandte Optik DGaO

"Light – a bridge between research, industry and society" Prof. Dr. Edward G. Krubasik
President of the German Physical Society DPG

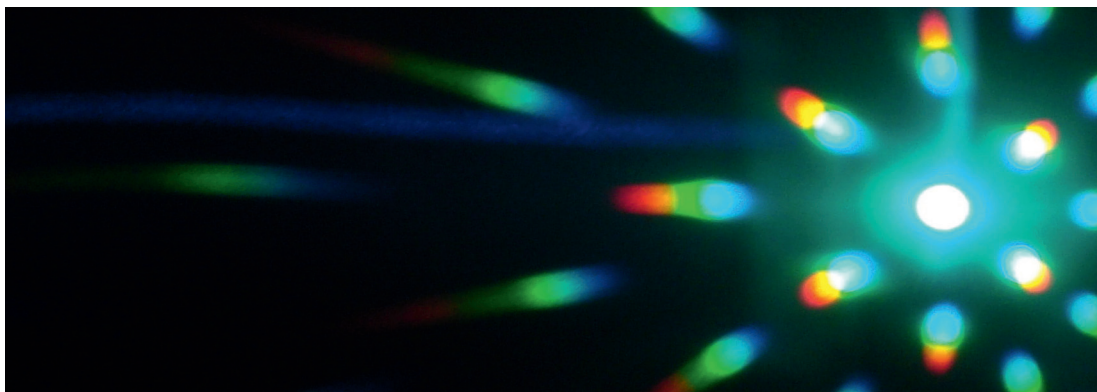
Welcome address "Recent highlights of photonics research in Europe" Prof. Dr. Seppo Honkanen
2015 President of the European Optical Society EOS
Prof. Dr. Jyrki Saarinen
Executive Director at EOS

"Challenges and trends in the german photonics industry sector" Prof. Dr. Andreas Tünnermann
Director Fraunhofer Institut für Angewandte Optik und Feinmechanik, Jena, Germany

"Light as a perspective to strengthen the european economic backbone" Dr.-Ing. Michael Mertin
President and CEO of JENOPTIK AG and President of Photonics21, Jena, Germany

"Optics and photonics as the backbone of physics in Europe" Dr. Luc Berge
European Physical Society EPS – Chair of the Quantum Electronics and Optics Division

- “Selected emerging areas of optics and photonics”
 Prof. Dr. Philip Russell
*2015 President of the Optical Society OSA and
 Director at the Max Planck Institute for the Science of Light, Erlangen, Germany*
-
- “Raising awareness of optics and photonics to the general public”
 Elizabeth A. Rogan
OSA CEO, Washington DC, USA
-
- “Society advocacy on behalf of the community:
 SPIE’s view of its growing importance”
 Prof. Toyohiko Yatagai
*2015 President of International Society for Optics and
 Photonics SPIE and Director of CORE – The Center for Optical
 Research and Education, Utsunomiya University, Japan*
 Dr. Eugene Arthurs
CEO at SPIE, Bellingham, USA
-
- “Modern teaching in optics at the College of Optical
 Sciences of the University of Arizona”
 Prof. Dr. James C. Wyant
*Founding Dean of the College of Optical Sciences,
 University of Arizona, USA*
-
- “Photonic quantum technology and future applications”
 Prof. Dr. Gerd Leuchs
University Erlangen-Nürnberg and Director at the Max Planck Institute for the Science of Light
-
- “Light sources for EUV lithography”
 Dr. Michael von Borstel
CEO of TRUMPF Lasersystems for Semiconductor Manufacturing
-
- “Building new scientific communities and European cohesion
 through the world’s largest laser research facility”
 Prof. Dr. Wolfgang Sandner
*Director General and CEO, ELI-DC International Association
 AISBL, The European Extreme Light Infrastructure ELI*
-
- “Optical and laser engineering at COLE, Singapore”
 Prof. Dr. Anand Asundi
*Director of COLE – Center for Optical and Laser Engineering, MAE,
 Nanyang Technological University, Singapore*



Optik-Kolloquium 2016

Optik in einer digitalen Welt

am 11. Februar 2016, Teilnehmer: ca. 140

Begrüßung und Einführung	Prof. Dr. W. Osten und Prof. Dr. A. Herkommer <i>ITO, Universität Stuttgart</i>
Schnelle digitale 3D-Formvermessung mit statistischer Musterprojektion	Prof. Dr. R. Kowarschik <i>Friedrich-Schiller-Universität, Jena</i>
Learning from Examples in Optical Imaging	Prof. Dr. D. Psaltis <i>Ecole Polytechnique Fédérale de Lausanne, Schweiz</i>
Grundsätze und Einsatzmöglichkeiten von Compressive Sensing und Sparse Representation in der bildgebenden Sensorik	Prof. Dr.-Ing. J. Ender <i>Universität Siegen</i>
Echtzeit-Bildverarbeitung in der Endoskopie	Dr. Johannes Fallert <i>Karl Storz, Tuttlingen</i>
Opto-digitale Methoden zur Erweiterung der Schärfentiefe in abbildenden optischen Systemen	M. Kamm <i>Sony Deutschland GmbH, EuTEC Stuttgart</i>
Case Study – Automotive Head-Up-Display	R. Födisch <i>LightTec, München</i>
Schaltbare flüssigkristallbasierte Lichtmodulatoren – Funktionsweise und Anwendungen	Dr. A. Hermerschmidt <i>HOLOEYE Photonics AG, Berlin</i>
Optikkonzepte für die digitale Zukunft – Auslegung optischer Systeme im digitalen Wandel	Dr. N. Kerwien <i>Carl Zeiss, Oberkochen</i>
Hochaufgelöste Mikroskopie großer Bildfelder durch Multispot-Abtastung mit diffraktiven Elementen	Prof. Dr. K.-H. Brenner <i>Universität Heidelberg, Mannheim</i>
Detection of Grating Asymmetries by Phase-structured Illumination	L. Gödecke <i>ITO, Universität Stuttgart</i>
Direktes Laserschreiben von mikrooptischen Systemen in 3D – in einem Schritt vom Digitalmodell zum Prototypen	S. Thiele <i>ITO, Universität Stuttgart</i>

Organized international conferences: 2015 – 2017

W. Osten:

SPIE Congress Optical Metrology 2015

June 21 – 25, 2015, Munich, Germany

W. Osten:

SPIE Conference “Optical Measurement Systems for Industrial Inspection IX”

June 22 – 25, 2015, Munich, Germany

W. Osten:

SPIE Conference
“Optical Micro- and Nanometrology VI”

April 04 – 07, 2016, Brussels, Belgium

W. Osten:

OSA Digital Holography and
3-D Imaging (DH) Conference

July 24 – 28, 2017, Heidelberg, Germany

W. Osten:

SPIE Congress Optical Metrology 2017

June 25 – 29, 2017, Munich, Germany

W. Osten:

SPIE Conference “Optical Measurement Systems for Industrial Inspection X”

June 25 – 29, 2017, Munich, Germany

W. Osten:

SPIE Conference
“Digital Optical Technologies”

June 25 – 29, 2017, Munich, Germany

W. Osten:

HoloMet 2017:
Future Challenges to Optical Imaging and
Measurement Technologies in Times of
Digital Transition

September 24 – 27, 2017, Stuttgart, Germany

Impressum:

Publisher: Institut für Technische Optik (ITO)
Universität Stuttgart
Pfaffenwaldring 9
D – 70569 Stuttgart
www.uni-stuttgart.de/ito

Editor: Dipl.-Ing. (FH) Erich Steinbeißer, ITO
ac.Cent werbeagentur gmbh, Leonberg (Layout)

Printing: Breitschuh & Kock GmbH, Kiel

Print run: 350

ISBN 978-3-923560-86-8

